THE UNIVERSITY
of EDINBURGH

The Hippo Pathway Regulates Caveolae Expression and Mediates Flow Response via Caveolae

Valentina Jana Laura Rausch (BSc, MSc)

A thesis submitted for the degree of

Doctor of Philosophy

November 2019

School of Clinical Sciences

THE UNIVERSITY *of* EDINBURGH

Contents

Abstract

The Hippo pathway is a key regulator of cell survival, proliferation and tissue homeostasis. In addition, it is vital for development and regeneration. The activity of the Hippo pathway depends on intra- and extra-cellular signals and is tightly regulated by diffusible chemicals as well as mechanical stimuli. The pathway comprises of a kinase cascade that controls the activity of YAP and TAZ, homologous transcriptional co-activators. Despite its central role in most cells the overall regulation of the Hippo pathway, especially originating from the plasma membrane, is not yet fully understood. Caveolae are 50-100 nm bulb-shaped plasma membrane invaginations that function in endocytosis, protection from mechanical stress and in cell signalling. Hence, the aim was to identify if caveolae and the Hippo pathway are functionally linked. This thesis reveals that the central caveolar components CAVEOLIN1 and CAVIN1 depend on YAP/TAZ. *CAVEOLIN1* and *CAVIN1* are direct YAP-TEAD target genes and YAP/TAZ are essential for the expression of caveolar components in mammalian cells and in zebrafish. Moreover, CAVEOLIN1 dictates YAP/TAZ subcellular localisation and inhibits their activity. Notably, in cells with diminished levels of caveolae, YAP/TAZ are hyperactive (nuclear), which led to increased induction of gene transcription. Finally, the activation of YAP/TAZ by shear stress is partly dependent on caveolae. These data link caveolae to Hippo pathway signalling in the context of cellular responses to mechanical stimuli and suggest feedback regulation between the Hippo pathway co-transcriptional activators YAP/TAZ and essential caveolae components.

Lay Summary

The development of most organs and the specialisation and survival of each cell of an organism depends on signals that the cell receives. One signalling pathway which is central for many functions of the body is the Hippo pathway. This pathway is a key cellular control centre and its activity is influenced by various stimuli. An example is the flow of liquid, like the blood flow in our vessels. The cells lining our blood vessels experience friction on their outer membranous layer when the blood passes by them. Capable of sensing the liquid flow are little structures in the outer membrane layer of the cell which are called Caveolae. In Latin Caveolae mean “little caves”. They have the shape of tiny cups inserted into the membrane of the cell. This thesis investigates if there is a functional link between the Hippo pathway and Caveolae, especially when a cell senses and responds to liquid flow.

One main discovery is that the Hippo pathway is important for the number of Caveolae. Consequently, only cells with a normal Hippo pathway contain physiological numbers of Caveolae. On the other hand, Caveolae were also discovered to influence the Hippo pathway activity. In the context of flow sensing, cells respond differently when they do not have a functional Hippo pathway and Caveolae. In normal cells, liquid flow strongly activates one part of the Hippo pathway, which induces the expression of genes and the secretion of molecules, which in turn activates neighbouring cells. In contrary, cells without Caveolae do not show this strong activation of the Hippo pathway as a response to liquid flow. Therefore, the Hippo pathway activation by liquid flow depends (at least partly) on Caveolae. As the Hippo pathway and Caveolae are both important for the development of blood vessels, their interaction might be central of the maintenance and renewal of blood vessels.

In conclusion, the interplay between the Hippo pathway and Caveolae is a new insight into how cells react to liquid flow and provides a new mechanism on how cells respond to mechanical stimuli in general. Consequently, future studies should focus on investigating the underlying mechanisms of the interaction between the Hippo pathway and Caveolae in order to pave the way for the development of new diagnostics and therapies in the cardiovascular field.

Declaration

I declare that this thesis is an original report of my research, has been written by me and has not been submitted for any previous degree. The experimental work is almost entirely my own work; the collaborative contributions have been indicated clearly and acknowledged. Due references have been provided on all supporting literatures and resources. I declare that this thesis was composed by myself, that the work contained herein is my own except where explicitly stated otherwise in the text, and that this work has not been submitted for any other degree or professional qualification.

Valentina J. L. Rausch

Acknowledgements

First of all, I want to thank Dr Carsten G. Hansen for his guidance and support throughout my project, while performing the experiments and writing this thesis. At the same time, I am very grateful to Dr Sonja Vermeren and Dr Alexander Hergovich for committing their time to examine this thesis. I also want to emphasise how fortunate I was to work in a lab group of people so supportive, understanding and cheerful, thank you Jiwon Park and Omar Salem, and Susanna Riley, Siyang Jia and Lisa Kölln. Further, I would like to thank Professor David Hay for his feedback on my project and initial technical advice. Moreover, I want to express my gratitude to the remaining members of my thesis committee Professor Elaine Dzierzak and Dr Yi Feng as well as the technical and administrative staff, in particular the postgraduate administrators Karen Colvin and Alexandrea Moreira. Finally, I want to say THANK YOU to everyone who accompanied me, to those who I met and those who I lost on my way to here. Thank you, Teşekkür ederim, muchas gracias, grazie mille, hvala puno and Dankeschön!!

List of Publications

Rausch, V.; Bostrom, J.R.; Park, J.; Bravo, I.R.; Feng, Y.; Hay, D.C.; Link, B.A.; Hansen, C.G. (2019) The Hippo Pathway Regulates Caveolae Expression and Mediates Flow Response via Caveolae. *Curr. Biol.* 29, 242–255e6.

Rausch, V.; and Hansen, C.G. (2019). Immunofluorescence study of endogenous YAP in mammalian cells. *Methods Mol. Biol.* 1893, 97–104.

Rausch, V.; and Hansen, C.G. (2019). The Hippo Pathway, YAP/TAZ, and the Plasma Membrane. *Trends in Cell Biology.* (in press) doi.org/10.1016/j.tcb.2019.10.005.

List of Figures

List of Tables

Abbreviations

2°AB	Secondary antibody
AP-1	Activator Protein-1
APS	Ammonium Persulfate
BOEC	Blood Outgrowth Endothelial Cells
bp	Base Pair
BSA	Bovine Serum Albumin
CAV	Caveolin
CCLE	Cancer Cell Line Encyclopedia
cDNA	Complementary DNA
CGL	Congenital Generalised Lipodystrophy
ChIP	Chromatin Immunoprecipitation
CLSM	Confocal Laser Scanning Microscopy
CO_2	Carbon Dioxide
CRISPR	Clustered Regularly Interspaced Short Palindromic Repeats
CTGF	Connective Tissue Growth Factor
CYR61	Cysteine-Rich Angiogenic Inducer 61
CytoD	Cytochalasin D
DNA	Deoxyribonucleic Acid
DAPI	4′,6-diamidino-2-phenylindo
DMEM	Dulbecco Modified Eagle Medium
DMSO	Dimethyl Sulfoxide
DSB	DANN Double Strand Break
DTT	Dithiothreitol
DYN2	Dynamin2
ECIS	Electric Cell-Substrate Impedance Sensing
ECL	Enhanced Chemiluminescence
ECM	Extracellular matrix
ef1a	Elongation Factor 1-alpha
eGFP	Enhanced Green Fluorescent Protein
EM	Transmission Electron Microsopy
FA	Focal Adhesion
FACS	Fluorescence-activated cell sorting
FBS	Fetal Bovine Serum
GAPDH	Glyceraldehyde 3-Phosphate Dehydrogenase
GFP	Green Fluorescence Protein
H_2O	Water
HEK	Human Embryonic Kidney
hpf	Hours Post Fertilisation
HPRT1	Hypoxanthine-Guanine Phosphoribosyltransferase 1
hr	Hour
HRP	Horseradish Peroxidase
HSP90	Heat Shock Protein 90
HUVEC	Human Umbilical Vein Endothelial Cells

IF	Immunofluorescence
IFN-γ	Interferon-gamma
IgG	Immunoglobulin G
IL-6	Interleukin 6
ISKNV	Infectious Spleen and Kidney Necrosis Virus
K_2HPO_4	Dipotassium Phosphate
KD	Knockdown (gene)
KH_2PO_4	Monopotassium Phosphate
KO	Knockout (gene)
LATS	Large Tumor Suppressor Kinase
LPA	Serum-Borne Lysophosphatidic Acid
M-CAT	Malonyl CoA-acyl Carrier Protein Transacylase
MAP4K	Mitogen-activated Protein Kinase Kinase Kinase Kinase
MCW	Medical College Wisconsin
MEF	Mouse Embryonic Fibroblasts
mM	Millimole
mRNA	Messenger Ribonucleic Acid
MRTF	Myocardin-related Transcription Factor
MST	Mammalian Ste20-like
$NaHCO_3$	Sodium bicarbonate
NDR	Nuclear dbf2-Related (kinases)
NF2	Neurofibromin 2
ng	Nanogramm
ns	Not Significant
nucl/cyto	Nuclear to cytoplasmic ratio
OD	Optical Density
p	Probability value
PACSIN	Protein kinase C and Casein Kinase Substrate in Neurons
PAH	Pulmonary Arterial Hypertension
PBS	Phosphate-Buffered Saline
PBST	PBS with added Triton-x-100
PCR	Polymerase Chain Reaction
PDL	Poly-D-Lysine
PECAM	Platelet Endothelial Cell Adhesion Molecule
PMSF	Phenylmethylsulfonyl Fluoride
PRKCDBP	Protein kinase C delta-Binding Protein
PTRF	Polymerase I and Transcript Release Factor
pYAP	Phosphorylated YAP
qPCR	Quantitative PCR
r	Pearson’s correlation coefficient
ROI	Region of interest
RT-qPCR	Reverse Transcriptase qPCR
S1P	Sphin-Gosine-1-Phosphophate
SD	Standard Deviation
SDPR	Serum Deprivation-Response Protein
SDS	Sodium Dodecyl Sulfate

SEM	Standard Error of the Mean
sgRNA	Single Guide RNA
shRNA	Short Hairpin RNA
SRF	Serum Response Factor
SWI	SWItch/Sucrose Non-Fermentable
TAZ	Ttranscriptional Co-activator with PDZ-binding Motif
TEAD	Transcriptional Enhancer Factor TEF
TEER	Transendothelial Electrical Resistance
TEMED	Tetramethylethylenediamine
U2OS	Human Osteosarcoma Cell Line
UCSD	Universitry of California, San Diego, USA
UoE	University of Edinburgh
v/v	Volume per Volume
VE	Vascular Endothelial
VEGF	Vascular Endothelial Growth Factor
VGLL4	Vestigial Like Family Member 4
VP	Verteporfin
w/v	Weight per Volume
WT	Wildtype
wwtr1	WW Domain-Containing Transcription Regulator Protein 1
YAP	Yes-Associated Protein

1. Introduction

1.1 The Hippo Pathway

1.1.1 Discovery of the Hippo pathway

The Hippo pathway is a key regulator of cell survival, development, regeneration and tumorigenesis [1, 2]. The first component of the pathway was discovered in Drosophila in 1995, when loss-of-function mutation of the one of the key kinases (Warts or Lats) resulted in accelerated proliferation and decreased cell death [3, 4]. However, it was only in the early 2000s that more components of the Hippo pathway, including the *Hippo* kinase (MST1/2 in mammals), were discovered [5-12]. With the identification of the Drosophila Yorkie (and mammalian YAP) and later transcription factors Scallop (Drosophila) and TEAD (mammals) the missing links between Warts/LATS and gene transcription were discovered and the combined realisation of the core Hippo pathway was established [13-19]. Since its discovery the Hippo pathway has been shown to be greatly conserved in a wide range of species, including mammals [7, 20], and the list of Hippo pathway components and interactors is constantly growing.

1.1.2 The role of YAP and TAZ as transcriptional regulators

The Hippo pathway regulates the phosphorylation and, thereby, the subcellular localisation of the co-transcriptional activators YAP/TAZ [21]. When the Hippo pathway kinase cascade is inactive, YAP/TAZ remain unphosphorylated and are therefore activated [7]. YAP (yes-associated protein) and its paralogue TAZ/*WWTR1* (transcriptional coactivator with PDZ-binding motif or WW-domain containing

transcriptional regulator 1) are homologs to the Drosophila *Yki* (*Yorkie*) [13, 15, 22]. YAP and TAZ are multi-domain proteins with several protein binding interfaces (**Figure 1**), e.g. WW domains or conserved phosphorylation sites [23].

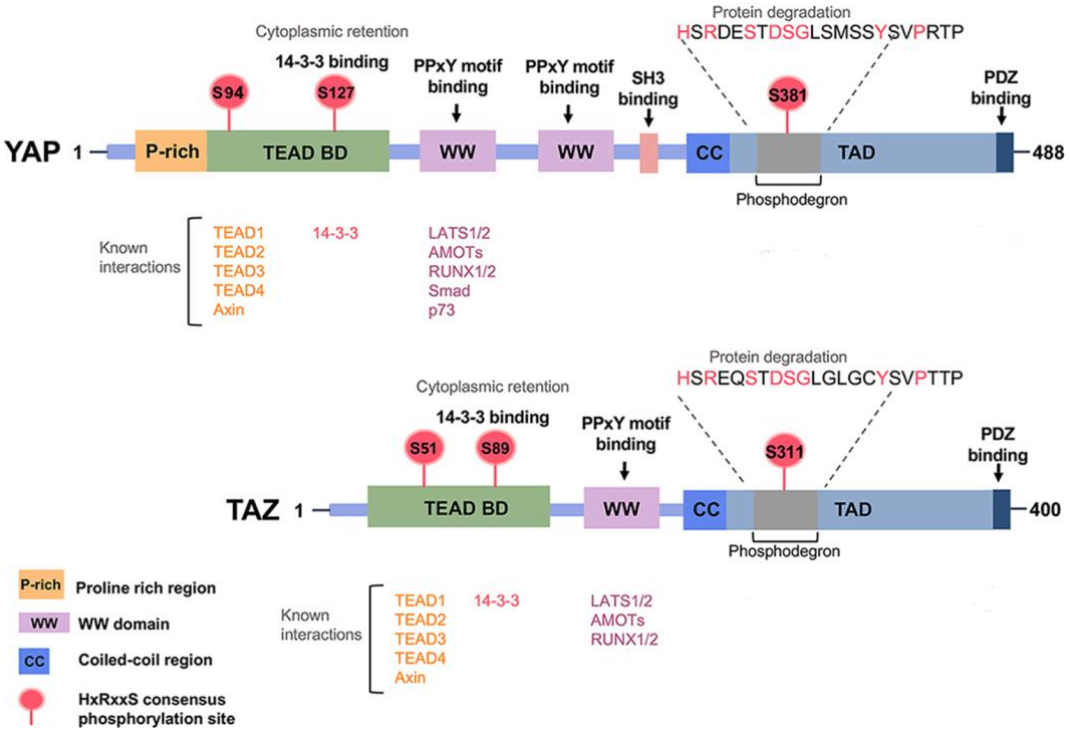

Figure 1: Diagram of YAP and TAZ proteins.

Representation of important regions and interaction sites of the isoforms 1 of both YAP and TAZ. Please refer to text for more details. Adapted from Chen, et al. [23].

Activated YAP and TAZ translocate into the nucleus, where they bind transcription factors like RUNX, SMAD and, mainly, TEADs (TEA domain transcription factor 1 - 4) [14, 15, 24]. As YAP/TAZ lack intrinsic DNA-binding regions, they depend on transcription factors to regulate gene transcription [14-16]. Essential for YAP/TAZ and TEAD interactions are serine residues in the highly conserved N-terminus of YAP/TAZ at the positions S94 for YAP and S51 for TAZ (**Figure 1**). YAP/TAZ interact with the

C-terminus of TEADs and form hydrogen bonds with tyrosine residues, for example at Y406 or Y421 of TEAD1 or Y429 of TEAD4 [15, 17, 18, 25, 26]. The YAP/TAZ-TEAD complexes then bind to M-CAT (muscle-specific cytidine-adenosine-thymidine sequence) and putative TEAD binding DNA motifs with the core sequence 5'-GGAATG-3' in both promoter and enhancer regions [26-29]. The YAP/TAZ-TEAD interactions induce expression of genes facilitating proliferation and inhibiting apoptosis, including connective tissue growth factor (*CTGF*) and cysteine rich angiogenic inducer 61 (*CYR61*) [15, 30].

1.1.3 LATS1/2-mediated YAP/TAZ inhibition

The activation of the Hippo pathway kinases large tumour suppressors 1/2 (LATS1/2) leads to the inhibitory phosphorylation of YAP/TAZ serine residues in their HxRxxS motifs (**Figure 1**) [22, 31, 32]. In the most common mammalian YAP isoform (#1) there are five conserved serine residues, S61, S109, S127, S164, S381, while TAZ (#1) is phosphorylated by LATS1/2 at S66, S89, S117 and S311 [22, 31, 33]. The YAP S127 is central to LATS-induced phosphorylation [31]. The LATS-mediated phosphorylation of YAP/TAZ is a signal for the interaction of YAP/TAZ with the phosphor-binding 14-3-3 protein family, resulting in their cytoplasmic sequestration and subsequent degradation [31, 34-36]. In YAP, phosphorylation at S381 is an important signal for ubiquitination. In TAZ the LATS1/2-mediated phosphorylation of S311 induces the phosphorylation at S314, which is a signal for TAZ ubiquitination. Therefore, LATS-induced YAP S381 and TAZ S311 phosphorylation (**Figure 1**) are markers of decreased YAP/TAZ stability Figure 1[34, 35]. In summary, the activity of the Hippo pathway results in YAP/TAZ inactivation and inhibition of YAP/TAZ-induced gene transcription.

1.1.4 The Hippo pathway core kinase cascade

The mammalian Hippo pathway core kinase cascade (**Figure 2,** in purple) comprises of the Ste20-like kinases 1/2 (MST1/2), which upon phosphorylation interact with and phosphorylate Salvador Family WW Domain Containing Protein 1 (SAV1) [6, 37]. Active MST1/2 further phosphorylate MOB kinase activator 1A/B (MOB1A/B) [38]. Both SAV1 and MOB1A/B act as scaffold proteins to facilitate the recruitment and activating phosphorylation LATS1/2 by MST1/2 [39, 40].

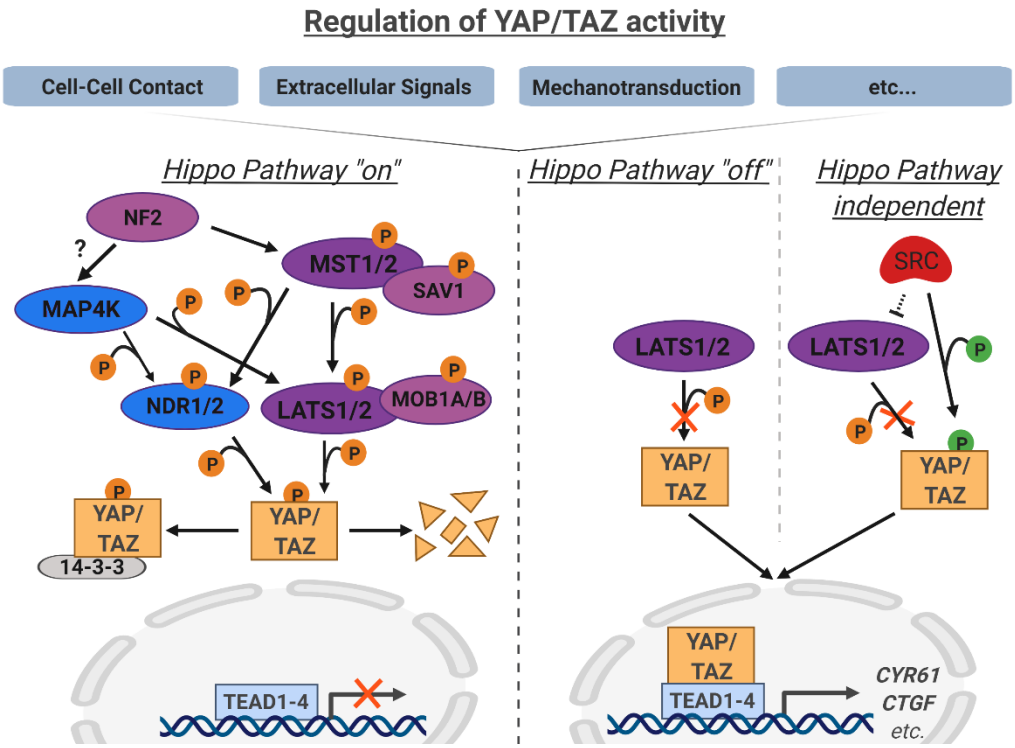

Figure 2: The Hippo pathway.

Simplified scheme of the interactions of (canonical, in purple) Hippo pathway components differentiating between the "on" stage, with the active kinase cascade, and the "off" stage, with no inhibitory phosphorylation of YAP/TAZ. MAP4K and NDR1/2 are exemplary for additions to the canonical Hippo kinase cascade. The SRC-mediated phosphorylation of YAP/TAZ is outlined to indicate one of the established Hippo pathway-independent activation mechanisms of YAP/TAZ. For details, please see text. Figure generated using BioRender.

An important upstream regulator of the Hippo pathway core kinase cascade is the tumour suppressor Neurofibromin 2 (NF2 or Merlin) [40, 41]. NF2 induces the phosphorylation of LATS1/2 by recruiting them to the plasma membrane where LATS1/2 are phosphorylated by MST1/2, which is accumulated at the plasma membrane due to the binding of SAV1 [40]. Activation of the Hippo pathway kinase cascade leads to the phosphorylation and inhibition of the transcriptional co-activator YAP and TAZ [13, 15, 22].

1.1.5 Expansion of the Hippo Pathway

In recent years an expansion of the Hippo pathway has occurred. Various effectors alter the response of Hippo pathway components. Besides MST1/2, more recently the MAP4Ks (mitogen-activated protein kinase kinase kinase kinase; MAP4K1/2/3/5 and MAP4K4/6/7) are now established LATS1/2 activating kinases (**Figure 2**) [42-45]. Potentially, NF2 mediates LATS1/2 phosphorylation, by-passing MST1/2 by activating MAP4Ks [21, 40, 42]. Recently, the Serine/Threonine Kinase 25 (STK25) has been confirmed as another mechanism of LATS1/2 phosphorylation [46]. STK25 mediates phosphorylation of LATS1/2 and presents a new way of upstream YAP/TAZ regulation [46]. Moreover, LATS1/2 are not the only members of the NDR (nuclear Dbf2 related) kinase protein family capable of phosphorylating YAP (**Figure 2**) [39, 43]. NDR1/2 (also known as STK38/STK38L) are highly conserved across species [47, 48]. NDR1 has been shown to be phosphorylated and therefore activated by MAP4K4 [49]. NDR1/2 phosphorylate YAP in a similar way to LATS1/2 and although NDR1/2 have not yet been proven to phosphorylate TAZ, they provide a LATS1/2-independent and therefore parallel regulation of YAP activity [43, 50]. The complexity and redundancy

of YAP/TAZ regulation enables the Hippo pathway to robustly respond to a large variety of stimuli in a timely, context and spatially specific manner.

Moreover, the classical view of YAP/TAZ being inhibited by phosphorylation is not clear cut. YAP was originally identified as a SRC interacting protein [16]. SRC-induced phosphorylation of YAP (at tyrosine 341, Y357 and Y394) and TAZ (at Y361) is activating (**Figure 2**) [51, 52]. In addition, SRC was shown to inhibit LATS phosphorylation and therefore activates YAP/TAZ via two different mechanisms [53, 54]. Finally, it is worth noting that TEAD transcription factors are not only regulated by the Hippo pathway, but also play a role in other signalling pathways like the Wnt pathway [55]. Likewise, YAP/TAZ regulate gene transcription not exclusively via TEADs [24, 25]. One example is YAP being a co-transcriptional activator for p73 to induce apoptosis [56, 57]. Consequently, accumulating research findings are constantly adding complexity to this central signalling pathway.

1.1.6 The Hippo Pathway: Function and Pathology

Since its discovery, the central role of the Hippo pathway as a regulator of essential functions in the cell and whole organisms became more and more apparent [58]. The importance of YAP and TAZ for the organism has become evident by knockdown and knockout models showing dramatic phenotypes [59]. Although YAP and TAZ have a large number of overlapping functions and in most cases compensate for each other, they are overall not interchangeable [60]. The phenotypes of knockout animals differ largely depending on which of the two co-transcriptional activators is affected. The YAP knockout in animals is lethal (in mice at E8.5), and leads to a shortened body axis and aberrant yolk sac vasculogenesis as well as increased body curvature in zebrafish [59, 61, 62]. Taz (Wwtr1) knockout mice on the other hand are viable and

reach adulthood. However, they die earlier than WT mice as a result of end stage kidney disease caused by renal cysts [63]. Yap/Taz double KO mice are not viable and die before the morula stage [64]. Due to severe consequences on the development and viability the effects of Yap/Taz double knockout in mice is investigated in inducible systems or conditional KO. In zebrafish, *yap/taz* knockout shows sever inhibition of posterior body elongation and leads to death at an early somitogenesis stage [65, 66]. YAP/TAZ transcriptional activity strongly depends on the interaction with TEAD. Thus, point mutations in the TEAD genes, which inhibit the interaction with YAP/TAZ proteins, lead to disease development. One example is the missense mutation at Y421 in TEAD1, which leads to Sveinsson's chorioretinal atrophy resulting in bilateral chorioretinal degeneration [17]. The deficiency of YAP/TAZ is detrimental while their hyperactivation in certain circumstances is potentially beneficial for the organism. For example, studies in the liver and heart showed that the induction of Yap/Taz activity can facilitate organ regeneration [67-69]. After partial hepatectomy, Yap activity increases, which leads to increased proliferation of hepatocytes, whereby the liver regains its original size [19, 70]. However, persistent YAP hyperactivation causes tumour development in multiple organs, including the liver [19, 68]. In general, YAP/TAZ hyperactivation, e.g. by loss-of-function mutations of components of the kinase cascade, is linked to tumour formation and progression [71]. However, intriguingly, only loss-of-function mutations of NF2 occurs frequently in a subset of cancers [72]. NF2 loss leads to YAP/TAZ hyperactivation, which results in disease onset and progression in malignant mesothelioma (prevalence of 40-50%) and schwannoma [72-74]. Increased YAP/TAZ activity is identified in most types of solid tumours, including cancers of the lung, breast and the gastrointestinal tract [75].

The stiffness of cancerous tissues differs from that of healthy tissues and this change affects YAP/TAZ activity [76, 77]. The Hippo pathway, in general, responses to alterations of the extracellular matrix (ECM) compositions [76-78]. Increased stiffness of the extracellular environment triggers a mechanotransductive response of YAP/TAZ and induces their activity [77]. The response of YAP/TAZ to changes of the ECM is linked to the actin cytoskeleton and cell tension, which is key in healthy tissues as it allows YAP/TAZ activation during cell proliferation [77, 79-81]. However, in fibrotic lungs, for example, increased ECM deposition induces nuclear accumulation and activation of YAP/TAZ in fibroblasts, which results in a self-sustaining fibrogenic feed forward loop [82]. Thus, a tight and dynamic regulation of the Hippo pathway is needed to maintain tissues homeostasis and allow controlled regenerative processes.

1.1.7 Regulation of the Hippo Pathway

Due to the central role of the Hippo pathway for multiple cellular processes a flexible and tight regulation of the Hippo pathway is indispensable [21, 83, 84]. The pathway is regulated by both soluble ligands and mechanical stimuli, and the cytoskeleton plays central roles in mediating these responses [2, 71, 77, 80, 85, 86]. Nevertheless, the complexity and context dependency of Hippo pathway regulation remains to be fully elucidated. One example, highlighting the increased molecular understanding of the regulation of the complex Hippo pathway, are G-protein-coupled receptors (GPCRs) [87]. Depending on the coupled G-protein, LATS1/2 are activated or inhibited. For example, the Gα proteins G12/13 are activated by soluble cues (i.e. serum-borne lysophosphatidic acid (LPA) and sphingosine-1-phosphophate (S1P) exposure) and inhibit LATS1/2, which results in YAP/TAZ activation [87, 88]. On the contrary, stimulation of GPCR with epinephrine or glucagon via GαS actives LATS1/2

and leads to the phosphorylation and inactivation of YAP/TAZ [87]. Besides chemical cues, mechanical stimuli are central for the Hippo pathway and YAP/TAZ activity regulation. Those stimuli can be cell intrinsic or extracellular. Small GTPases regulate cytoskeletal dynamics, which in turn influence YAP/TAZ [89]. For example, the RhoA GTPase activates YAP/TAZ by interfering with the activity of the YAP/TAZ inhibitor AMOT. RhoA stabilises the interaction between F-actin and AMOT, which blunts the activity of AMOT. On the other hand, RhoA facilitates the AMOT-induced inhibition of NF2 [89, 90]. Furthermore, cell morphology dependent F-actin stress fibre organisation regulates YAP/TAZ localisation. At low cell density cells are spread and flat and contain many F-actin fibres, while high density cells are more compact and stress fibres are reduced. F-actin fibres induce LATS1/2 activity and therefore YAP/TAZ inactivation [86, 91]. The regulation of the Hippo pathway activity by contact inhibition is a mechanism that contextually controls cell proliferation and tissue size [31, 80]. Finally, the crosstalk between the Hippo pathway, YAP/TAZ and focal adhesions (FA) is a mechanism that allows the cell to sense and respond to multiple mechanical stimuli [79]. YAP/TAZ, for example, regulate FA via activation of Rho-GTPases, which are also integral parts of FA assembly and stability [77, 91]. Integrins are essential FA components and are partly regulated by YAP/TAZ-TEAD. Consequently, loss of YAP/TAZ-TEAD activity dramatically changes the overall cellular composition of integrins [15, 79]. Furthermore, YAP deficiency is associated with disrupted integrin subunit interaction which results in a reduction of FA number [79]. Another consequence of loss of YAP activity is the reduction of expression of FA components vinculin and zyxin, important components mediating linkage of FA with the cytoskeleton [79]. Thus, YAP/TAZ activity is important for FA integrity and the interaction between FA and the cytoskeleton [79]. Besides FA other plasma membrane elements are interacting with YAP/TAZ, like primary cilia, clathrin-coated

pits, clathrin plaques as well as, revealed in this thesis, caveolae. The interaction with plasma membrane elements adds new complexity to the regulation and impact of the Hippo pathway.

1.2 Caveolae

1.2.1 Discovery and Abundance of Caveolae

With the advances in electron microscopy mid of the past century, caveolae structures were first described in 1953. The flask-like membrane invaginations discovered in heart endothelium were named plasmalemma vesicles [92, 93]. Two years later the name caveolae, Latin for “little caves” (*intracellulares*) was used for the first time when describing those uncoated plasma membrane structures found in gall bladder epithelium [92, 94]. The original focused investigations of caveolae were performed by the group, which discovered them, and they concluded that caveolae are part of the endocytic system of the cell [93]. However, it was only in 1992 that CAVEOLIN1 (CAV1) the main structural component and molecular marker of caveolae was discovered [95]. Today, caveolae are no longer seen as key for bulk steady state endocytosis, but are recognised as pleomorphic multifunctional plasma membrane domains [96].

Caveolae are 50-100 nm bulb-shaped structures formed by a 70S complex of protein components (CAVEOLIN1-3 and CAVIN1-4 proteins) (**Figure 3**) as well as various lipid components (cholesterol and glycosphingolipids) [97-99]. The CAVEOLIN/CAVIN oligomere form tissue specific caveolar complexes, which are central for the biogenesis of caveolae. Depending on the cell type, caveolae are

formed by different proportions of CAVEOLIN and CAVIN complexes [98, 100, 101]. CAVEOLIN3 (originally named M-Caveolin) and CAVIN4 are muscle specific caveolar proteins [98, 101]. CAV1 is essential for caveolae formation in non-muscle cells, whereas CAVIN1, formally known as polymerase I and transcript release factor (PTRF), is critical for caveolae formation throughout [102-105]. Furthermore, the overall abundance of caveolae varies significantly not only between healthy and cancerous cells but also between cell types [106]. Caveolae are hardly found in hepatocytes and not present in the kidney proximal tubule [107, 108]. However, they are highly abundant in endothelial cells, adipocytes and myocytes, where they make up large parts of the plasma membrane, pointing towards their increased functional importance for specific cell types [102, 109, 110].

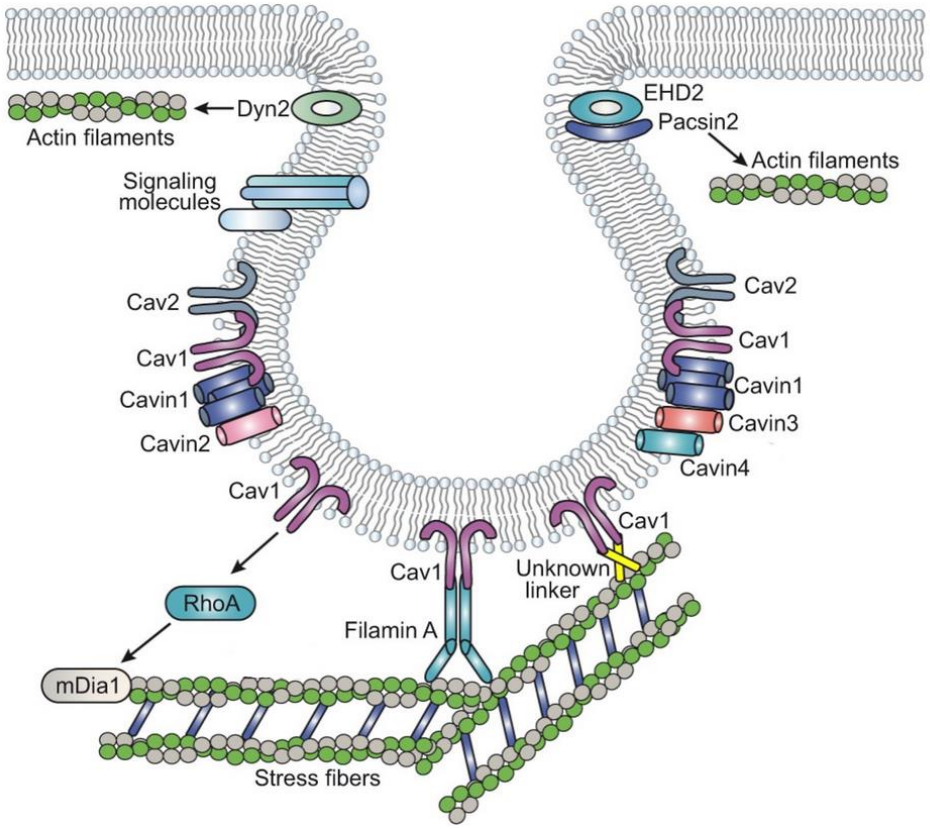

Figure 3: Caveolae.

Structure of caveolae and interactions of caveolar components with cytoskeletal elements. Please see text for more details. Adapted from Echarri and Del Pozo [111].

1.2.2 The Caveolae Structure

The main caveolae components, CAVEOLINs, are integral membrane proteins with both their C- and N-terminal region localised in the cytoplasm [96]. CAVEOLINs have four distinct protein regions; the N-terminus, a conserved scaffolding region, an intramembrane domain as well as the C-terminus, which forms a hairpin structure in the membrane [112]. CAV1 hetero-oligomerises with CAV2 in the Golgi and this complex is transported to and fused with the plasma membrane [113-115]. The C-terminus of CAV1 is palmitoylated while its N-terminus is regulated by SRC-mediated phosphorylation (at tyrosine14) [116, 117] (**Figure 4**). Cav1 by itself is capable of forming caveolae-like structures in bacterial systems [118].

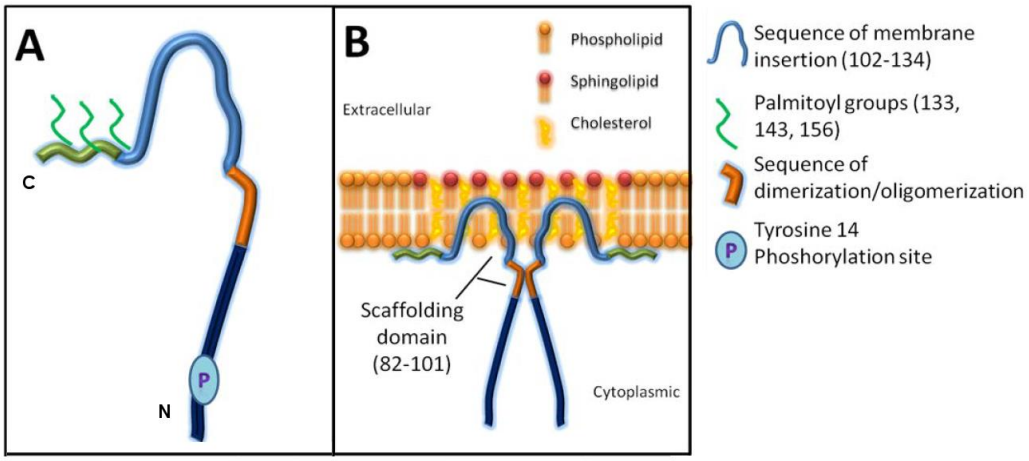

Figure 4: Representation of CAVEOLIN1.

A: Scheme of the CAVEOLIN1 protein domains. **B:** Membrane localisation of CAVEOLIN homodimer in the plasma membrane. Please see text for details. Adapted from Lobos-Gonzalez, et al. [119].

However, in mammalian cells and *in vivo* CAVIN proteins (CAVIN1 in particular) are, essential components of the caveolae bulb [103, 104, 120, 121]. Notably, the stability of CAVIN proteins in non-muscular derived cell types depends on CAV1 expression, CAV1 stability likewise dependents on CAVIN1 expression, indicating the co-dependence of CAV1 and CAVIN1 for caveolae structures [102, 103, 105]. CAVINs form several distinct heterocomplexes, which associates with caveolae to facilitate the stability of the caveolae bulb [102, 122-125]. CAVIN2-4 are CAVIN1 homologs and associates with caveolae only in the presence of CAVIN1. CAVIN2 has high membrane affinity and facilitates stabilisation of CAVIN1 at the plasma membrane [125]. At the neck of caveolae structures EHD (epidermal growth factor receptor substrate 15 [Eps15] homology-domain-containing) accumulate (**Figure 3**) [126-128]. There is a high sequence similarity between EHD1-4, however, it is EHD2, which the most important EHD protein for promotion of caveolar clusters and the mechanoprotective abilities of caveolae [129]. Upon loss of EHD2 proteins, the structure of the bulb remains, however the morphology of the caveolar neck changes [126, 129]. In addition, EHD1, 3 and 4 accumulate at caveolae, especially in EHD2-deficient cells, which might compensate for EHD2 loss [129]. Besides CAVEOLIN, CAVIN and EHD proteins, PACSINs (protein kinase C and casein kinase substrate in neurons proteins) are essential for caveolae stability and morphology. PACSIN2 (also known as SYNDAPIN2) has a BAR domain, which promotes the formation of membrane curvatures [101, 130, 131]. Knockdown of Pacsin2 results in the loss of caveolae structures in fibroblasts and epithelial cells, while knockout of Pacsin3 led

to a reduced number of caveolae in murine muscle cells [126, 130, 132]. In vertebrate cells, these caveolar components are spatially and timely coordinated in order to ensure caveolae formation and stability [96]. Good progress has been made on the molecular details of how these caveolar protein complexes are formed [96, 99, 123], however in great part the biological functions of caveolae and the distinct components of the CAVEOLIN and CAVIN complexes are still not well understood.

1.2.3 Caveolae: Function and Pathology

Caveolae are involved in a large variety of processes. They function in endocytosis, maintenance of the membrane lipid composition and are involved in signalling. Moreover, caveolae are central for mechanosensing and protection from mechanical stress [133, 134].

Although initially described as endocytic elements caveolae do not appear to be crucial cargoes for substances and plasma membrane components within the cells [97]. It is speculated that endocytosis performed by caveolae facilitates the recycling and a dynamic adjustment of caveolae abundance at the plasma membrane [96]. Moreover, as highly specialised plasma membrane domains, caveolae exhibit a specific profile of lipids compared to other regions of the membrane with increased glycosphingolipids and cholesterol content [135]. The palmitoylation sites CAV1 possesses as well as its scaffolding domain are important for cholesterol binding [117, 136-138]. CAVINs have lipid-binding properties themselves, e.g. binding of phosphatidylserine or phosphoinositide [124, 125, 139]. As a consequence, lack of caveolae results in different types of lipodystrophy [96]. Patients with non-functional CAV1 develop congenital generalised lipodystrophy (CGL), a rare genetic disorder, which is characterised with a nearly total loss of body fat [140]. Similarly, Cav1 KO

mice are leaner and have smaller adipocytes and lipid droplets emphasising the importance of Cav1 for lipid homeostasis [141]. In addition, the loss-of-function mutation of CAVIN1 is linked to lipodystrophy in patients [142].

Caveolae interact with various signalling pathways. They play roles in cell growth, migration, survival and death as well as various cancer-associated processes [143]. The main caveolae component, CAV1, for instance has been reported to interact with the K-RAS oncogene, Rho GTPases, G proteins and their receptors as well as a range of kinases, like SRC or protein kinase A [144-148]. However, detergent insolubility and the resistance to extract caveolae without harsh detergents, make interaction studies challenging [134, 149]. Only recently the *in vitro* analysis of isolated caveolae was successful and promises new insight into the interactome of caveolae [150].

Mechanical stress triggers remodelling of the actin cytoskeleton and the plasma membrane. Caveolae provide membrane plasticity, which allows the cell to accommodate changes in tension [111]. The membrane invaginations associate with actin stress fibres, which regulate their organisation and trafficking [95, 111, 151-153]. The significance of the cytoskeleton for caveolae is indicated by the fact that caveolar curvature depends, besides on cholesterol, on stress fibres [95, 111, 154, 155]. An excess in stress fibres leads to increased membrane tension and is accompanied by increased accumulation of CAV1 at the plasma membrane as well as caveolae flattening [151, 156, 157]. The physical interaction of caveolae and stress fibres is assumed to depend at least partly on the actin cross linker filamin A [155, 158, 159]. Besides Filamin A, EHD2 might be another element linking caveolae with stress fibres as EHD2 silencing increases CAV1 motility [127]. Another protein which is localised at the neck of caveolae is DYNAMIN2 (DYN2). It regulates actin polymerisation and caveolar endocytosis [151, 152, 160]. Furthermore, CAV1 activates RhoA and

therefore a signalling pathway which is central for mechanotransduction and the control of actomyosin contractility [111, 161]. RhoA mediates force-induced cytoskeletal reorganisation, a process which requires CAV1 [162]. RhoA silencing results in reduced alignment of stress fibres with CAV1 [152]. Thus, caveolae are tightly interlinked with the cytoskeleton to sense and regulate responses to mechanical stimuli. One cell type which experiences persistent mechanical stress and shows a high abundance of caveolae are endothelial cells. For example, up to 70% of the plasma membrane in alveolar endothelium is covered by caveolar [163-165]. CAV1 is a key feature of the vascular system, where it plays a role in the nitric oxide pathway to regulate contractility of vessels and capillary tubule formation [98, 166-168]. As a consequence, it is not surprising that upon loss of Cav1, mice develop hypertrophic cardiomyopathy leading to heart failure as well as lung fibrosis with pulmonary arterial hypertension (PAH) [140]. In the endothelium, CAV1 deficiency induces a constitutive hyperactivation of the nitric oxide pathway, which is important for regulation of blood pressure [169, 170]. Therefore, the high number of caveolae in endothelial cells is not coincidental. The blood flow in vessels exhibits a constant mechanical force on the endothelium, termed shear stress. In this process, caveolae do not only influence the remodelling of blood vessels but also harbour mechanoprotective properties [110, 171-173]. Under severe cell stretching caveolae appear to flatten in order to increase the surface to volume ration of the cell and therefore protect the cell from bursting [174]. Upon flattening of the caveolae bulb caveolar components, e.g. CAVINs and EHDs, are released from the bulb into the cytoplasm [109, 173, 174]. Part of dissociated EHD2 accumulates in the nucleus and induces transcription of genes involved in receptor interactions with the extracellular matrix (ECM) as well as genes of the TNF-α or K-Ras pathways [153, 175]. Cytoplasmic CAVIN complexes interact with CAVEOLIN complexes at the plasma

membrane and regenerate the full morphological caveolae structures [153]. Caveolae influence the composition and homeostasis of the ECM. Cav1 knockout in mammary glands induced the expression of ECM components, e.g. fibronectin and collagen, resulting in an increased ECM stiffening [176]. Deficiency of Cavin1 in adipocytes also increased the expression of fibronectin and collagen [177]. Similar results were obtained in murine fibroblasts, when Cav1 knockout induced elastin and collagen expression [178]. This can, at least partly, be explained by the co-dependence of protein stability between CAV1 and CAVIN1, as the deficiency of CAV1 destabilises CAVIN1 [102, 105, 125]. As a consequence, Cav1 KO mice show increased prevalence of lung fibrosis due to the fact that Cavin1 no longer inhibits collagen and fibronectin expression [179]. Accordingly, CAVIN1 loss-of-function mutation leads to cardiac fibrosis as well as morphological and functional impairments of the lung and muscular dystrophy [142, 180, 181]. Also, dysregulation of CAVEOLIN3 expression is characteristic in different muscle disease phenotypes, e.g. limb gridle muscular dystrophy, rippling muscle disease, hyperCKemia, cardiomyopathy, distal myopathy or Duchenne muscular dystrophy [167, 182, 183]. Furthermore, CAVEOLIN3 was to be central for myotube formation and is therefore functionally important in skeletal muscles [184]. In conclusion, caveolae are distinctive versatile and pleomorphic plasma membrane organelles, which enable the cell to respond to a large variety of stimuli in a flexible manner.

1.3 Mechanotransduction

1.3.1 Types and Functions of Mechanotransduction

Cells constantly experience at least one type of mechanical force, as they are exposed to gravity, adhesion, pressure, tension or shear stress. These physical stimuli trigger cellular reactions allowing the organism to respond and adapt to changes of their environment [185]. The translation of physical forces into biochemical signals by a tightly structured signalling network is called mechanotransduction [185-187]. The cellular response is diverse and ranges from proliferation and angiogenesis to differentiation and apoptosis [186, 188, 189]. Flow and shear stress are major forms of mechanical cellular stimuli. The blood flow in vascular systems exposes endothelial cells to stretching forces, hydrostatic pressure and most importantly tangential forces in the form of shear stress [190]. Flow is predominantly considered laminar, without turbulences or mixture and occurs mostly in straight arterial regions. On the other hand, turbulent or oscillatory flow occurs in branched or curved vessels and induces besides laminar also random movements [190]. Shear stress is the frictional force in the endothelium generated by blood flow and expressed in force-area unit (Dyn/cm^2). The strength of shear stress strongly depends on the vessel type and the quality of flow, ranging for example from one Dyn/cm^2 in smaller venous areas to 30 Dyn/cm^2 in greater arteries [191]. As the quality of shear stress is so variable a timely and adaptive response is needed. This cellular response is achieved by a wide range of sensors and integrative pathways that coordinate subcellular signalling processes [185]. In endothelial cells a range of proteins and plasma membrane domains are central mechanosensors and are capable in adapting to changes in shear stress; examples are adhesion molecules like PECAM1 (Platelet Endothelial Cell Adhesion Molecule 1), receptor 2 for VEGF (Vascular Endothelial Growth Factor), ion channels

and caveolae [192, 193]. Moreover, shear stress affects the cytoskeleton, which by itself may act as a mechanosensor and transducer enabling the cell to sense and respond to complex mechanical stimuli [165, 189].

1.3.2 Mechanotransduction: A Possible Link Between the Hippo Pathway and Caveolae

Both the Hippo pathway and caveolae are regulated by mechanical stimuli, including shear stress [21, 58, 78, 194]. Importantly, how mechanical signals are sensed at the plasma membrane and transduced via the Hippo pathway is currently not well understood. As caveolae are important mechanosensors and protectors, further understanding of their overall function as mechanotransducers, including the downstream effectors are warranted [96, 111]. Since both the functional regulation of the Hippo pathway and caveolae are still not fully understood, I sought to investigate whether the Hippo pathway and caveolae are functionally integrated in the process of sensing shear stress. Elucidating the regulation of the Hippo pathway of and by caveolae in connection to mechanical stimuli reveals insights into clinically important processes and enhances our knowledge of tissue growth dysregulation and differentiation.

2. Hypothesis and Aims

Given that both the Hippo pathway and caveolae are capable of sensing mechanical stress, the central hypothesis of this thesis is that ***there is a mutual, regulatory interaction between caveolae and the Hippo pathway*** which impacts the ability of cells to sense shear stress.

Consequently, this thesis aims to:

1. **Assess whether components of caveolae and their abundance depend on YAP/TAZ**
2. **Determine whether YAP/TAZ activity is influenced by caveolae**
3. **Determine the potential regulation of YAP/TAZ by caveolae in the response to shear stress**

3. Materials and Methods

Parts of this section have been taken from Rausch, et al. [195] and adapted with the consent from authors.

3.1 Mammalian Cell Culture and Cell Lines

3.1.1 General Cell Culture

All cell lines were cultivated at 37°C in a humidified, 5% CO_2 atmosphere. HEK 293A, HEK 293T and U2OS cells were cultivated in high glucose DMEM (Gibco) supplemented with 1% penicillin/streptomycin (v/v), 2 mM glutamine, and 10% fetal bovine serum (FBS) unless stated otherwise. The HEK 293A and HEK 293T cell lines are human epithelial cells originating from embryonic kidney of a female. The wildtypes (WT) as well as the HEK 293A YAP/TAZ and LATS1/2 double knockout cell lines were kindly provided by Professor Kun-Liang Guan lab, University of California, San Diego (UCSD) [196, 197]. HEK 293A cell lines were used to perform experiments while HEK 293T cells where used for virus generation. The U2OS cell line originates from human epithelial from the bone of a female suffering from osteosarcoma. The U2OS wildtype was kindly provided by Professor Jack Dixon (UCSD). Cells were periodically tested with the MycoZap kit (Lonza, cat# LT07-818) by A.F. Howie (University of Edinburgh, UoE) for mycoplasma contamination but were not authenticated.

Generation of Stable Knockdown (KD), Knockout (KO) and Re-Expression Cell Lines

KD cell lines were generated by retrovirus mediated shRNA knockdown. The virus was generated in HEK 293T cells which were seeded into a 6-well the day before transfection to reach a confluency of about 70-80%. Using the GenJet transfection reagent (SignaGen Laboratories) the cells were co-transfected with pMD2G (200 ng/well) and pSPAX2 (400 ng/well) plasmids (from the Kun-Liang Guan lab, UCSD) and with pKLO.1-vectors (400 ng/well) coding for shRNAs targeting YAP, TAZ and TEADs 1/3/4 (construct #1 and #2) [15, 197] as well as of CAV1 (construct #1 and #2) and CAVIN1 (construct #1 and #2), see Table 1.

Table 1: Constructs used for shRNA-mediated knockdown

Construct	Source	Identifier
pMD2.G	Professor Kun-Liang Guan lab (UCSD)	N/A
pSPAX2	Professor Kun-Liang Guan lab (UCSD)	N/A
pLKO.1	Professor Kun-Liang Guan lab (UCSD)	N/A
shRNAScramble	Sigma-Aldrich	see [15]
shRNA YAP	Sigma-Aldrich	TRCN0000300325
shRNA TAZ	Sigma-Aldrich	TRCN0000370007
shRNA CAV1 #1	Sigma-Aldrich	TRCN0000007999
shRNA CAV1 #2	Sigma-Aldrich	TRCN0000008002
shRNA CAVIN1 #1	Sigma-Aldrich	TRCN0000430242
shRNA CAVIN1 #2	Sigma-Aldrich	TRCN0000446514
shRNA TEAD1/3/4 #1 and #2	Professor Kun-Liang Guan lab (UCSD)	see [15]

All shRNA constructs carry the pLKO.1 backbone (puromycin selection)

48 hours after transfection, the virus was harvested by aspirating and filtering (low binding syringe filters, Corning #431220) the medium of the transfected cells. The cells of interest were seeded the day before and the medium was exchanged with fresh 10 µg/ml polybrene containing medium shortly before adding 50-100 µl of virus solution to each well. Following a 6-8 hours

incubation the cell medium was changed. Stable cell lines were generated following puromycin (1 µg/ml) selection.

The generation of CRISPR/Cas9-mediated KO cell lines is depicted in **Figure 5**. At first, two sets of complementary oligo nucleotides containing the sgRNA (single guide RNA) were annealed. Thereafter, they were ligated into a linearised pSpCas9(BB)-2A-Puro (PX459 *V2.0*, Addgene #48139) plasmid at the BbsI restriction site, to generate the different KO vectors. The generated plasmids were inserted into Dh5α *E.coli* bacteria. After transformation separate bacteria colonies were picked and plasmids were extracted after propagation (as in 3.4.1). Vectors with the correct insertion of the sgRNA were identified by sequencing (performed by Source BioScience).

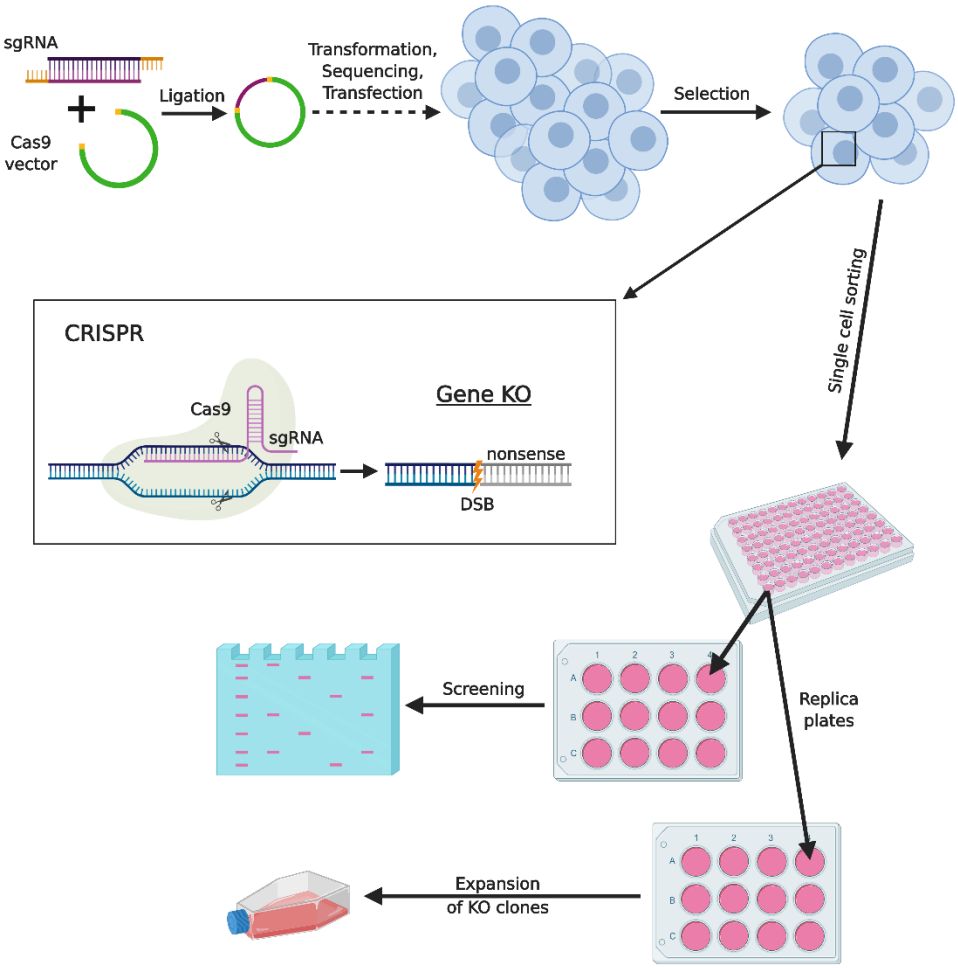

Figure 5: Generation of CRISPR/Cas9-mediated KO cell lines.

For details on the procedure please refer to text. The generated DNA double stand break (DSB) by the RNA-guided nuclease Cas9 is repaired mostly by non-homologous end joining which can result in a nonsense mutation and the inactivation of the gene function, which equals a KO.

Guide sequences were designed using http://crispr.mit.edu. For YAP and TAZ KO, previously generated constructs were used [197]. CRISPR sgRNA oligos are listed in Table 2. The CAV1 KO sgRNAs target sequences in the second exon of the human CAV1 gene (**Figure 6**).

Table 2: Guide sequences utilised for CRISPR/Cas9-mediated knockout (5' → 3')

Target	Forward Primer	Reverse Primer
CAV1#1	CACCGAGTGTACGACGCGCACACCA	AAACTGGTGTGCGCGTCGTACACTC
CAV1#2	CACCGTTTAGGGTCGCGGTTGACC	AAACGGTCAACCGCGACCCTAAAC
YAP#1	CACCGCATCAGATCGTGCACGTCCG	AAACCGGACGTGCACGATCTGATGC
WWTR1 (TAZ)#1	CACCGTGTCTAGGTCCTGCGTGACG	AAACCGTCACGCAGGACCTAGACAC
NF2	CACCGTCCATGGTGACGATCCTCA	AAACTGAGGATCGTCACCATGGAC

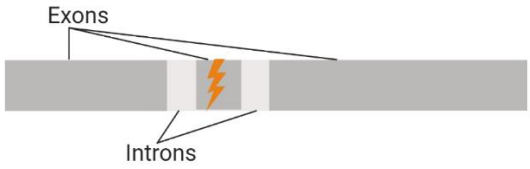

Figure 6: Recognition site of the sgRNA for CRISPR/Cas9-mediated CAV1 KO.

Representation of the human CAV1 gene. Dark grey: Exons. Light grey: Introns. Arrow: Localisation of the sequence complementary to the sgRNA oligoes of CAV1#1 and #2 as in Table 2.

Cells were transfected with the PX459 plasmid, containing the annealed sgRNA guide sequence, using LipoD293 or GenJet transfection reagent (SignaGen Laboratories). Clonal YAP, TAZ (WWTR1) and CAV1 KO cell lines were generated by transient transfection of CRISPR constructs, followed by two days of puromycin (1 µg/ml) selection and one day recovery in medium without puromycin. Subsequently, cultures were single cell sorted into 96-well plates by means of the BD FACS Aria II (with the assistance of the QMRI flow cytometry team, UoE) containing DMEM supplemented as above however with 20% FBS to improve cell survival. Five to ten 96-well plates pre construct were prepared. Weekly, plates were checked for colony formation and evaporated

medium was replaced with fresh medium. After two to four weeks single cells formed colonies. Separately, colonies were detached from the 96-well plate using trypsin and 1/3 of the cell suspension was transferred into one and the remaining 2/3 were seeded into a second 24-well plate. In these two replicate plates single cell cultures were expanded and screened for positive knockouts by Western blot analysis. In detail, cells of one of the replica plates were prepared for protein lysates and expression of the protein of interest was analysed on a full-length Western blots, in order to check for truncated proteins, as in **Figure 7**. In addition, and if available, several antibodies recognising distinct parts of the targeted proteins were used. Positive knockout clones were transferred from the remaining replica plates and expanded.

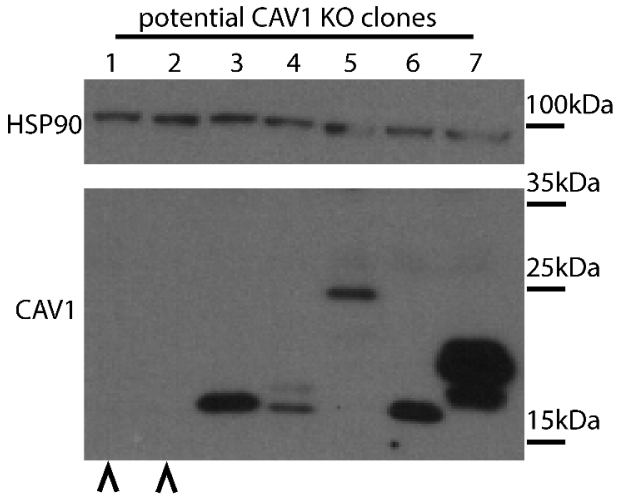

Figure 7: Example of KO clone screening.

Example Western blot of the screening of CAV1 KO clones. Clone1 and 2 are potential CAV1 KO (indicated by arrow heads). Their cultures in the replica plate were expanded and used for experiments. HSP90 served as loading control.

To generate U2OS CAV1 re-expressing cell lines, shCAV1 cells were transfected with CAV1-GFP plasmid (#14433, Addgene) and stable exogenous CAV1-expressing cells were established by G418-selection (1 mg/ml). Plasmids encoding either myc-

tagged WT or mutant YAP (S94A flag-tagged or 5SA myc-tagged) as well as flag-tagged WT or mutant TAZ (S51A flag-tagged) are listed in Table 3. HEK 293A CAV1 re-expressing cell lines were generated by lentiviral transduction of CAV1 KO cells with a pBabe vector carrying the open reading frame of human CAV1. Furthermore, HEK 293A LATS1/2 KO cells transfected with plasmids carrying LATS1 WT or K/R kinase loss-of-function mutant and cell lines were established by hygromycin B selection (4 µl/ml). Please note, the exogenously expressed constructs were not normalised to WT expression levels.

Table 3: Re-expression plasmids used

Target	Source	Identifier
Cav1-GFP	Originally from Ari Helenius (Addgene #14433)	N/A
pBabe-CAV1	This study (generated by GeneWIZ)	N/A
pBabe	Addgene	#1764
CAVIN1-mCherry	Doctor B. Nichols Lab Cambridge University	see [125]
pCMV Flag-YAP	Professor Kun-Liang Guan lab San Diego (UCSD)	see [15]
pQCXIH-Myc-YAP (S5A)	Professor Kun-Liang Guan lab, (UCSD) (Note, also encodes S128A, S131A, and S163A) (Addgene #48139)	N/A
pQCXIH-Myc YAP	Addgene	#33091
pQCXIH-Myc YAP S94A	Addgene	#33094
pBabe-Flag TAZ (WT)	Professor Kun-Liang Guan lab (UCSD)	N/A
pBabe-Flag TAZ (S89A)	Professor Kun-Liang Guan lab (UCSD)	N/A
pQCXIH-HA LATS1 (WT)	Professor Kun-Liang Guan lab (UCSD)	N/A
pQCXIH-HA LATS1 (K/R)	Professor Kun-Liang Guan lab (UCSD)	N/A

3.1.2 BOEC (Blood Outgrowth Endothelial Cells) Isolation, Differentiation and Culture of Primary Endothelial Cells

Isolation of endothelial progenitor cells from human blood and subsequent differentiation was performed following a recently established protocol [198]. Briefly, 60 ml of whole human blood were diluted 1:1 in phosphate-buffered saline without calcium and magnesium (PBS, Gibco), layered over a density gradient solution (Ficoll-Paque Plus, GE Healthcare) and centrifuged. The buffy coat and about 2/3 of the plasma were transferred into a fresh tube, diluted 1:1 with PBS and centrifuged. The resulting pellet was resuspended in 7.5 ml EGMTM-2 Endothelial Cell Growth Medium-2 (cat# CC-3162; complete, with 20% FBS and no penicillin/streptomycin) and seeded into a collagen-coated T75 flask (Corning, #354236). The medium was exchanged every other day until colonies became visible.

Primary endothelial cells were cultured in T25 flasks (Corning, without additional coating) and kept in EGMTM-2 Endothelial Cell Growth Medium-2 and passaged once to twice a week.

3.2 *In vitro* Assays

3.2.1 Verteporfin Treatment of Cell Lines

HEK 293A WT cells were seeded into 6-wells and the next day treated with 6.45 µM verteporfin (Sigma) with 1.87% (v/v) dimethyl sulfoxide (DMSO, Sigma) or DMSO

only. After 18 hours, mRNA was extracted using the RNase kit (QIAGEN, cat#74136), and RT-qPCR was performed as described in 3.3.2.

3.2.2 Soft Agar Colony Formation Assay

2x DMEM was supplemented with 20% FBS, 2% penicillin/streptomycin and 2% L-glutamine. In 6-well plates (Corning) a bottom layer of 1% agarose (w/v in H_2O) mixed 1:1 with 2x complete DMEM was poured. For the top layer 5000 cells (per well) were added to 2x DMEM supplemented with 1.7 g/l $NaHCO_3$ (Roth) and mixed with 0.7% warm agarose. The agarose cell mix was carefully pipetted on top of the bottom layer. After solidification at room temperature 0.5-1 ml of 1x complete DMEM was added per well. Cells were transferred to a cell incubator and cultivated under standard cell culture conditions. Medium was exchanged once to twice per week. Eight weeks after seeding cells were fixed and stained with 0.005% crystal violet in methanol (Thermofisher) overnight. After methanol-destaining of the agarose, abundance of colonies was documented by a Leica M205 fluorescence stereo-microscope at a magnification of 10x (for representation) and 50x (for quantification). The number of colonies (of at least 50 µm in diameter) per well were quantified manually by means of ImageJ and numbers of colonies were analysed using GraphPad (Prism).

3.3 Molecular and Biochemical Assays

3.3.1 Western Blotting

Cell lysates were prepared by lysing cells in reducing lysis buffer (200 mM Tris pH6.8, 8% SDS, 0.1% bromophenol blue, 40% glycerol, 20% beta-mercaptoethanol). Samples were hereafter transferred to a 1.5 mL Eppendorf tube and boiled at 95°C

for 10 min. If samples were not run straight away, they were stored at -20°C. SDS gels of a thickness of 1 mm were casted in glass plates. Resolving gels of 7-12% SDS were prepared by mixing 375 mM Tris (pH8.8), 0.1% (w/v) SDS, 0.1% (w/v) APS, 0.08% (v/v) TEMED and the appropriate amount of water and acrylamide. Following polymerisation of the resolving gel, about 1 ml of stacking gel (composition as above, however at 5% SDS and made up with 520 mM Tris, pH6.8) was poured on top of it and a 15-well comb was inserted into the stacking gel before polymerisation. Samples were loaded onto the gels and the PageRuler pre-stained protein ladder (cat# 26616, Fisher Scientific) was used to determine protein sizes. Gels were run at 100V using the Bio-Rad system and running buffer (24.8 mM Tris, 189.5 mM Glycine, 0.1% [w/v] SDS). Subsequently, proteins were “wet” transferred onto a methanol-activated polyvinylidene difluoride (PVDF) membrane (Sigma). Pre-chilled (4°C) transfer buffer (25 mM Glycine, 190 mM glycine, 20% [v/v] methanol) was used and transfer was conducted at 0.5mA for 80 minutes in the cold room. The membrane was then incubated in 5% milk/TBS-T blocking solution (TBS-T: 20 mM tris [pH7.5], 150.6 mM NaCl, 0.1% [v/v] TWEEN20) for 45 minutes, briefly rinsed with TBS-T, cut and incubated with the appropriate antibodies (diluted in 5% BSA/TBS-T) overnight at 4°C at low agitation. Antibodies used for Western blotting are listed in Table 4. The next day membranes were washed in TBS-T for 2x 10 minutes and 1x 15 minutes. Followed by an incubation in HRP-conjugated secondary antibodies (listed in Table 4) diluted 1:10,000 in 5% milk/TBS-T for 1 hour. After washing as above blots were developed using Immuno Western ECL mix (Millipore), X-ray films (SLS) and an X-ray developer Ecomax (Photon imaging systems). Besides conventional SDS gels Western blotting was performed with Phos-Tag gels. Therefore, 15 µl Phos-Tag reagent (Wako chemicals) and 25 µl of 10 mM $MnCl_2$ were added to each 7.5% (w/v) polyacrylamide gel while the subsequent steps remained the same. For densitometric

quantification of protein levels with ImageJ and the value of the protein of interest was normalised to the loading control of the same lane.

Table 4: Antibodies used for Western blotting

Target	Dilution	Source	Identifier
Anti-YAP/TAZ	1:1000	Santa Cruz Biotechnology	Cat# sc-101199
Anti-CYR61	1:1000	Santa Cruz Biotechnology	Cat# sc-13100
Anti-CTGF	1:1000	Santa Cruz Biotechnology	Cat# sc-14939
Anti-GAPDH	1:10,000	Santa Cruz Biotechnology	Cat# sc-25778
Anti-CAV1	1:1000	BD Biosciences	Cat# BD610060
Anti-CAV2	1:500	BD Biosciences	Cat# BD610684
Anti-HSP90	1:10,000	BD Biosciences	Cat# BD610418
Anti-panTEAD	1:1000	Cell Signaling Technology	Cat# 13295
Anti-YAP p127	1:1000	Cell Signaling Technology	Cat# 4911S
Anti-YAP p397	1:1000	Cell Signaling Technology	Cat# 13619
Anti-NF2	1:1000	Cell Signaling Technology	Cat# 6995S
Anti-LATS1	1:1000	Cell Signaling Technology	Cat# 3477
Anti-LATS2	1:1000	Cell Signaling Technology	Cat# 5888
Anti-CAVIN1	1:1000	Cell Signaling Technology	Cat# 69036
Anti-YAP	1:1000	Abcam	Cat# ab52771
Anti-YAP (active)	1:1000	Abcam	Cat# ab205270
Anti-GFP	1:1000	Abcam	Cat# ab6556
Anti-CAVIN3	1:1000	Bethyl	Cat# A302-419A
Anti-CAVIN2	1:1000	Atlas Antibodies	Cat# HPA039325
Anti-Myc	1:1000	Cell Signaling Technology	Cat# 2276
Anti-VA-Cadherin	1:1000	Santa Cruz Biotechnology	Cat# sc-1506
Anti-PECAM1	1:1000	Cell Signaling Technology	Cat# D87F2
Anti-Goat IgG/HRP	1:10,000	DAKO	Cat# P044901
Anti-Rabbit IgG/HRP	1:10,000	DAKO	Cat# P044801
Anti-Mouse IgG/HRP	1:10,000	DAKO	Cat# P044701

3.3.2 Quantitative Reverse Transcription PCR (RT-qPCR) and Primers

For RT-qPCR mRNA was extracted from cells using the RNeasy plus mini kit (QIAGEN) and quantified using the Nanodrop. Complementary DNA (cDNA) was generated using High-Capacity cDNA Reverse Transcriptase kit (Applied Biosystems). qPCR was performed on 1 ng of cDNA using the Brilliant III Ultra-Fast SYBR® Green QPCR Master Mix (Agilent Technologies) and the LightCycler® 96 System (Roche) according to manufactures instruction. In mammalian cells expression levels of all genes analysed were normalised to Hypoxanthine-guanine phosphoribosyltransferase (*HPRT1*) levels. Human specific primers (5 µM per primer per reaction) against *YAP*, *TAZ, CYR61, CTGF, TEAD1, CAV1, CAVIN1* and *HPRT1* were used. Primer sets against caveolar components *CAV1* and *CAVIN1* were designed using primerbank [199], the remaining were taken from Hansen, et al. [197]. Methods to harvest and prepare cDNA from zebrafish embryos were performed by Jonathon R. Bostrom (Link lab, Medical College Wisconsin [MCW]) and have previously been reported [66, 200]. I performed the qPCR analysis zebrafish cDNA as described above, while expression levels were normalised to Elongation factor 1-alpha (*ef1a*) [66]. Sequences of primers are listed in Table 5.

Table 5: Sequences of primers used for RT-qPCR (5' → 3')

Target	Forward Primer	Reverse Primer
CAV1	GCGACCCTAAACACCTCAAC	ATGCCGTCAAAACTGTGTGTC
cav1 fish	CGATGTGGTGAAGGTGGACTTT	TCAGCAGCCTGTAGCACCAAT
CAVIN1	GAGGACCCCACGCTCTATATT	CCCCGATGATTTTGTCCAGGA
cavin1b fish	AAACGTCTGGAGAGCAACGAGA	GCCACA TTCACTTTCGAACCC
CTGF	CCAATGACAACGCCTCCTG	TGGTGCAGCCAGAAAGCTC
ctgf fish	CTGCACAGCCAGAGATG	CACTTCCCAGGCACTTT
CYR61	AGCCTCGCATCCTATACAACC	TTCTTTCACAAGGCGGCACTC
cyr61 fish	CCGTGTCCACATGTACATGGG	GGTGCATGAAAGAAGCTCGTC
ef1a fish	TCTCTCAATCTTGAAACTTATCAATCA	AACACCCAGGCGTACTTGAA
TEAD1	ATGGAAAGGATGAGTGACTCTGC	TCCCACATGGTGGATAGATAGC
YAP	CCAAGGCTTGACCCTCGTTTTG	TCGCATCTGTTGCTGCTGGTTG
TAZ (WWTR1)	AATGGAGGGCCATATCATTCGAG	GTCCTGCGTTTTCTCCTGTATC
HPRT1	AGAATGTCTTGATTGTGGAAGA	ACCTTGACCATCTTTGGATTA

If not stated otherwise, primers are specific to human genes. All primers have been obtained from Integrated DNA Technologies, Inc.

3.3.3 Chromatin Immunoprecipitation qPCR (ChIP-qPCR)

ChIP was performed on HEK 293A cells using the ChIP-IT® Express Enzymatic kit (Active Motif Inc.). For immunoprecipitation anti-mouse IgGs (#12102270, Fisher Scientific), anti-rabbit IgGs (#11805935, Fisher Scientific), anti-TEF-1 (TEAD1, #610923, BD Bioscience) and anti-YAP (ab52771, Abcam) antibodies were used. Subsequent DNA clean up (by DNA Clean & Concentrator™-5, Zymo Reseach) was followed by DNA quantification by qPCR analysis and output was normalised to the input DNA. Primers specific to sequence of the promoter of *CAV1* promoter (*CAV1*

prom) or *CAVIN1* promoter (*CAVIN1 prom*) as well as for regions within the genes, *CAV1* in gene (*CAV1 ingene*) and *CAVIN1* in gene (*CAVIN1 ingene*), were used to quantify the yield of the ChIP. *CTGF (CTGF prom)* was used as a control. For primer sequences please refer to Table 6.

Table 6: Sequences of primers used for qPCR (5' → 3') (ChIP)

Target	Forward Primer	Reverse Primer
CAV1 prom	TGGCATAACCTGTTGGCATA	CCCAAACGCTTCGAAATAAG
CAV1 ingene	CCTCCGTGTCTCAGTGGTTT	TCACCTTGCTTGCCTTTCTT
CAVIN1 prom	TTTCAGAATCTCCTGGTCCAC	TTGCTCTCTGTTTCCCTCTCA
CAVIN1 ingene	GCAGTTTTGAGGAGGCAAAG	AAATGCTTCCTGGCCCTTAT
CTGF prom	CTTTGGAGAGTTTCAAGAGCC	TCTGTCCACTGACATACATCC

3.3.4 Proximal Promoter Cloning and Luciferase Assay

The sequence of the upstream proximal promoter regions of *CAV1* and *CAVIN1* were obtained from http://genome.ucsc.edu and examined for M-CAT, muscle-specific cytidine-adenosine-thymidine sequence (CATTCC-A/T) and predominant TEAD binding site, and putative TEAD (G/A-G-A/T/C-ATG) binding motifs [201]. gDNA was isolated from MeT5A cells and used to amplify the sequences of the promoter regions of both CAV1 and CAVIN1 (primers see Table 7). pGL3-basic vectors carrying upstream proximal promoter regions of either CAV1 (-1800 to +200bp) or CAVIN1 (-1250 to +150bp) were generated by restriction cloning and insertion into the multiple cloning site using Mlu1/Xho1 (*CAV1*) or Kpn1/Mlu1 (*CAVIN1*) respectively. A short

version (-500 to +200bp) of the *CAV1* promoter was also generated, which does not harbour any predicted TEAD recognition sites. Sequences and orientation of the insert in the vector were verified by Sanger sequencing (performed by Source BioScience). HEK 293A YAP/TAZ KO cells were seeded into a 12-well plate ($1x10^5$ cells/well) and two days later co-transfected with one of the plasmids above, renilla plasmid and pCMV Flag-YAP using GenJet transfection reagent. 36-48 hours after transfection cells were lysed using lysis buffer (91.5 mM K_2HPO_4, 8.5 mM KH_2PO_4, 0.2% Triton-X-100 [v/v], 1 mM DTT, 1 mM PMSF) and lysates were transferred into a white 96-well plate (Corning). Luminescence was induced by using the Dual-Glo® luciferase assay system (Promega) and was detected by a Biotek HT plate reader. Luciferase activity was normalised to renilla signal.

Table 7: Primers used for cloning plasmids carrying promoter regions

Target	Sequence
CAVIN1 (-1250)	TAAGGTACCCCCCGGGTTCAAGTGATT
CAVIN1 (+150)	TTATGACGCGTGGAAGGGAGGAGAGCTAGC
CAVEOLIN1 (-1800)	TTATGACGCGTCTGCAGTGACCTATGAATGCA
CAVEOLIN1 (-500)	TTATGACGCGTCTTATTTCGAAGCGTTTGGG
CAVEOLIN1 (+200)	TTATGCTCGAGGTATTGTATGGGGGGAAAAAAAG

3.3.5 Flow cytometry Analysis

Intracellular labelling of proteins and analysis of their expression on a single cell basis was performed by flow cytometry assay. BOECs and HEK 293A cells were trypsinised

and resuspended in medium, centrifuged, washed once with 1x PBS (without calcium and magnesium), centrifuged again and washed a second time with FACS buffer (0.5% BSA, 0.2 mM EDTA in PBS). The cell number was determined and $1.5x10^5$ cells/well were seeded into a round-bottom 96-well plate (Corning). The plate was centrifuged at 300 g for 5 minutes and the FACS buffer was discarded. Cells were resuspended in 100 µl Zombie aqua (#423101, BioLegend) solution (1:100 in 1x PBS) and incubated for 10 minutes in the dark. The plate was centrifuged, as before, and cells were washed once with 150 µl PBS per well. PBS was discarded and cells were resuspended in 100 µl of Fix/Perm solution (1:3 concentrate [#00-5123-43] in diluent [#00-5223-56], Invitrogen). The plate was wrapped in tin foil and cells were incubated overnight at 4°C. The next day, the plate was centrifuged, and cells were washed twice with 1x permeabilisation buffer (from 10x [#00-8333-56] diluted in PBS, Invitrogen). Subsequently, cells were incubated in 100 µl/well blocking solution (5% goat serum [sigma] in 1x permeabilisation buffer) for 10 minutes in the dark at room temperature. Without removing the blocking solution, 50 µl of primary antibody solution, at a final dilution of 1:100 (in permeabilisation buffer), were added per well. Antibodies against CAV1 (#BD610060), VE-Cadherin (#D87F2) and PECAM1 (#SC1506) were used (see also Table 8). After 30 minutes of incubation in the dark, the plate was centrifuged, and cells were washed twice with permeabilisation buffer. 100 µl/well secondary antibody solution were added (anti-mouse AF647 [#1030-31, SouthernBiotech] or anti-rabbit AF647 [#Z25308, Invitrogen] diluted 1:400 in permeabilisation buffer). In the dark, the cells were incubated for 30 minutes with secondary antibodies. Afterwards the cells were washed two more times in permeabilisation buffer and finally resuspended in 100 µl FACS buffer. For analysis the cells were transferred into FACS tubes and resuspended in additional 150 µl of FACS buffer. The flow cytometry analysis was performed on the 5 LSRFortessa (BD

Biosciences) and with the assistance of Shonna Johnston (UoE). The gating was as follows; side scatter area vs forward scatter area (SSC-A/FSC-A) to identify cells. forward scatter height vs area (FCS-H/FCS-A) to sort for singlets. To identify live cells (alive at the time of fixation), Zombie aqua positive cells were detected. Finally, cells labelled with the AF647 fluorophore were detected. As the primary antibodies were not conjugated with a fluorophore, secondary antibodies had to be used. In order to test for background signal by unspecific binding of secondary antibodies, cells were incubated with secondary antibodies only. Furthermore, to be able to detect autofluorescence in the range of the secondary antibodies used, one well per cell line remained unlabelled with antibodies and only the signal of Zombie aqua was detected.

3.4 Microbiological Techniques

3.4.1 Generation of Competent Dh5α *E.coli*

Chemically competent *E.coli* bacteria (initial stock kindly provided by Sonja Vermeren, UoE) were generated following a method using rubidium chloride. An overnight culture of *E.coli* in LB (Luria Bertani) medium (1% tryptone, 0.5% yeast extract, 1% NaCl, pH7.5) was diluted 1:100 in 5 ml YT++ medium (0.8% tryptone, 0.5% yeast extract, 0.5% NaCl 3.5 mM NaOH) and incubated for 3.5 hours at 37°C in an orbital shaker. This culture was then used to inoculate 100 ml of pre-warmed YT++ medium, which was cultured until the bacteria suspension reached an OD_{600} of 0.45-0.55. The bacterial suspension was then divided into pre-chilled 50 ml Falcon tubes in 50 ml aliquots, the suspension was left on ice for 5 min and subsequently pelleted at 1700 g for 15 min at 4°C. On ice, the pellets were resuspended each in 10 ml of ice cold TFB1 buffer (30 mM potassium acetate, 50 mM $MnCl_2$, 100 ml $RbCl_2$, 10 mM $CaCl_2$,

15% glycerol, pH5.8, sterile filtered), which was followed by a 10 min incubation on ice. The suspension was then centrifuged as above, and the supernatant was discarded. The bacteria pellets were resuspended in each 2 ml of ice-cold TFB2 (10 mM Na-MOPS, 75 mM $CaCl_2$, 10 mM $RbCl_2$, 15% glycerol, pH7, sterile filtered). The competent bacteria suspension was aliquoted as 100 µl portions into pre-cooled (on ice) 1.5 ml tubes and snap frozen in an ethanol-dry ice bath and stored at -80°C.

3.4.2 Transformation of Competent Dh5α *E.coli*, DNA Propagation and Isolation

Transformation of competent Dh5α *E.coli* bacteria was carried out by heat shock, whereupon bacteria were seeded onto selective agar. In detail, after thawing on ice, bacteria were incubated with plasmids for 30 minutes on ice and heat-shocked at 42°C for 45 seconds, followed by a 2-minute incubation on ice. Bacteria were resuspended in 900 µl LB medium (10 mg/ml bacto-tryptone, 5 mg/ml yeast extract, 10 mg/ml NaCl, pH7.5) and incubated at 37°C in a bacteria shaker. After one hour, cells were pelleted, resuspended in 50-100 µl of LB, while 10-50 µl of this solution was plated onto LB agar with selection (e.g. 100 µg/mL carbenicillin) and incubated at 37°C. The following day single clones were picked and used to inoculate LB medium (with appropriate selection) and propagated by overnight incubation in an orbital shaker at 37°C. The next day plasmids were harvested using the EZNA KIT PLASMID MINI I (Q-SPIN) kit (Omega Biotek). Glycerol stocks of bacteria were generated by resuspending fresh bacteria suspension 1:1 in sterile 50% glycerol and stored at -80°C.

3.5 Zebrafish Assays

3.5.1 Zebrafish Husbandry and Mutants

Danio rerio Zebrafish (ZDR strain) were kept by Dr Isabel Ribeiro Bravo at the Bioresearch & Veterinary Services Aquatics facility (UoE) or by the Link lab (MCW). The following lines were used by the Link lab to generate *yap/taz* (*wwtr1*) double homozygous mutants; *yap1*^{mw48} (c. 158-161del), this allele has a 4 bp deletion within exon1 [66] and *wwtr1*^{mw49} (c. 156-160del), this allele has a 5 bp deletion within exon1 [66]. In addition, *cav1/cav3* double homozygous mutants were obtained by the Link lab and have been described elsewhere [202]. I performed qPCR on cDNA obtained from *yap/taz* KO zebrafish (see 3.3.2) and whole zebrafish immunohistochemistry on cav1/cav3 KO fish (see 3.6.2). For details on the methodology of the remaining experiments with zebrafish models please refer to Rausch et al. [195].

3.5.2 Zebrafish Yap Localisation Reporter

Yap localisation was assessed specifically in zebrafish epidermal cells which express a GFP-labelled Tead-binding deficient mutant version of Yap (GFP-YapS54A) as well as a nuclear marker (H2A-mCherry). Experiments with these reporter zebrafish were kindly performed by the Link lab (MCW) and analysed by Carsten G. Hansen (UoE). For details please refer to Rausch et al. [195].

3.6 Microscopy

3.6.1 Immunocytochemistry (Immunofluorescence)

The preparation of cells for immunofluorescence (IF) staining is explained in great detail in Rausch and Hansen [203]. The antibodies used for this method are listed in Table 8. Image acquisition was performed by a Zeiss 780 inverted confocal laser scanning microscope (CLSM) utilising a Plan-Apochromat 63x/1.4 Oil DIC M27 objective. Microscope settings were kept constant between samples for direct comparison. Image acquisition and quantification were generously carried out by Carsten G. Hansen (UoE) and is explained in detail in Rausch et al. [195]. Quantified were five to 15 cells of each population in eight to 15 images per condition. The experiments were carried out 2-3 times.

Table 8: Antibodies used for immunocytochemistry and flow cytometry

Target	Dilution	Source	Identifier
Anti-YAP/TAZ	1:100	Santa Cruz Biotechnology	Cat# sc-101199
Anti-CAV1	1:500	BD Biosciences	Cat# BD610060
Anti-CAV2	1:100	BD Biosciences	Cat# BD610684
Anti-YAP	1:300	Abcam	Cat# ab52771
Anti-CAVIN1	1:300	Abcam	Cat# ab48824
Anti-GFP	1:300	Abcam	Cat# ab6556
Anti-CAV1	1:300	Jørgen Vinten, University of Copenhagen	See [204]
Anti-Myc	1:500	Cell Signaling Technology	Cat# 2276
Anti-TEAD1	1:100	BD Biosciences	Cat# 610923
Anti-FLAG	1:200	Cell Signaling Technology	Cat# 2368
Anti-PECAM1	1:400	Santa Cruz Biotechnology	Cat# SC1506
Anti-VE-Cadherin	1:400	Cell Signaling Technology	Cat# D87F2
Anti-Rabbit IgG 2°AB, Alexa Fluor 488	1:400	Thermo Fisher Scientific	Cat# A-11008
Anti-Rabbit IgG 2°AB, Alexa Fluor 594	1:400	Thermo Fisher Scientific	Cat# A-11037
Anti-Mouse IgG 2°AB, Alexa Fluor 594	1:400	Thermo Fisher Scientific	Cat# A-11032
Anti-Mouse IgG 2°AB, Alexa Fluor 488	1:400	Thermo Fisher Scientific	Cat# A-11029
Anti-Rabbit IgG 2°AB, Alexa Fluor 633	1:400	Thermo Fisher Scientific	Cat# A-21071
Anti-Mouse IgG 2°AB, Alexa Fluor 647	1:400	SouthernBiotech	Cat# 1030-31
Anti-Rabbit IgG 2°AB, Alexa Fluor 647	1:400	Invitrogen	Cat# Z25308

2°AB: Secondary antibody

3.6.2 Whole Zebrafish Immunohistochemistry

For whole mount immunohistochemistry fixed zebrafish embryos were washed in PBST and stored in 100% methanol at -20°C overnight. This was followed by rehydration in solutions of incrementally increased PBST concentration (25%, 50%, 75% PBST in methanol) and a final wash in PBST. Subsequently, embryos were incubated in blocking buffer (10% goat serum, 0.2% BSA in PBST) for several hours at room temperature. For labelling of YAP, embryos were left in blocking solution with anti-YAP antibody (#13584-1-AP, Proteintech) at 4°C overnight. After rigorous washing in PBST, embryos were incubated in blocking solution containing secondary antibody (Alexa Fluor 633, A21071, Thermofisher), which was followed by another extensive washing procedure. Nuclei were labelled by Hoechst 3342 (Thermofisher). Finally, embryos were dehydrated in glycerol solutions (30%, 50%, 80% glycerol/PBS) and stored in antifadent (AF1, Citifluor). Labelled zebrafish embryos were mounted in antifadent onto glass slides and microscopic images were taken using the Leica SP8 CLSM utilising a HC PL APO 40x oil CS2 objective. The nuclear to cytoplasmic YAP ratio in individual cells was kindly determined by Carsten G. Hansen (UoE), for details please see Rausch et al. [195].

3.6.3 Transmission Electron Microscopy (EM)

Zebrafish embryos were collected at the 12-somite stage and prepared as previously described [200]. Four embryos were analysed for each genotype. Sample preparation and imaging was generously performed by the Link lab (MCW). Quantification was kindly conducted in a genotype-blinded manner by Carsten G. Hansen (UoE). For

details on sample preparation, imaging and quantification please refer to Rausch et al. [195].

3.6.4 Shear Stress Studies

Cells were cultured under laminar flow using the Kirkstall Quasi Vivo® QV500 system with a Parker (PF22X0103) peristaltic pump. HEK 293A cells were seeded onto Thermanox^{TM} 13 mm coverslips (#174950, ThermoFisher), or (for IF) poly-D-lysine coated glass coverslips and grown to confluency in complete DMEM containing 10% FBS. The coverslips were transferred into the QV500 system and cells were cultured in DMEM (with supplements as described above) containing 0.1% FBS and a constant flux of 4.7 and $2.1x10^{-5}$ Dyn/cm^2, respectively. After 18 hours cells were harvested and analysed by RT-qPCR, Western blotting or IF.

3.6.5 Statistics and Data Presentation

Data is represented with probability (p) values used by "*" $p<0.05$, "**" $p<0.01$ and "***" $p<0.001$. All data originated from at least three independent biological replicates if not directly stated otherwise. Data was analysed using Fiji (ImageJ), Excel (Microsoft) and Prism (GraphPad) software. All statistical analysis and graphs were generated using Prism software. All IF based scatter plots were tested and analysed by unpaired (Student's) t-test, whereas all other data was analysed using Mann-Whitney, if not specifically mentioned in the figure legends. Data are represented as mean ± standard error of the mean (SEM) or standard deviation (SD) as highlighted in figure legends.

4. Results

4.1 YAP and TAZ Drive Caveolar Protein Expression

YAP and TAZ regulate the expression of a large variety of genes. Here, the importance of YAP/TAZ for the expression of two main caveolar components was investigated. YAP/TAZ as well as LATS1/2 HEK 293A double KO cell lines, were previously described [196, 197]. These genome edited cell lines were central to determine the dependence of caveolar gene and protein levels on YAP/TAZ activity and analysed by immunofluorescence, RT-qPCR and Western blotting. Furthermore, the established YAP/TAZ and LATS1/2 double KO cell lines allowed for the verification of antibodies against YAP/TAZ and YAP used for this study (**Figure 8**) [197, 203].

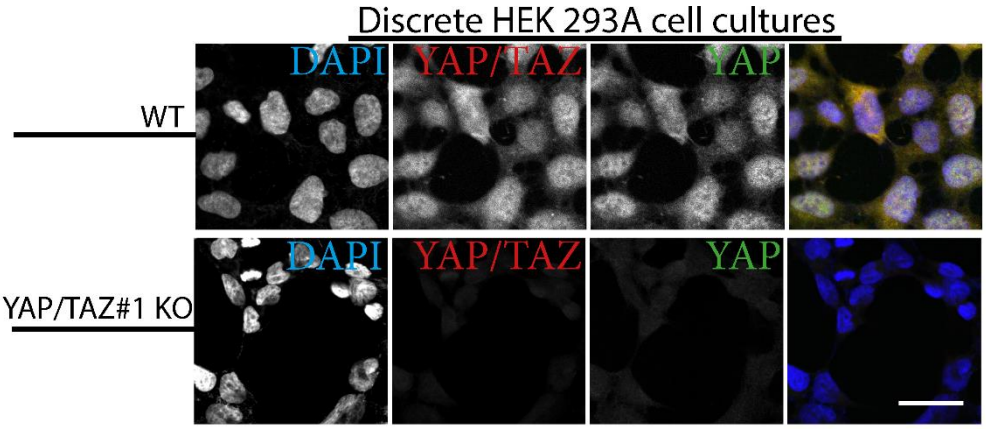

Figure 8: Validation of antibody specificity.

Confocal laser scanning microscopy (CLSM) images of discrete HEK 293A cell cultures of WT and YAP/TAZ#1 double KO cells, respectively. Cells were fixed and labelled for YAP/TAZ (red), YAP (green) and counterstained with DAPI (blue); Antibodies against YAP/TAZ (Santa Cruz, sc101199) and YAP (Abcam, ab52771). The single channel images visualise the specificity of the antibodies. Scale bar = 15µm.

A strong reduction of both CAV1 or CAVIN1 signals became evident in two independent YAP/TAZ KO cell lines (#1 and #2) compared to WT cells (**Figure 9A,B**). On the other hand, LATS1/2 KO cells, compared to WT cells, showed increased CAV1 and CAVIN1 signal (**Figure 9A-C**). LATS1/2 are negative regulators of YAP/TAZ [13]. LATS1/2 KO causes YAP/TAZ hyperactivity, as indicated by the nuclear accumulation of YAP/TAZ signal (**Figure 9C,D**). The quantification of relative CAV1 and CAVIN1 signal in the YAP/TAZ#1 KO compared to WT cells showed a significant reduction of the two central caveolar components, while this signal was increased in LATS1/2 KO cells (**Figure 9E,F**).

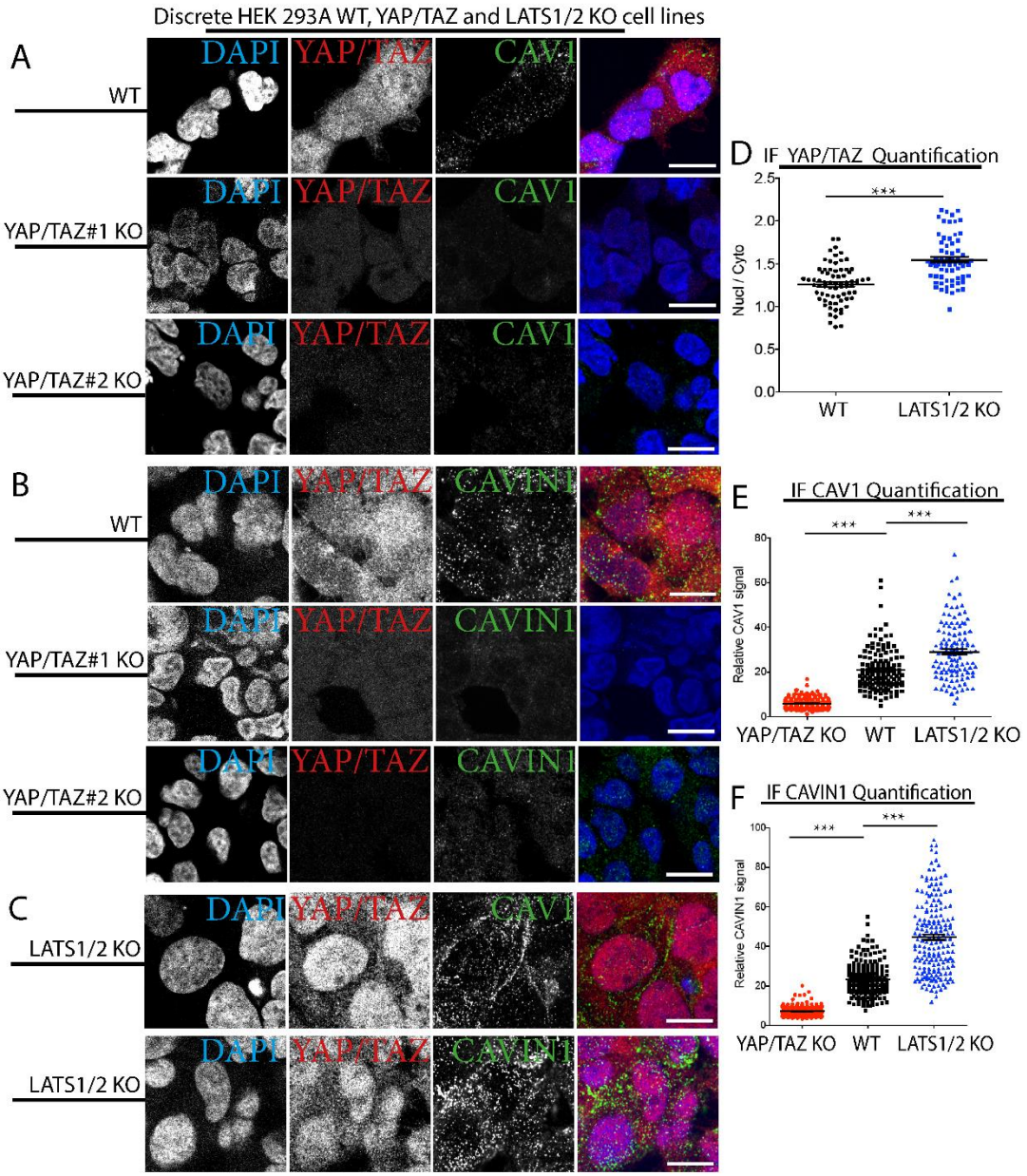

Figure 9: CAV1 and CAVIN1 depend on YAP/TAZ expression.

A-C: CLSM images of discrete HEK 293A cell cultures of WT and two independent YAP/TAZ KO cell lines (A and B) and LATS1/2 KO cells (C). Cells were fixed and labelled for YAP/TAZ (red) and either CAV1 or CAVIN1 (green) and counterstained with DAPI (blue). Samples were all imaged in parallel and with similar settings to allow for direct comparison between cell lines. Scale bar = 15µm. **D:** Quantification of nuclear to cytoplasmic signal of YAP/TAZ in WT cells (as in A and B) and LATS1/2 KO cells (as in C). **E:** Quantification of relative CAV1 signal in YAP/TAZ KO, WT and LATS1/2 KO cells. **F:** Quantification of relative CAVIN1 signal in YAP/TAZ KO, WT and LATS1/2 KO cells. For D-F: Each dot represents one cell. n ≥ 80. T-test, mean ± SEM.

Along with CAV1 and CAVIN1, YAP/TAZ-deficient cells, unlike LATS1/2 KO cells, had a strong reduction of CAV2 expression (**Figure 10**). This indicates that the levels of these important caveolar proteins are positively correlated with YAP/TAZ activity.

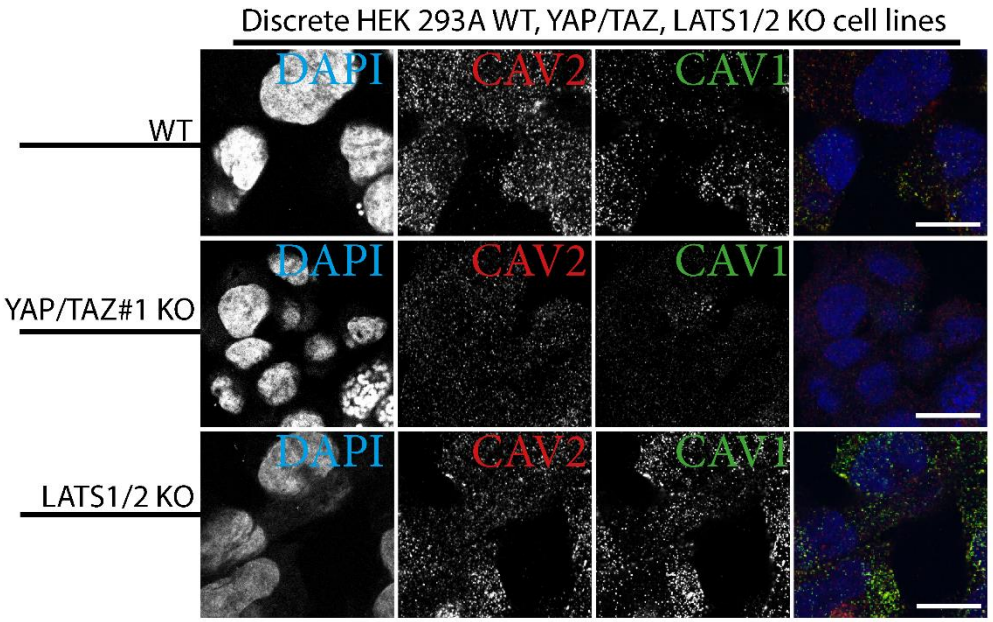

Figure 10: CAV2 depends on YAP/TAZ expression.

CLSM images of discrete HEK 293A cell cultures of WT, YAP/TAZ#1 KO and LATS1/2 KO cells. Cells were fixed and labelled for CAV2 (red), CAV1 (green) and counterstained with DAPI (blue). Samples were all imaged in parallel and with similar settings to allow for direct comparison between cell lines. Scale bar = 15µm.

To determine whether YAP/TAZ-dependent caveolar protein expression is a cell-intrinsic effect, and not solely due to paracrine interactions, mixed (WT and KO) cell populations were analysed by immunofluorescence assays. The specificity of the antibodies used (**Figure 8**), allowed for directly comparison of CAV1 and CAVIN1 expression between WT and YAP/TAZ KO cells in a mixed culture (**Figure 11**). As in

the discrete cultures, CAV1, CAVIN1 as well as CAV2 protein expression were drastically reduced in YAP/TAZ-deficient cells both qualitatively (**Figure 11A-C**) and quantitatively (**Figure 11D,E**). An effect which was reproduced in a second YAP/TAZ KO cell line (#2) (**Figure 11F,G**) and indicates a cell-intrinsic dependence of caveolar proteins on YAP and TAZ.

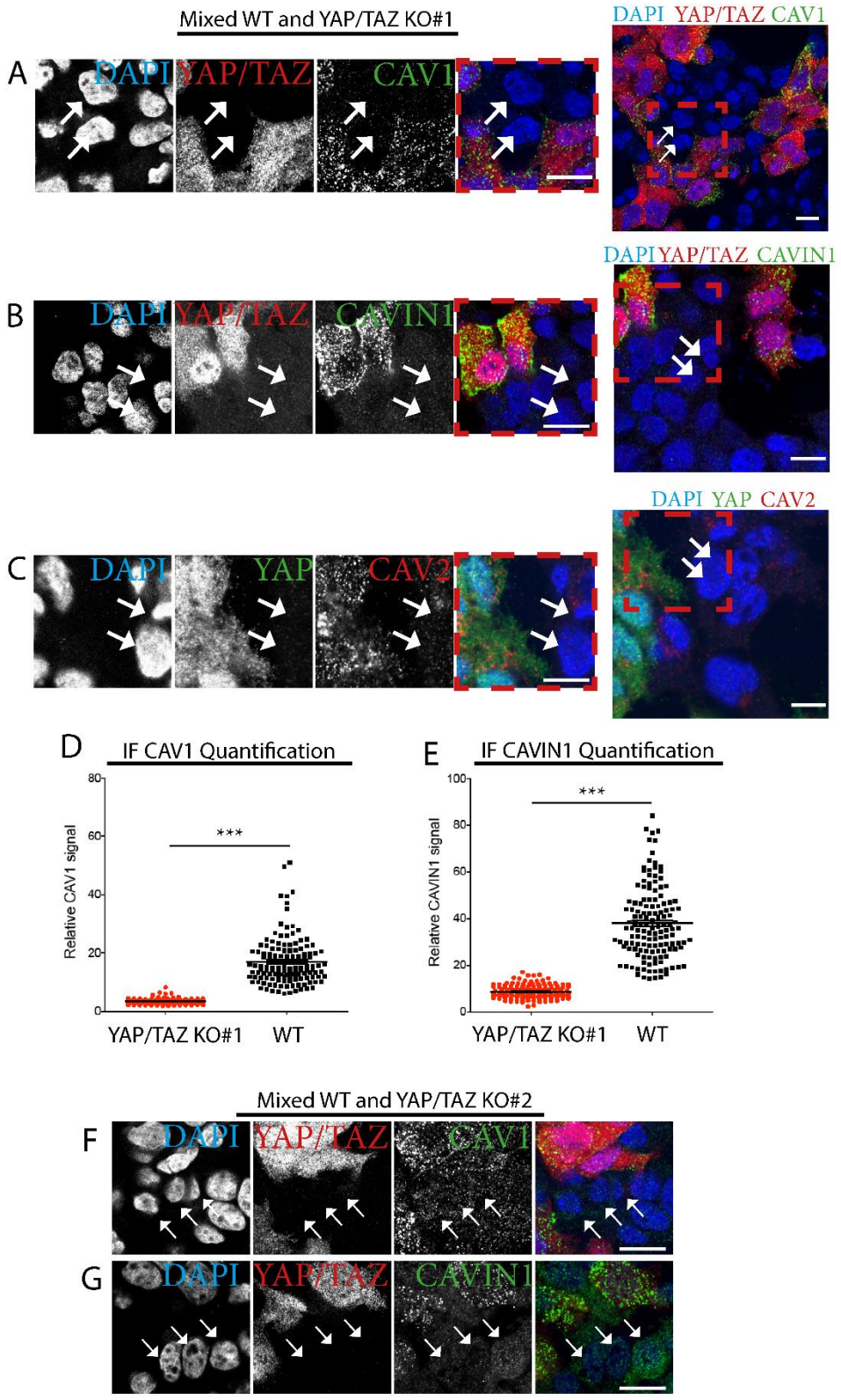

Figure 11: YAP/TAZ regulate CAV1 and CAVIN1 expression cell-intrinsically.

A-C: CLSM images of mixed cultures of fixed HEK 293A WT and YAP/TAZ#1 KO cells labelled for YAP/TAZ (red in **A** and **B**), CAV1 (green in **A**), CAVIN1 (green in **B**) or YAP (green in **C**) and CAV2 (red in **C**) and counterstained with DAPI (blue). Arrows indicate KO cells. On the right, zoom-out image of cell culture, highlighting the selected zoom-in by the red dashed-line box. Scale bars = 15µm. **D:** Quantification of relative CAV1 signal in YAP/TAZ KO and WT cells (as in A). **E:** Quantification of relative CAVIN1 signal in YAP/TAZ KO and WT cells (as in B). For D and E: Each dot represents one cell. n ≥ 120. T-test, mean ± SEM. **F** and **G:** Images as in A and B but of WT and YAP/TAZ#2 KO cells.

In addition, exogenous plasmid-based re-expressed CAV1 and CAVIN1 in YAP/TAZ KO cells co-localised within, or close to, plasma membrane domains (**Figure 12A**). This localisation is comparable to the localisation of endogenous CAV1 and CAVIN1 in WT cells (**Figure 12B**). These data indicate that YAP and TAZ are required for the expression of the essential caveolar proteins CAV1 and CAVIN1, but YAP and TAZ do not determine the cellular localisation of CAV1 and CAVIN1.

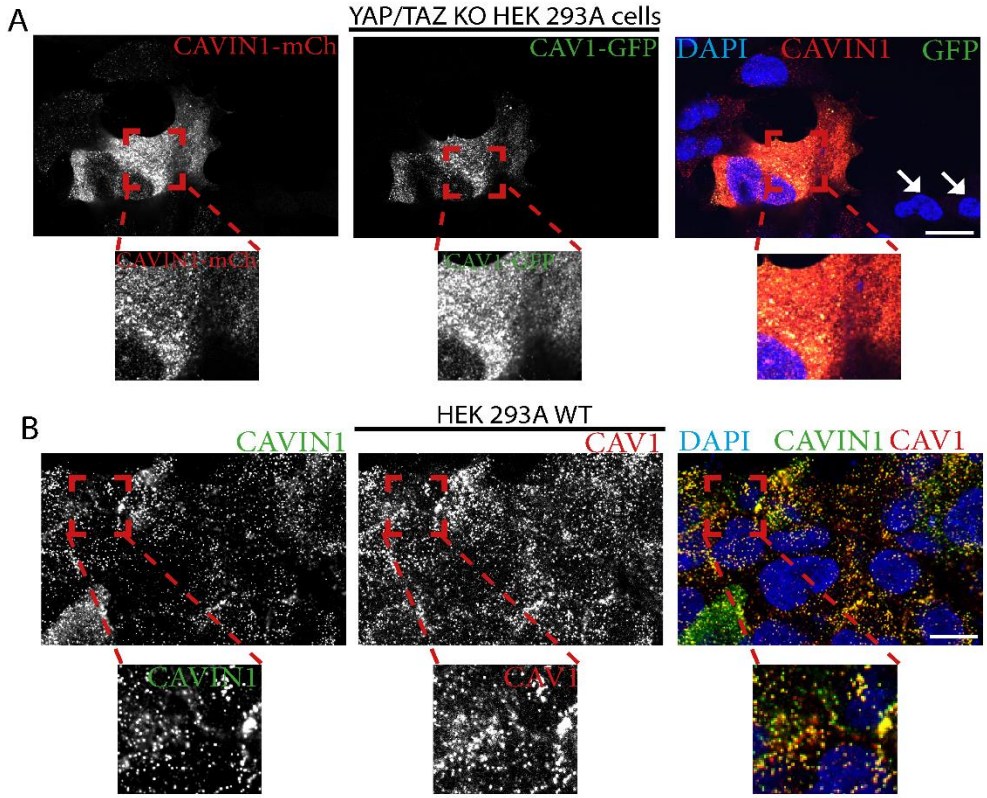

Figure 12: Exogenous expression of CAV1 and CAVIN1 form caveolae-like plasma membrane domains in YAP/TAZ KO.

A: Expression of CAVIN1-mCherry (red) and CAV1-GFP (green) in HEK 293A YAP/TAZ KO cells. Cells were fixed and processed for CLSM imaging. Note the co-localisation of CAV1 and CAVIN1 in plasma membrane domains. Red boxes indicate inserts shown below. Arrows: untransfected cells. Scale bar = 20 µm. **B:** CLSM images of HEK 293A WT cells fixed and processed for immunofluorescence, labelled for endogenous CAVIN1 (green), CAV1 (red) and counterstained for DAPI (blue). Note, CAV1 and CAVIN1 co-localise as in A. Red boxes indicate inserts shown below. Scale bar = 20 µm.

The correlation between YAP/TAZ and the expression of caveolar components was mirrored by total protein levels. Western blotting analysis revealed a dramatic reduction of CAV1, CAV2 and CAVIN1 (as well as CAVIN3) protein levels in both YAP/TAZ KO (#1 and #2) cell lines (**Figure 13A,B**). In addition, it is worth noting that the reduction of LATS2 protein levels in YAP/TAZ KO cells

(**Figure 13A,B**) goes along with reports in the literature on the positive regulation of LATS2 transcription by YAP/TAZ [196]. On the other hand, in the LATS1/2 KO cell lines YAP was hypo-phosphorylated, as seen by the downshift of the YAP signal in the PhosTag gel-based Western blot (**Figure 13C**). Consequently, in LATS1/2 KO cells YAP (and TAZ) were active and the expression of the caveolar components was increased (**Figure 13A-C**).

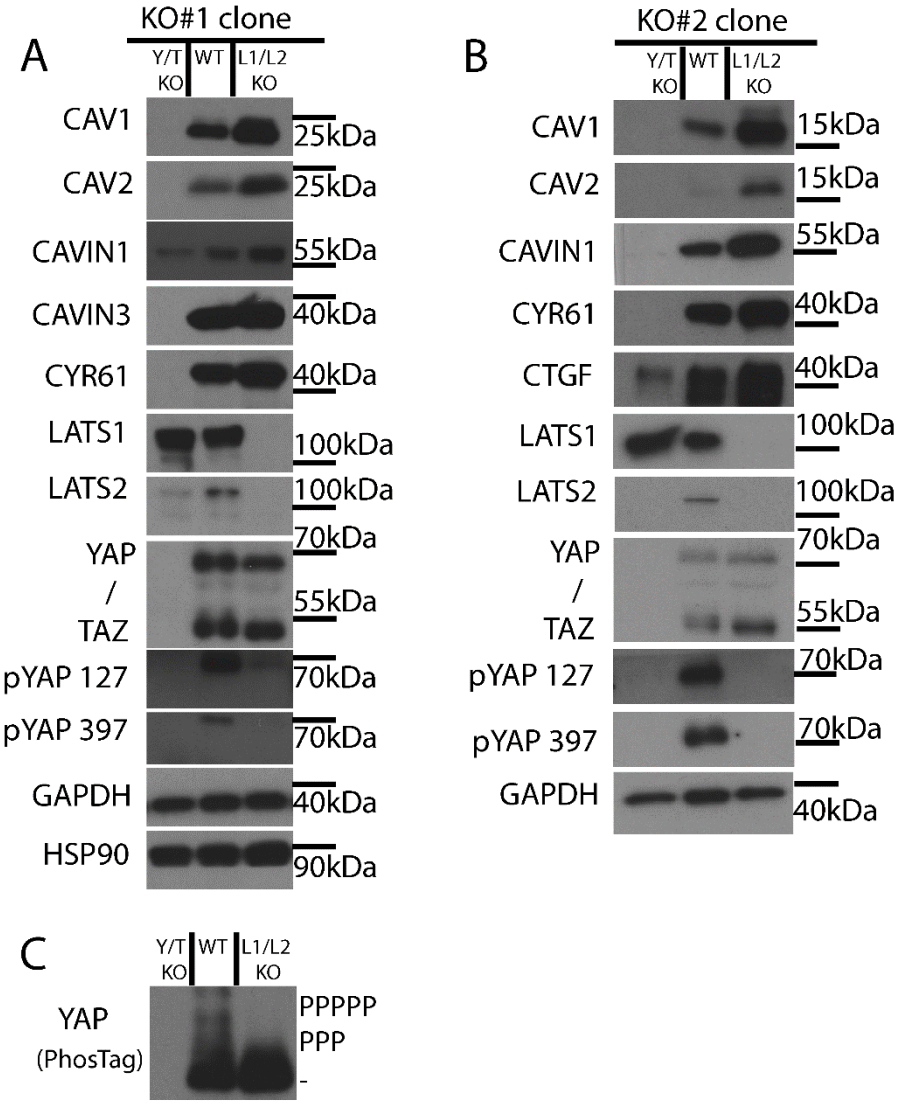

Figure 13: YAP/TAZ activity is important for expression of caveolar proteins.

Western blot analysis of cell lysates from YAP/TAZ (Y/T) KO, WT and LATS1/2 (L1/L2) KO cells. GAPDH and HSP90 served as loading controls. Depending on the protein tested n ≥ 3. **A:** Western blots of YAP/TAZ#1 KO, WT and LATS1/2#1 KO. **B:** Western blots of YAP/TAZ#2 KO, WT and LATS1/2#2 KO. **C:** Western blot based on a PhosTag SDS-gel blotted for YAP protein of lysates as in A.

Re-introduction of LATS1 into the LATS1/2 KO cells reversed this effect, while a kinase-dead version (K/R) did not (**Figure 14A**). Only LATS1/2 KO cells expressing the fully functional version of LATS1, but not the K/R mutant revealed an increase of phosphorylated YAP (**Figure 14B**). On total protein levels, cells expressing the K/R mutant behaved similar to the KO, while the LATS1 WT expressing cells had increased levels of the YAP/TAZ target CYR61 as well as CAV1 and CAVIN1 (**Figure 14A**). These data demonstrate the importance of LATS1/2-dependent phosphorylation-mediated regulation of YAP/TAZ activity for the expression of central caveolar components.

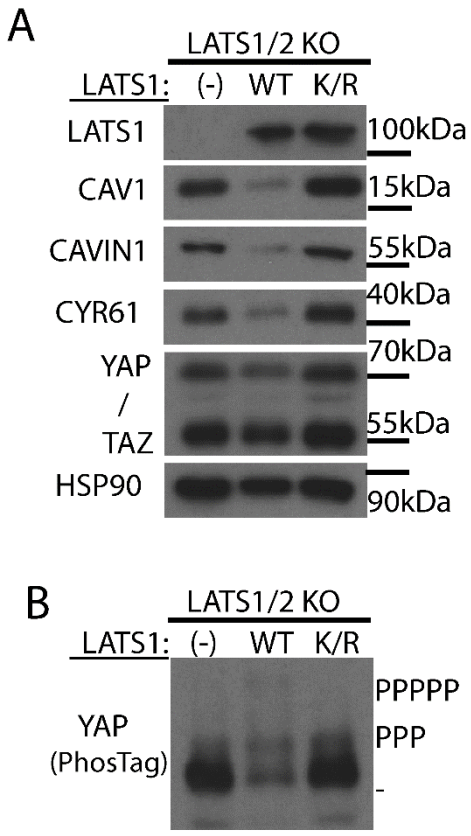

Figure 14: Active LATS1 inhibits caveolar protein expression.

A: Western blot of HEK 293A LATS1/2 KO cells stably expressing vector control (-), LATS1 WT or a mutant LATS1 kinase-dead (K/R). **B:** Western blot based on a PhosTag SDS-gel probing for YAP protein of lysates as in A. Depending on the protein tested n ≥ 3.

4.2 Expression of Caveolar Components Depends Transcriptionally on YAP/TAZ Activity

Since YAP and TAZ are transcriptional co-activators and the expression of central caveolar proteins depends on their activity (as seen in 4.1), I sought out to determine whether YAP/TAZ activity directly regulates caveolar gene expression. RT-qPCR analyses revealed a significant decrease of not only the well-known YAP/TAZ target genes *CYR61* and *CTGF* but of *CAV1* and *CAVIN1* mRNA in both YAP/TAZ KO cell lines (**Figure 15A-C**). In the LATS1/2 KO cells, with hyperactive YAP/TAZ, an increase in *CYR61*, *CTGF* and *CAVIN1* mRNA was apparent (**Figure 15A,B**). Re-expressing WT but not the kinase-dead K/R version of LATS1 in the LATS1/2 KO cells led, as on protein levels (**Figure 14A**), to a decrease of both YAP/TAZ target genes as well as *CAVIN1* (**Figure 15D**). In addition, exogenous expression of hyperactive YAP (5SA mutant) increased *CAV1* and *CAVIN1* expression (**Figure 15E**). Consequently, YAP/TAZ activity regulates the expression of caveolar components on transcriptional level.

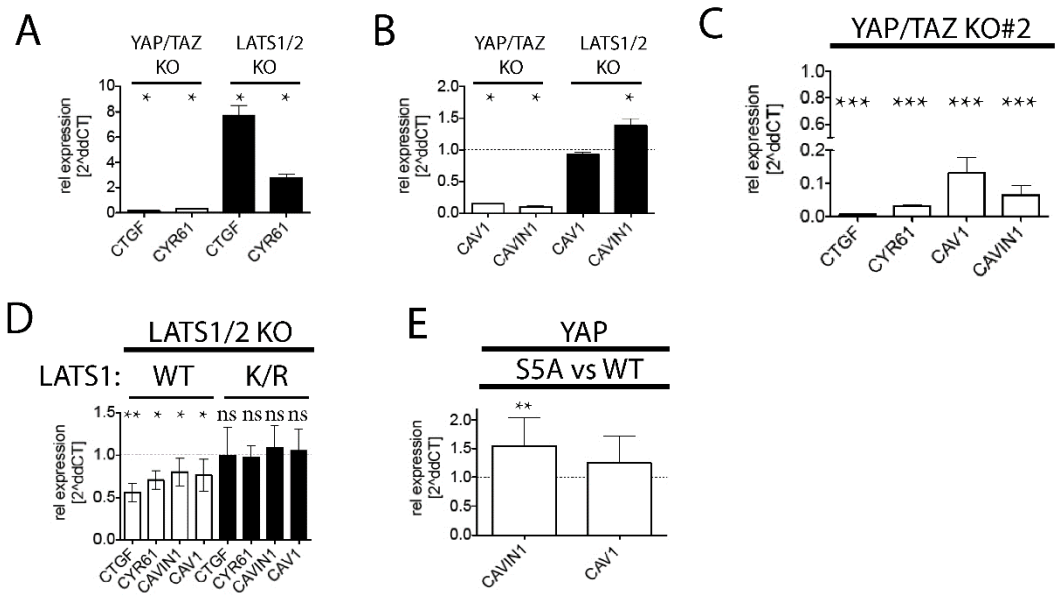

Figure 15: Active YAP/TAZ induce transcription of caveolar gene.

A: RT-qPCR analysis of expression of established YAP/TAZ target genes in HEK 293A YAP/TAZ#1 KO and LATS1/2 KO relative to WT cells. **B:** RT-qPCR analysis of expression of essential caveolar genes in HEK 293A YAP/TAZ#1 KO and LATS1/2 KO relative to WT cells. **C:** RT-qPCR analysis as in A and B of HEK 293A YAP/TAZ#2 KO cells. n = 2 **D:** RT-qPCR analysis of expression of established YAP/TAZ target genes and essential caveolar genes in HEK 293A LATS1/2 KO stably expressing LATS1 WT or a kinase-dead (K/R) LATS1 relative to LATS1/2 KO cells. n ≥ 2 **E:** RT-qPCR analysis of expression of essential caveolar genes in HEK 293A cells stably expressing the constitutive active S5A version of YAP relative to cells stably expressing YAP WT. n ≥ 3. Mann-Whitney test, mean ± SD.

4.2.1 YAP/TAZ-TEAD Interaction is Important for CAV1 and CAVIN1 Expression

YAP and TAZ are co-transcriptional activators, however as they do not contain any DNA binding domains, they are incapable of inducing gene transcription by themselves. They bind to transcription factors, e.g. TEAD1-4, and as a complex locate to distal enhancer and promoter regions of Hippo pathway regulated genes [15, 18, 25, 30, 205]. The expression of caveolar components (CAV1, CAV2, CAVIN1,

CAVIN3) depends on YAP/TAZ expression and activity (see above), however whether the central caveolar genes *CAV1* and *CAVIN1* are transcriptionally regulated via TEAD was unclear. Therefore, I analysed the expression of CAV1 and CAVIN1 in cells deficient for TEADs as well as cells where the interaction between YAP/TAZ and TEAD was inhibited.

A drug, which inhibits the YAP-TEAD interaction is verteporfin [206]. Clinically, verteporfin is used as a photosensitiser in photodynamic therapy [207]. Verteporfin binds YAP leading to a conformational change, which inhibits the ability of YAP to bind TEADs [206]. Verteporfin further appears to affect the Hippo pathway by increasing the levels of 14-3-3, which induces YAP/TAZ cytoplasmic retention [208, 209]. After treating cells with verteporfin there was a significant reduction of both *CYR61* and *CTGF* as well as *CAV1* and *CAVIN1* mRNA levels relative to untreated cells (**Figure 16**).

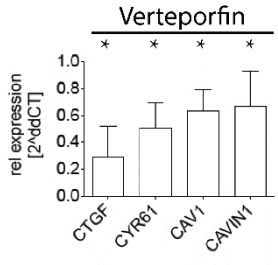

Figure 16: YAP-TEAD interaction important for caveolar gene expression.

Verteporfin treated HEK 293A WT cells analysed by RT-qPCR for expression of YAP/TAZ target genes and central caveolar components relative to cells not treated with verteporfin. n ≥ 4. Mann-Whitney test, mean ± SD.

Importantly, the specificity of verteporfin has recently come under scrutiny, when, e.g. no effect was detected in melanoma model [210]. Therefore, in order to not only rely on drug treatments, a genetic approach was adopted to analyse the TEAD-dependency further. YAP binds to TEAD via forming a hydrogen bond at its serine 94 [15, 25]. In a complementary approach a WT or a TEAD binding-deficient version of

YAP (S94A), mutated at serine residue 94, or the equivalent TAZ (S51A), mutated at its TEAD interaction site, serine residue 51, were stably (re-)introduced into YAP/TAZ KO HEK 293A cells. Analysing total protein levels, it was evident that there was an increase of CYR61, CAV1 and CAVIN1 protein in cells expressing YAP-WT compared to YAP/TAZ KO and YAP-S94A cells (**Figure 17A**). Immunofluorescent labelling of CAV1 and CAVIN1 revealed a rescue of their expression in cells transfected with the YAP-WT but not the TEAD binding-deficient YAP-S94A mutant. This YAP-TEAD binding rescue occurs in a cell-intrinsic manner as proven by a mixed cell culture approach (**Figure 17B-G**). The induction of CAV1 and CAVIN1 expression in YAP-WT expressing cells was significantly elevated compared to the YAP/TAZ KO and the YAP-S94A cells (**Figure 17D,G**). The increase of CAV1 and CAVIN1 expression was mirrored when comparing the above results with TAZ-WT re-expressing and TAZ-S51A expressing cells (**Figure 17H,I**). Consequently, these results emphasise that the expression of essential caveolar components depends on the interaction of YAP/TAZ with TEAD.

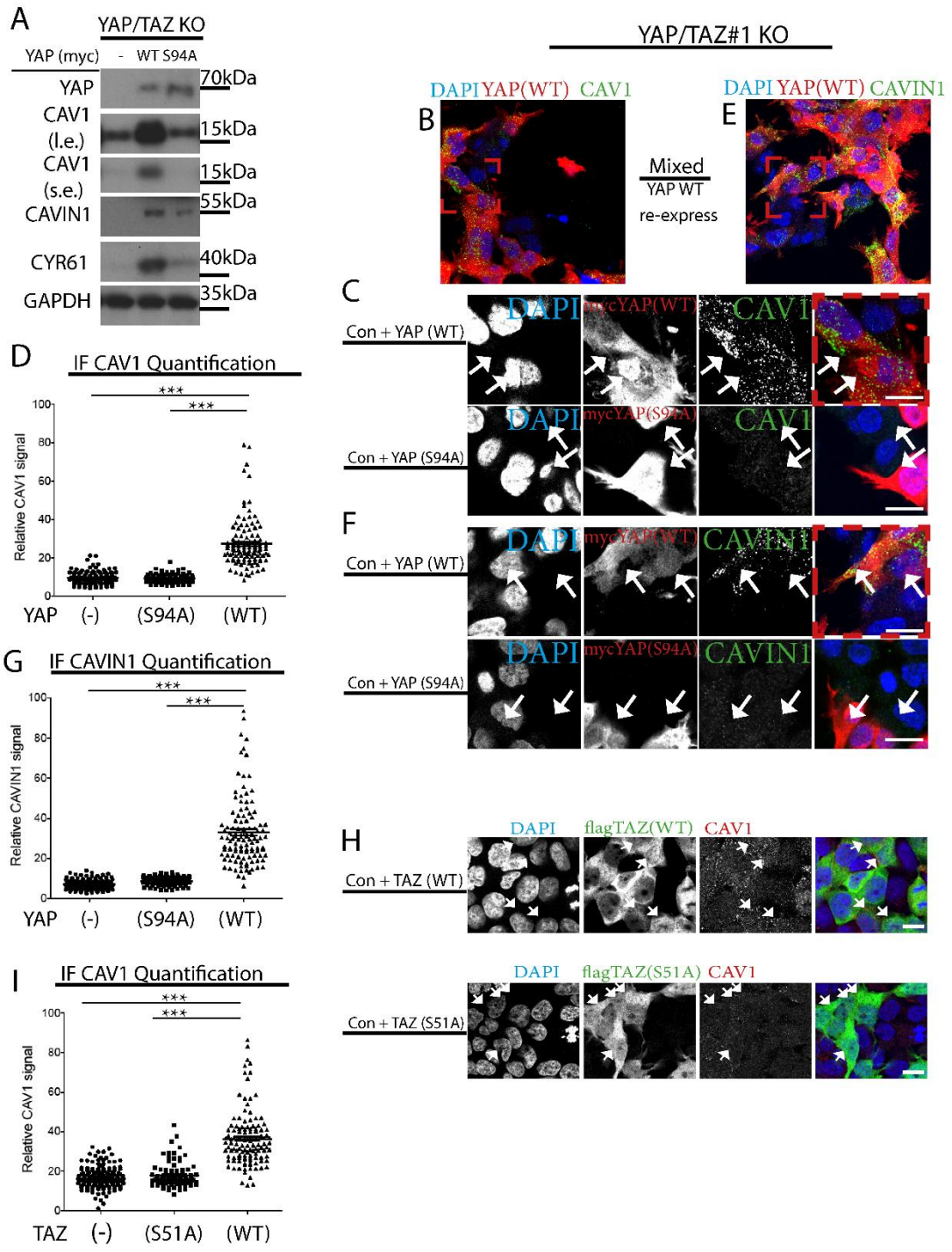

Figure 17: YAP/TAZ-TEAD interaction important for caveolar protein expression.

A: Western blot analysis of lysates from HEK 293A YAP/TAZ#1 KO cells stably expressing vector control (-), myc-tagged WT YAP or the TEAD-binding-deficient YAP S94A. l.e. = long exposure, s.e. = short exposure. Depending on the protein tested n ≥ 2. **B:** Zoom-out image of cells as in C indicated by the red dashed-line box. **C:** CLSM images of mixed HEK 293A cultures YAP/TAZ#1 KO cells stably expressing vector control, myc-tagged YAP WT or YAP S94A. Cells were fixed

and labelled for myc (red), CAV1 (green) and counterstained with DAPI (blue). Arrows: Cells expressing the myc tag. **D:** Quantification of relative CAV1 signal of cells as in C. **E:** Zoom-out image of cells as in F indicated by the red dashed-line box. **F:** CLSM images of mixed HEK 293A cultures YAP/TAZ#1 KO cells stably expressing vector control, myc-tagged YAP WT or YAP S94A. Cells were fixed and labelled for myc (red), CAVIN1 (green) and counterstained with DAPI (blue). Arrows: Cells expressing the myc tag. **G:** Quantification of relative CAVIN1 signal of cells as in F. **H:** CLSM images of mixed HEK 293A cultures YAP/TAZ#1 KO cells stably expressing vector control, flag-tagged TAZ WT or the TEAD-binding-deficient TAZ S51A. Cells were fixed and labelled for flag (green), CAV1 (red) and counterstained with DAPI (blue). Arrows: Cells expressing the flag tag. **I:** Quantification of relative CAV1 signal of cells as in H. For C, F and H: Samples were all imaged in parallel and with similar setting to allow direct comparison. Scale bar = 15µm. For D, G and I: Each dot represents one cell. n ≥ 100. T-test, mean ± SEM.

A significant increase of *CAV1* and *CAVIN1* mRNA was only detected in cells expressing the WT but not the TEAD-binding-deficient version of YAP or TAZ (**Figure 18A,B**). This apparent dependence of CAV1 and CAVIN1 expression on the YAP/TAZ-TEAD interaction was an encouragement to analyse the role of TEADs in the expression of central caveolar components.

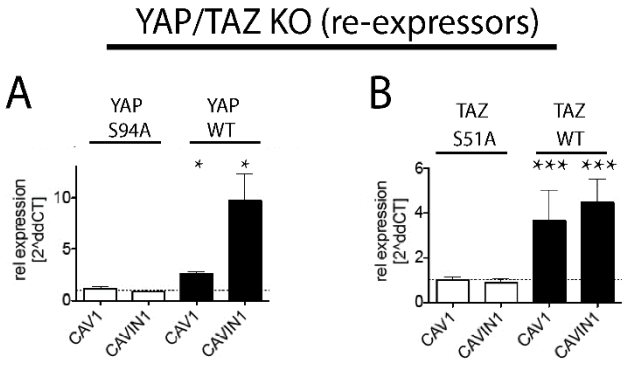

Figure 18: YAP/TAZ-TEAD interaction essential for caveolar gene expression.

A: RT-qPCR analysis of expression central caveolar components in HEK 293A YAP/TAZ#1 KO cells stably expressing YAP S94A or WT, relative to KO cells. **B:** RT-qPCR analysis as in A but of cells stably expressing TAZ S51A or WT, n ≥ 2. Mann-Whitney test, mean ± SD.

Therefore, shRNA-induced TEAD1/3/4 KD in HEK 293A cell lines (which naturally lack detectable TEAD2) were utilised to investigate changes in CAV1 and CAVIN1

expression (**Figure 19**). In discrete cultures of TEAD KD cells a reduction of CAV1 and CAVIN1 signal was detected by immunofluorescence assays compared to control cells (**Figure 19A-C**). Quantifying the relative signal of CAV1 and CAVIN1 revealed a significant reduction of the two essential caveolar components in TEAD-deficient cells (**Figure 19D,E**). Those results were mirrored in mixed cultures, indicating that it is not merely a paracrine effect but that the two essential caveolar components directly depend on TEAD expression (**Figure 19F-I**).

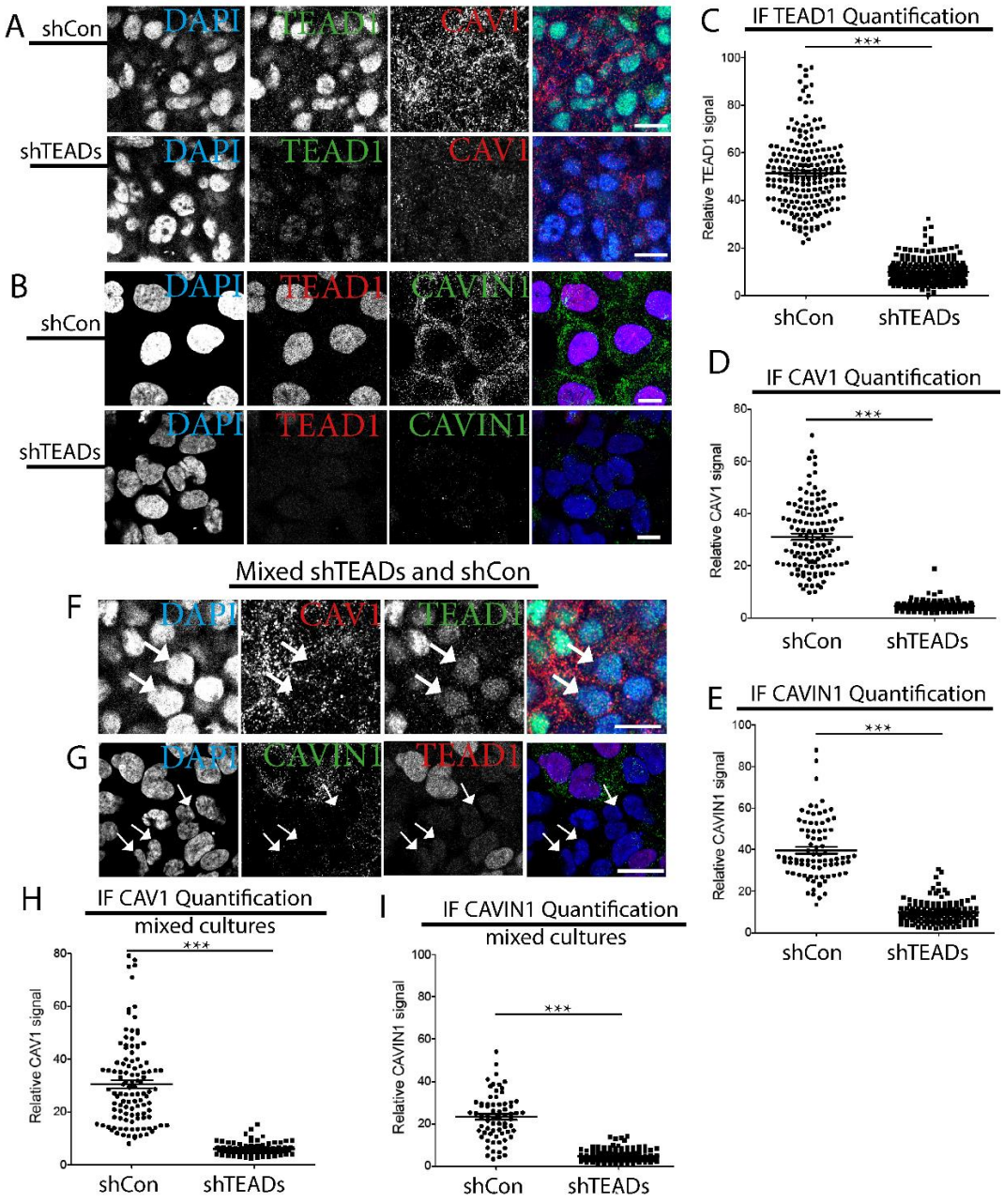

Figure 19: Expression of CAV1 and CAVIN1 depends on TEAD.

A and **B:** CLSM images of discrete cultures of HEK 293A shCon or shTEADs (TEAD1/3/4, cell line #1) treated cells. Cells were fixed and labelled for TEAD1 (in A green, in B red), CAV1 (red in A) or CAVIN1 (green in B) and counterstained with DAPI (blue). Scale bars = 15 µm. **C:** Quantification of relative TEAD1 signal in control and TEADs KD cells as in A and C. **D:** Quantification of relative CAV1 signal in control and TEADs KD cells as in A. **E:** Quantification of relative CAVIN1 signal in control and TEADs KD cells as in B. **F** and **G:** CSLM images of mixed cultures of shCon and shTEAD#1 cells. Cells were fixed and labelled (in F) for CAV1 (red) and TEAD1 (green) or (in G) CAVIN1 (green) and TEAD1 (red) and counterstained with DAPI (blue). Scale bars = 15 µm. **H:** Quantification of relative CAV1 signal in control and TEADs KD cells as in F. **I:** Quantification of relative

CAVIN1 signal in control and TEADs KD cells as in G. For C-E, H and I: Each dot represents one cell. n ≥ 90. T-test, mean ± SEM.

The caveolar TEAD dependence was further examined by total protein analysis (**Figure 20A**). Evidence that the regulation of the two essential caveolar genes *CAV1* and *CAVIN1* are transcriptionally regulated by YAP/TAZ-TEAD was delivered by RT-qPCR analysis of two independent TEAD-deficient cell lines. The results reveal a significant reduction of *CAV1* and even more drastically *CAVIN1* (**Figure 20B,C**). In conclusion, these data show that TEAD transcription factors and their interaction with YAP and TAZ is central for CAV1 and CAVIN1 expression.

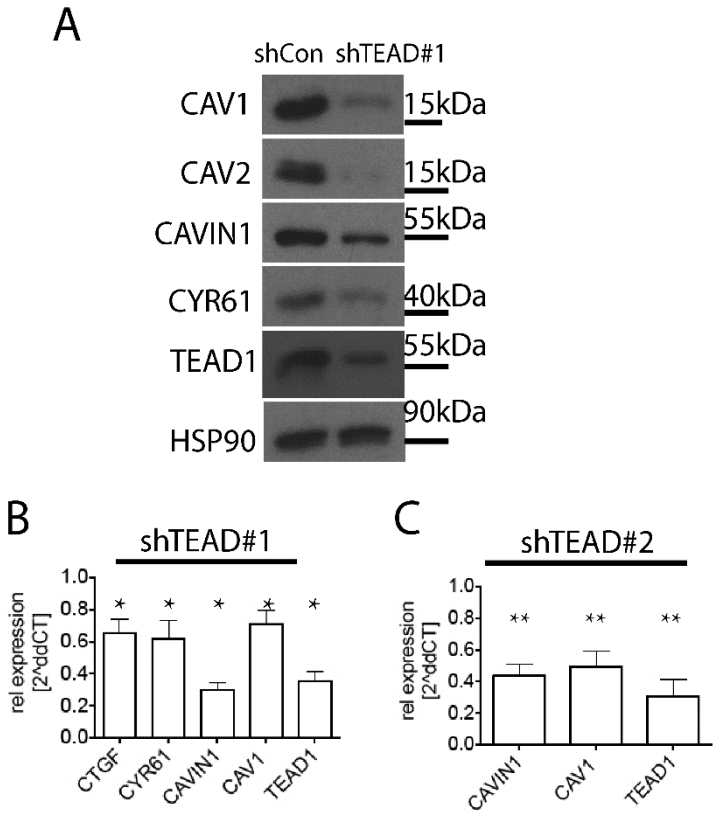

Figure 20: TEAD is required for expression of caveolar components.

A: Western blot analysis of cell lysates from HEK 293A control or TEAD1/3/4 #1 KD cell lines. HSP90 served as loading controls. **B:** RT-qPCR analysis of expression established YAP/TZA target genes and central caveolar components in HEK 293A cells TEAD1/3/4 #1 KD cells, relative to control cells. n ≥ 3. Mann-Whitney test, mean ± SD. **C:** RT-qPCR analysis as in B but of a second TEAD1/3/4 (#2) KD cell line. n = 3.

4.2.2 *CAV1* and *CAVIN1* are Direct Targets of YAP and TAZ-TEAD

I performed luciferase promoter assays to determine whether the transcription factors TEAD localise at the promoter region of *CAV1* and *CAVIN1*. Therefore, sequences of proximal genomic regions of either *CAV1* or *CAVIN1* were inserted into a plasmid upstream of the open reading frame of a luciferase gene. A long version of the *CAV1* promoter (-1800 to +200bp) as well as a sequence of the *CAVIN1* promoter (-1250 to +150bp) harbour five and four predicted TEAD binding sites, respectively. While a short version of the *CAV1* promoter region does not contain any TEAD recognition motifs (**Figure 21A**). When co-expressed with YAP, only cells with the plasmids containing genomic regions of *CAV1* and *CAVIN1* covering the TEAD binding sites showed increased luciferase activity. While the short *CAV1* genomic region does not affect luciferase activity (**Figure 21B**).

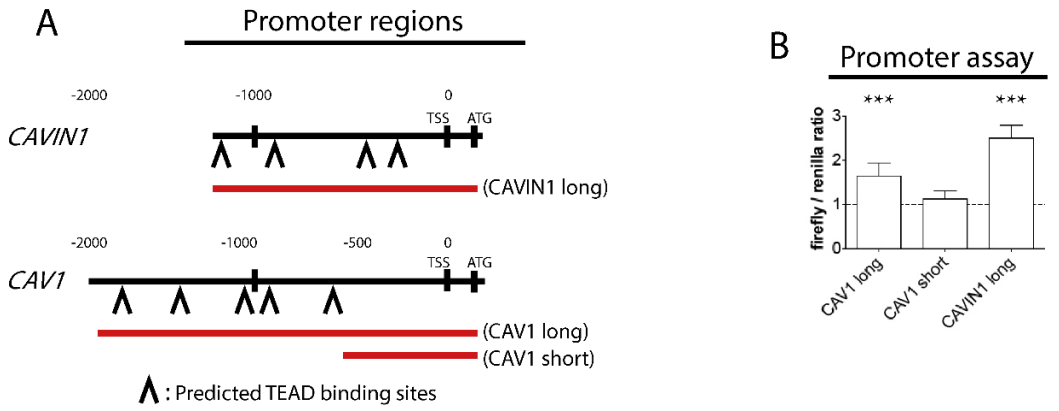

Figure 21: YAP drives *CAVIN1* and *CAV1* promoter activity.

A: Diagram of the CAVIN1 and CAV1 proximal promoter regions. Numbering in base pairs (bp) from transcription start site (TSS). ATG: Start codon. Red line: Representations of the regions contained in the luciferase reporter plasmid. Arrow heads: Predicted TEAD recognition motifs (including degenerate). The short fragment of the CAV1 promoter region (-500 to +200 bp) does not contain any predicted TEAD recognition motifs, while the long fragments of both CAV1 (-1,800 to +200bp) and CAVIN1 (-1,250 to +150bp) do. **B:** HEK 293A YAP/TAZ#1

KO cells were transfected each with one of the plasmids with fragments of promoter regions as in A together with either a YAP or a vector control plasmid. Luciferase activity was measurable in cells transfected with the plasmids carrying promoter regions of CAV1 and CAVIN1 with TEAD binding motifs. n = 3. Mann-Whitney test, mean ± SD.

To verify the results obtained above with the overexpressing approach, I next aimed to show YAP-TEAD binding to proximal promoter regions of *CAV1* and *CAVIN1* endogenously in cells. Therefore, chromatin immunoprecipitation (ChIP) was performed. At first, the binding of TEAD1 to the promoter regions of *CAV1* and *CAVIN1*, respectively, was verified. Performing the immunoprecipitation with a TEAD1 specific antibody, the subsequent qPCR analysis revealed enrichment of the proximal caveolar promoters bearing TEAD binding sites, but not of the in-gene negative controls (**Figure 22A**). Next, to assess whether YAP localises at the proximal promoters of *CAV1* and *CAVIN1,* an immunoprecipitation was performed with an antibody against YAP. Again, the promoter regions of *CAV1* and *CAVIN1* were enriched (**Figure 22B**). Finally, to prove that the YAP-TEAD complex binds to the promoters of *CAV1* and *CAVIN1* the ChIP assay was performed with the TEAD KD cell line #1. Here the immunoprecipitation with the YAP specific antibody and subsequent qPCR analysis resulted in no enrichment of the promoter regions of *CAV1* and *CAVIN1* (**Figure 22C**). In conclusion, the YAP-TEAD complex physically interacts with the proximal promoter regions of the two essential caveolar genes *CAV1* and *CAVIN1*. In summary, these data show that YAP/TAZ activity and their interaction with TEAD regulate the expression of central caveolar components and that *CAV1* and *CAVIN1* are direct transcriptional targets of the YAP/TAZ-TEAD complex.

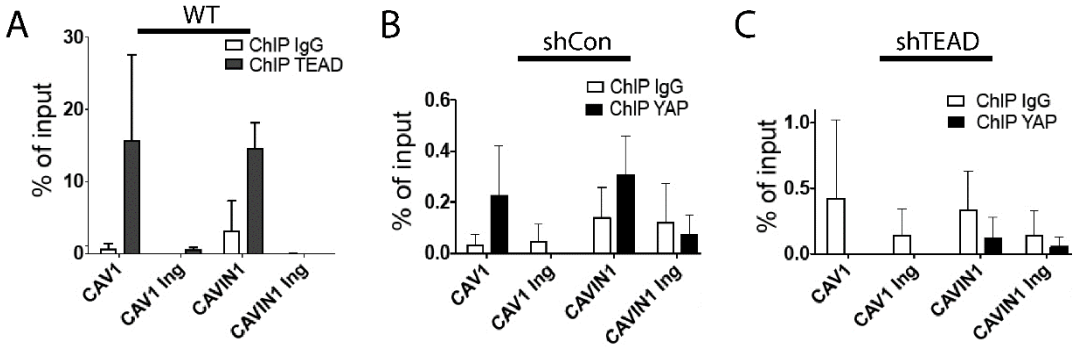

Figure 22: YAP-TEAD1 physically bind to the promoter regions of *CAV1* and *CAVIN1*.

A-C: qPCR analysis of chromatin immunoprecipitation (ChIP) in HEK 293A cells. The precipitated DNA was quantitated using primers specific for a promoter region or a control in-gene (Ing) region. Data are means ± SD of triplicates from a representative experiment. **A:** Immunoprecipitation was performed with an antibody against TEAD1 in HEK 293A WT cells. **B:** Immunoprecipitation was performed with an antibody against YAP in HEK 293A control (shCon) cells. **C:** Immunoprecipitation was performed with an antibody against YAP in HEK 293A TEAD1/3/4 KD (#1) cells.

4.2.3 YAP/TAZ Activity-dependent Expression of Caveolar Components is a Widespread Phenomenon

The conclusion that caveolar gene expression depends on YAP/TAZ activity, was further supported by a cancer cell line which, is known to have a functional Hippo pathway [87] and shows high relative expression and correlation between *CYR61* and *CAV1* as well as of *CAVIN1* [195]. U2OS is a human osteosarcoma cell line and was used to further establish the CAV1 and CAVIN1 dependency on YAP/TAZ-TEAD. Different KO and KD U2OS cell lines were therefore generated. I aimed to generate CRISPR/Cas9-mediated YAP/TAZ double KO cell lines based on U2OS. However, even after multiple repeated attempts, with verified active guide sequences, I was not able to obtain a viable YAP/TAZ double KO U2OS cell line. This is an indicator of the

central role of YAP and TAZ for those osteosarcoma derived cells. The KO of YAP or TAZ in combination with the KD of TAZ or YAP showed a strong reduction of CYR61 and, importantly, of both CAV1 and CAVIN1 expression in U2OS cells (**Figure 23A-C**).

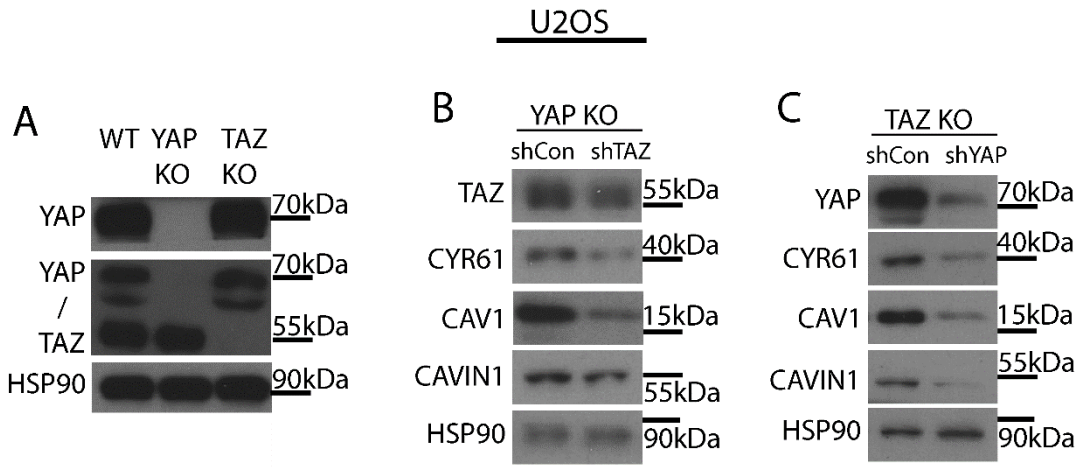

Figure 23: YAP/TAZ dictate caveolar protein expression in U2OS cells.

Western blot analysis of cell lysates from U2OS cells. HSP90 served as loading controls. Depending on the protein tested n ≥ 2. **A:** Comparison of protein levels in U2OS WT, YAP KO and TAZ KO cells. **B:** YAP KO cells with control (shCon) or TAZ KD. **C:** TAZ KO cells with control or YAP (shYAP) KD.

4.2.4 The Role of the Upstream Hippo Pathway and NF2 for Caveolae

Above, I verified the central roles of not only YAP/TAZ, but also other Hippo pathway components, e.g. LATS1/2 and TEADs, for the expression of CAV1 and CAVIN1 (see 4.1). Another important Hippo pathway regulator is Neurofibromatosis type 2 (NF2, also known as merlin) [211-215]. NF2 is an upstream activator of the kinase cascade and, consequently, an inhibitor of YAP/TAZ and the most commonly mutated Hippo pathway tumour suppressor [2, 21]. NF2 KO in U2OS cells resulted in nuclear accumulation of YAP/TAZ (**Figure 24A,B**). The increased nuclear localisation of YAP

goes along with its hypo-phosphorylation profile seen by PhosTag-analysis, an effect, which is reversed upon NF2 re-expression (**Figure 24C**). The activation of YAP (and TAZ) was accompanied by increased CAV1 and CAVIN1 protein levels (**Figure 24D**). Interestingly, the induction of caveolar gene expression both on protein and mRNA levels was blunted by re-introduction of NF2 (**Figure 24E,F**). Thus, the re-expression of NF2 indicates that CAV1 and CAVIN1 expression is inhibited by NF2. In order to assess the role of downstream Hippo pathway components in the context of NF2 deficiency, KD of YAP, TAZ and TEADs, respectively, was induced in NF2 KO cells. Deficiency of TEADs and TAZ in particular led to a reduction of CAV1 in U2OS WT cells (**Figure 24G**). Correspondingly, the KD of TEADs and TAZ in NF2 KO cells had a strong negative effect on CAV1 expression, which grossly cancelled out the CAV1 induction due to NF2 KO U2OS cells (**Figure 24G**). Importantly, TEAD deficiency led to reduced *CYR61*, *CAV1* and *CAVIN1* mRNA expression both in WT and NF2 KO cells (**Figure 24H,I**). Consequently, as in HEK 293A cells (**Figure 19**), the expression of CAV1 and CAVIN1 in U2OS cells is TEAD-dependent.

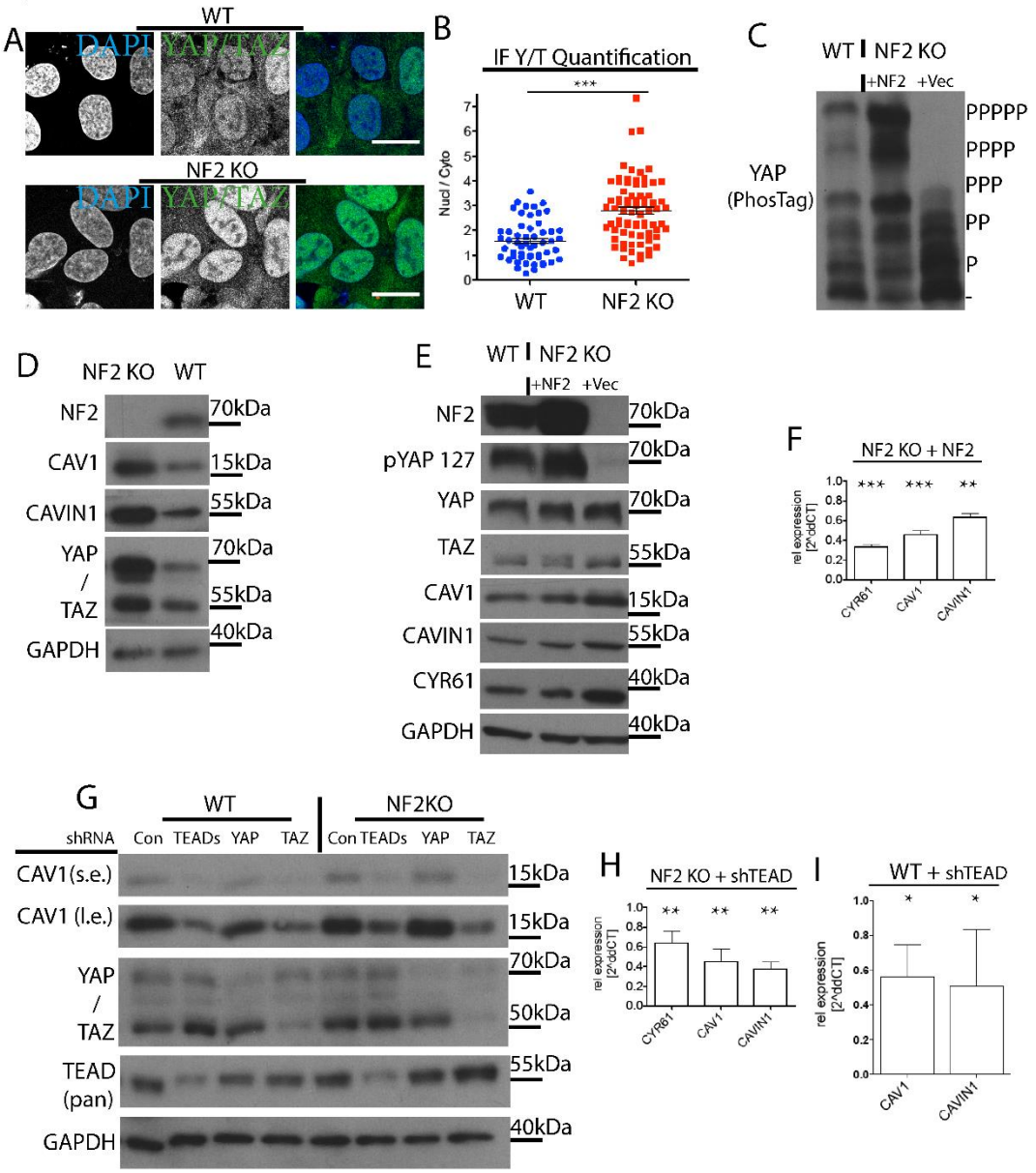

Figure 24: NF2 supresses expression of caveolar components.

A: CLSM images of discrete U2OS cell cultures of WT and NF2 KO lines. Cells were fixed and labelled for YAP/TAZ (green) and counterstained with DAPI (blue). Samples were imaged in parallel and with similar settings to allow direct comparison between cell lines. Scale bar = 20µm. **B:** Quantification of nuclear to cytoplasmic signal of YAP/TAZ (Y/T) in WT and NF2 KO cells (as in A). Each dot represents one cell, n ≥ 80. Mean ± SEM. **C:** Western blot based on a PhosTag SDS-gel probing for YAP protein of cell lysates of U2OS WT and NF2 KO cells re-expressing either a vector (control) or NF2. **D:** Western blot analysis of cell lysates from U2OS NF2 KO and WT cells. **E:** Western blot analysis of cell lysates from lysates as in C. **F:** RT-qPCR analysis of U2OS NF2 KO cells re-expressing NF2, relative to NF2 KO. n = 2. Mean ± SD. **G:** Western blot analysis of cell lysates from U2OS WT and NF2 KO cells with shRNA-induced KD of genes depicted. D, E and G: GAPDH served as loading control. **H:** RT-qPCR analysis in U2OS NF2 KO cells with TEAD1/3/4 #1 KD, relative to NF2 KO. n ≥ 2. Mean ±

SD. **I:** RT-qPCR analysis in U2OS WT cells with TEAD1/3/4 #1 KD, relative to WT. n ≥ 2. Mann-Whitney test, mean ± SD.

4.2.5 YAP/TAZ Activity Governs Expression of Caveolar Components also *in vivo*

Combined KO of YAP and TAZ in both mice and zebrafish is embryonic lethal [59, 66, 216]. *In vitro* YAP/TAZ-deficiency has a strong impact on caveolar gene expression as shown above. To examine if the dependence of caveolae on YAP/TAZ is also present across species and *in vivo* we examined zebrafish embryos. 12-somite-stage Yap/Taz KO fish were compared to age- and background-matched WT embryos. Samples for electron microscopy were prepared (by the Link Lab) and Carsten G. Hansen quantified the abundance of caveolae structures in the fish epidermis. Yap/Taz-deficient epidermal cells have strongly decreased caveolae numbers compared to WT fish (**Figure 25A,B**). To determine if the reduction of caveolar structures was a result of diminished caveolar gene expression, I performed qPCR analysis on cDNA samples of those fish embryos (provided by the Link Lab). Relative to the WT, Yap/Taz KO embryos showed a downregulation of the well-known Yap/Taz target genes, *cyr61* and *ctgf* as well as *cav1* and *cavin1* (**Figure 25C**). In conclusion, upstream regulators and downstream components of the Hippo pathway are key mediators for caveolar gene expression across cell lines and YAP/TAZ-TEAD harbour a central role for caveolae expression.

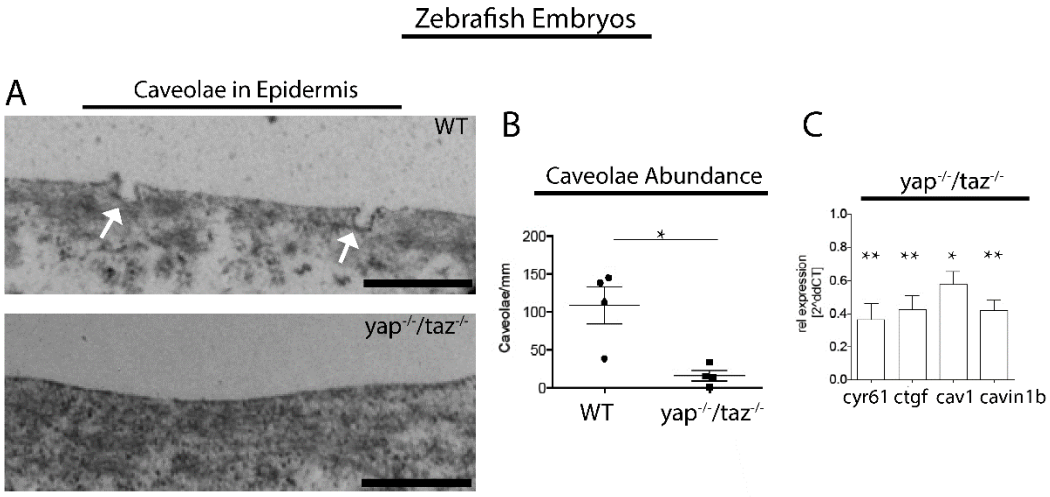

Figure 25: Reduction of caveolae in yap/taz KO zebrafish.

A: Electron microscopic micrographs from epidermis cells from WT and *yap/taz* KO zebrafish embryos. Arrows: Examples of caveolae at the plasma membrane. Scale bar = 500 nm. Samples and images obtained by the Link lab (MCW). Quantification performed by Carsten G. Hansen (UoE). **B:** Quantification of caveolae abundance per millimetre in images as in A. n = 4. Mean ± SEM. Quantification performed by Carsten G. Hansen (UoE). **C:** RT-qPCR analysis to five zebrafish embryos of each genotype. n = 3. Mann-Whitney test, mean ± SD. Sample were prepared by the Link lab (MCW), while I performed the qPCR analysis.

4.3 CAV1 and CAVIN1 Inhibit YAP/TAZ Activity

The understanding of the regulation of the Hippo pathway and YAP/TAZ activity is still incomplete. However, it is well-established that Hippo pathway components and some of its effectors are part of feedback responses [2, 196]. Hence, I sought to determine whether the central caveolar components CAV1 and CAVIN1 regulate YAP/TAZ activity.

4.3.1 CAV1 and CAVIN1 deficiency Induces YAP/TAZ Activity *in vitro*

Initial experiments with CAV1 U2OS KD cells revealed an induction of YAP/TAZ activity, indicated by the decrease of the inhibitory S127-phosphorylation of YAP, and an increase in CYR61 and CTGF protein levels (**Figure 26A**). In addition, these data confirmed the dependence of protein stability of CAVIN1 and CAVIN2 on CAV1 expression [102] (**Figure 26A-D**). Employing the mixed cell culture approach allows the investigation of whether YAP/TAZ hyperactivation was a result of paracrine effects. Immunofluorescence labelling of YAP/TAZ and CAV1 revealed an increased nuclear localisation of YAP/TAZ in CAV1 KD compared to control cells (**Figure 26E,F**). These results are in agreement with increased CYR61 protein expression in three independent CAV1 KD cell lines compared to control cells (**Figure 26G,H**). In order to determine whether the increase in CYR61 and CTGF levels are due to induction of YAP/TAZ-TEAD transcriptional activity, mRNA levels in shCAV1 and shCAVIN1 cells were analysed. Both the CAV1 and the CAVIN1 deficiency led to higher *CYR61* and *CTGF* gene expression (**Figure 26I,J**).

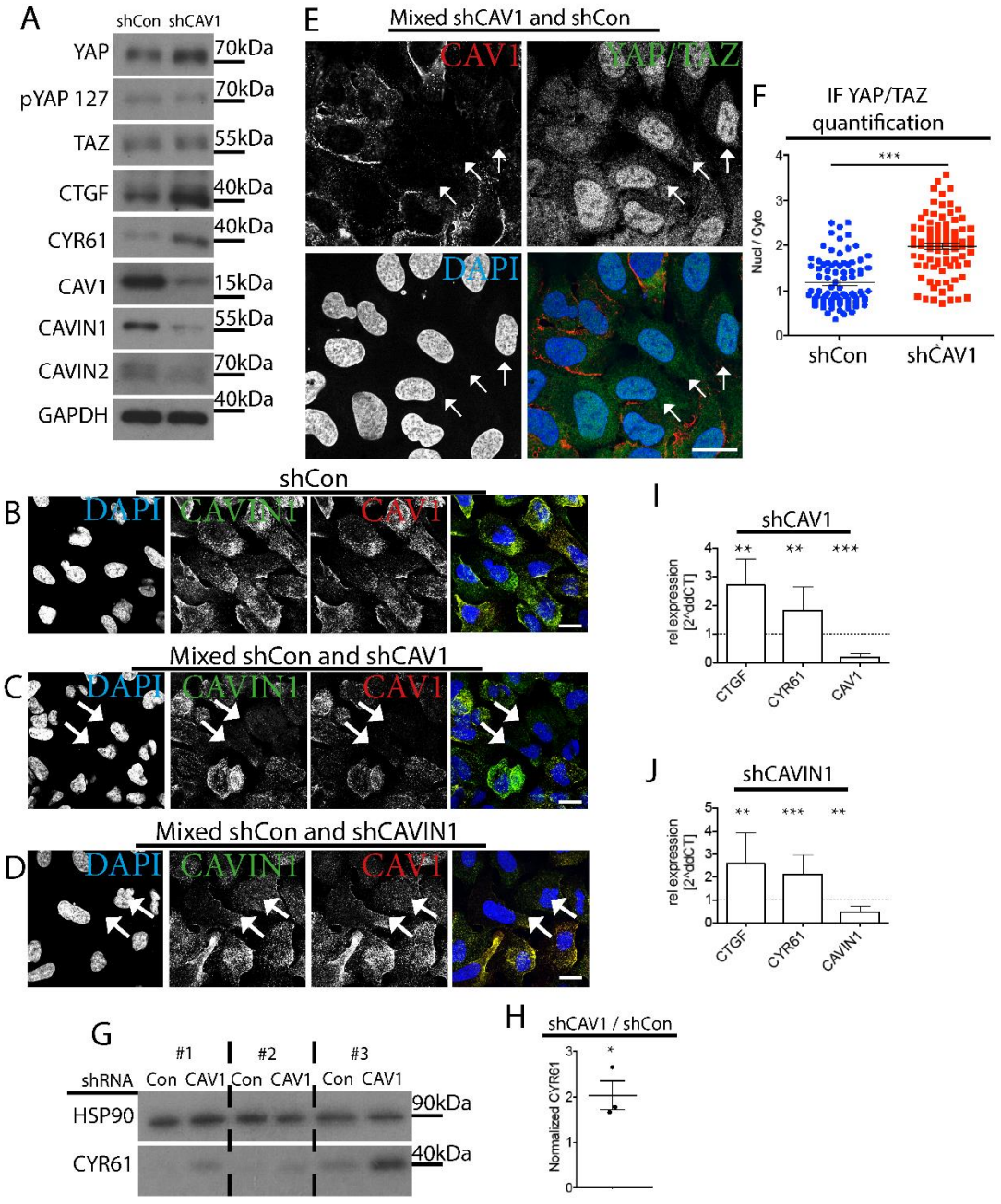

Figure 26: Caveolae inhibit YAP/TAZ activity.

A: Western blot analysis of cell lysates from U2OS control (shCon) and CAV1 KD (shCAV1) cells. GAPDH served as loading control. Depending on the protein tested n ≥ 2. **B-D:** CLSM images of cultures of fixed U2OS shCon (in B), mixed shCon and shCAV1 (in C) or mixed shCon and shCAVIN1 (in D) cells labelled for CAVIN1 (green), CAV1 (red) and counterstained with DAPI (blue). Arrows indicate CAV1 or CAVIN1 KD cells. Scale bars = 20µm. **E:** CLSM images of mixed cultures of fixed U2OS shCon and shCAV1 cells labelled for CAV1 (red), YAP/TAZ (green) and counterstained with DAPI (blue). Arrows indicate CAV1 KD cells. Scale bar = 20µm. **F:** Quantification of nuclear to cytoplasmic ratio of YAP/TAZ signal in images as in B. Each dot represents one cell, mean ± SEM. n ≥ 100. **G:** Western blot analysis of cell lysates from U2OS shCon and three

independent shCAV1 cell lines showing increased CYR61 protein expression in shCAV1 cells. n ≥ 2. **H:** Quantification of relative CYR61 protein levels from Western blot in G, normalised to the loading control HSP90. T-test, mean ± SEM. **I** and **J:** RT-qPCR analysis of expression of established YAP/TAZ target genes in shCAV1 or shCAVIN1 relative to shCon. n ≥ 3. Mann-Whitney test, mean ± SD.

The induction of YAP/TAZ activity (nuclear localisation) was reversed upon re-introduction of CAV1 into U2OS CAV1 KD cells (**Figure 27A**). The nuclear to cytoplasmic ratio of YAP/TAZ was reduced in CAV1 KD cells expressing CAV1-GFP (**Figure 27B**) and protein levels as well as mRNA expression of CYR61 and CTGF decreased as a result of re-expression of CAV1 (**Figure 27C,D**). In addition, CAV1 re-expression also rescued CAV2 and CAVIN1 expression (**Figure 27E,F**). Notably, both CAV1 and CAVIN1 are required for the stability of the caveolin/cavin complex [102, 103, 105]. The loss of one of the components therefore causes destabilisation of the other caveolae components [102, 122, 125]. In summary, CAV1 acts as a negative regulator of YAP/TAZ activity in U2OS cells. To further verify caveolar components as inhibitors of YAP/TAZ activity, shRNA-induced KD of CAV1 and CAVIN1 was examined in HEK 293A cells. The deficiency of only one of the central caveolar elements, CAV1 or CAVIN1, was sufficient to increase YAP/TAZ activity and CYR61 protein expression (**Figure 27G**). Furthermore, RT-qPCR analysis of two independent HEK 293A shCAV1 cell lines confirmed that caveolae deficiency led to increased expression of YAP/TAZ target genes (**Figure 27H**). Consequently, these data suggest that caveolae function as upstream negative regulators of YAP/TAZ activity.

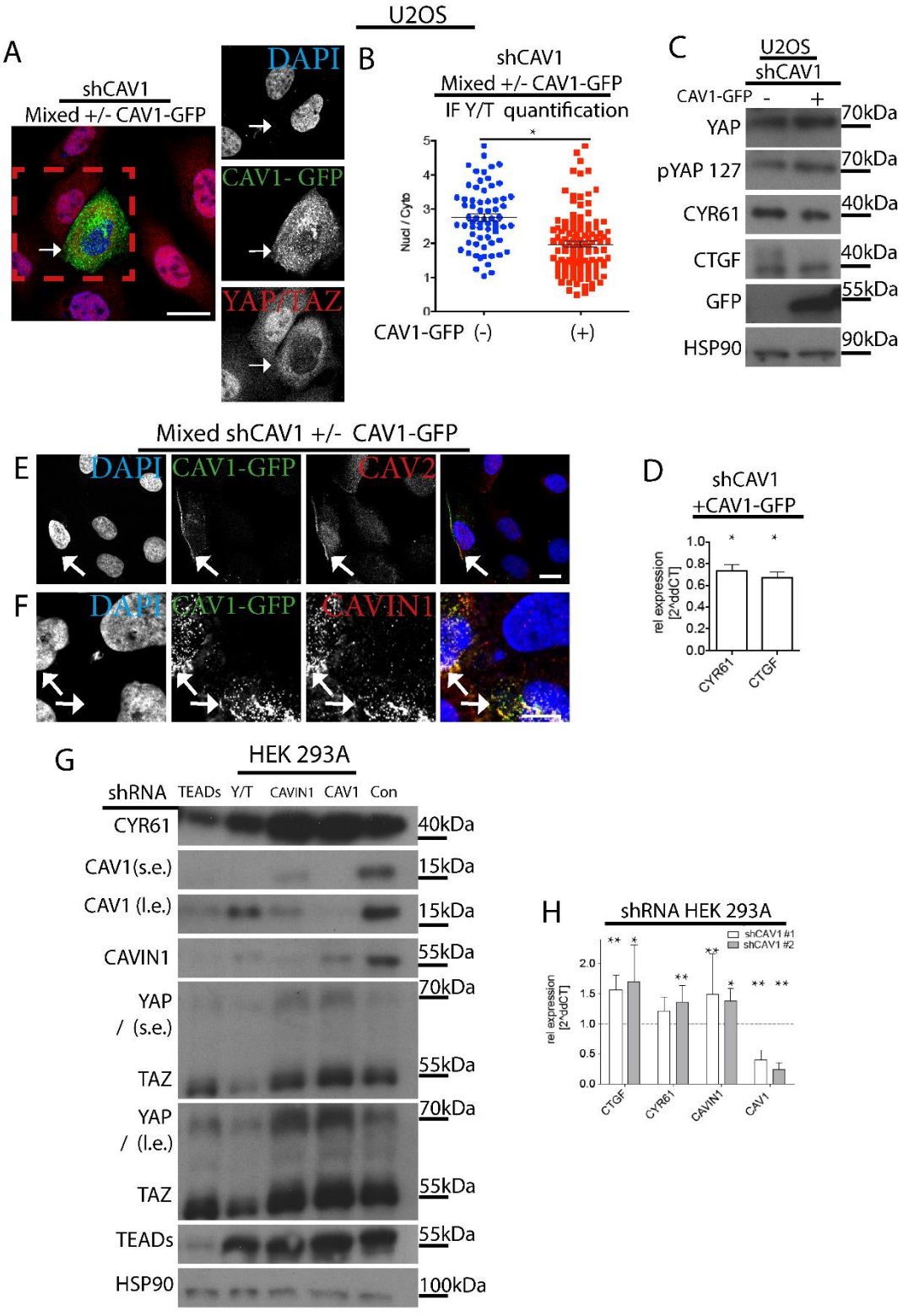

Figure 27: Verifying the inhibitory effect of CAV1 on YAP/TAZ activity in different cell lines.

A: CLSM image of a mixed culture of U2OS shCAV1(#1) cells expressing a control construct or CAV1-GFP. Cells were fixed and labelled for GFP (green), YAP/TAZ (red) and counterstained with DAPI (blue). Arrow indicates a CAV1-GFP expressing cell. Red dash-line box highlights zoom-in images as in the right. Scale bar = 10 µm. **B:** Quantification of nuclear to cytoplasmic ratio of YAP/TAZ (Y/T) signal in cells control (-) and CAV1-GFP expressing shCAV1 cells (as in A). Each dot represents one cell. T-test, mean ± SEM. n ≥ 80. **C:** Western blot analysis of lysates from U2OS shCAV1 (-) control and CAV1-GFP (+) expressing cells. HSP90 served as loading control. **D:** RT-qPCR analysis of two of the establish YAP/TAZ target genes in CAV1-GFP expressing U2OS shCAV1 cells relative to control cells. n ≥ 2. Mann-Whitney test, mean ± SD. **E** and **F:** CLSM images of mixed cultures of U2OS shCAV1 cells expressing CAV1-GFP (+) or vector control (-). Cells were fixed and labelled for GFP (green), CAV2 (red in E) or CAVIN1 (red in F) and counterstained for DAPI (blue). Scale bar = 10 µm. **G:** Western blot analysis of HEK 293A cells with shRNA-induced KD as indicated (Y/T = YAP/TAZ). HSP90 served as loading control. **H:** RT-qPCR analysis of two independent HEK 293A shCAV1 cell lines relative to shCon. n = 3. Mann-Whitney test, mean ± SD.

4.3.2 Caveolae are Negative Regulators of YAP/TAZ Activity *in vivo*

In order to investigate whether the inhibitory effect of caveolae was conserved in other systems and *in vivo*, YAP/TAZ activity was analysed in Cav1/Cav3 KO zebrafish, which lack caveolae [202]. Immunofluorescence labelling of Yap in the epidermis of 48 hours post fertilisation (hpf) fish revealed nuclear accumulation of endogenous Yap in Cav1/Cav3 KO compared to background- and stage-matched WT zebrafish (**Figure 28A,B**). Since Yap/Taz double-KO is lethal at a very early stage of embryonic development [66], it was not possible to fully verify the specificity of the anti-Yap antibody used here at this developmental stage. In addition, as well as to validate the finding above, WT zebrafish were compared to the Cav1/Cav3 KO when expressing the eGFP-Yap-S54A reporter. The Yap-S54A mutant is incapable of binding to Tead transcription factors [66]. The WT and Cav1/Cav3 KO zebrafish co-expressed the eGFP-Yap-S54A reporter and the nuclear marker H2A-mCherry in their epidermis. Imaging and quantification revealed a significant nuclear accumulation of Yap in the

KO compared to WT fish (**Figure 28C,D**). Consequently, these data substantiate the findings of the inhibition of the nuclear translocation of YAP by caveolae *in vivo*. Finally, the transcriptional activity of Yap/Taz in Cav1/Cav3 KO fish was compared to WT fish. In the KO fish mRNA levels of both well-established Yap/Taz-Tead target genes *ctgf* and *cyr61* were significantly increased relative to the expression in WT zebrafish (**Figure 28E**). In conclusion, these data confirm increased activity of YAP upon caveolae deficiency both *in vivo* and across species.

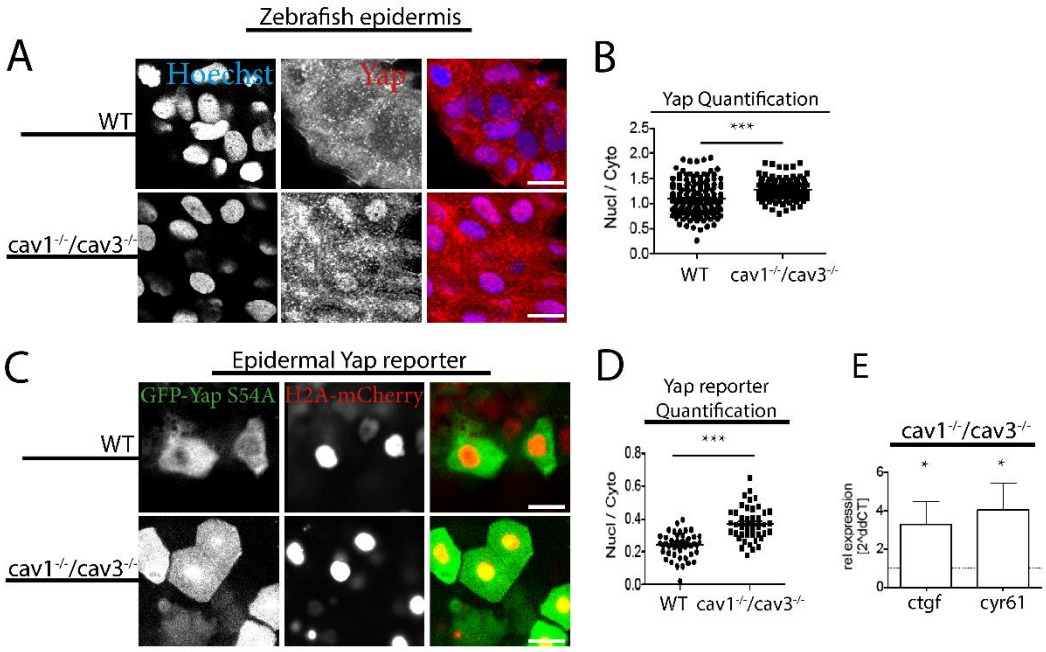

Figure 28: Caveolins are negative regulators of YAP/TAZ activity *in vivo*.

A: CLSM images of epithelial cells from WT and *cav1/cav3* KO zebrafish embryos (at 48hpf) labelled for Hoechst (blue) and Yap (red). Scale bars = 25 µm. **B:** Quantification of nuclear to cytoplasmic ratio of YAP signal in images as in A. Each dot represents one cell. n ≥ 120. Mean ± SEM. **C:** CLSM images of epidermal cells from *cav1/cav3* KO and WT zebrafish embryos expressing epidermal eGFP-Yap S54A (Tead binding-deficient zebrafish Yap mutant) and H2A-mCherry (nuclear marker). Scale bars = 20 µm. **D:** Quantification of nuclear to cytoplasmic ratio of eGFP-Yap from images as in C. Each dot represents one cell. n > 50 from each genotype. n ≥ 80. Mean ± SEM. **E:** RT-qPCR analysis from *cav1/cav3* KO zebrafish embryos (48hpf) relative WT. Mean ± SD. B and D: Quantification performed by Carsten G. Hansen (UoE). C and E: Sample preparation and analysis performed by the Link lab (MCW).

4.3.3 CAV1 Regulates YAP/TAZ via Upstream Hippo Pathway Kinases

In LATS1/2 KO cells YAP/TAZ are hyperactive (**Figure 9**) [196, 197]. To determine whether the CAV1-induced inhibition of YAP/TAZ activity is Hippo pathway-dependent, CAV1 deficiency was induced in LATS1/2 KO cells (**Figure 29A**). Immunofluorescence labelling of YAP and CAV1 as well as RT-qPCR analysis of two independent HEK 293A CAV1 KD cell lines revealed that CAV1 deficiency does not further induce YAP/TAZ nuclear accumulation and transcriptional activity in LATS1/2 KO cells (**Figure 29B-D**). In summary, these data indicate that the inhibition of YAP/TAZ by caveolae likely occurs via the Hippo pathway.

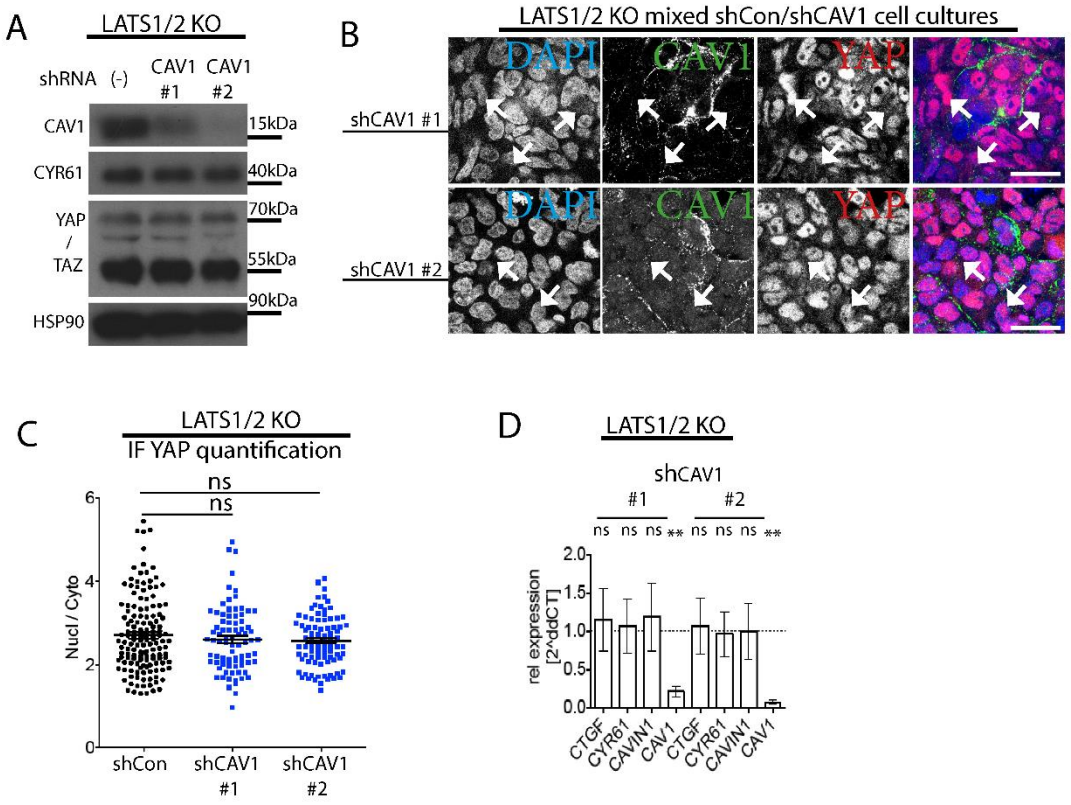

Figure 29: CAV1 regulates YAP/TAZ activity via LATS1/2.

A: Western blot analysis of lysates from HEK 293A LATS1/2 KO cells with or without shRNA-induced CAV1 KD. HSP90 served as a loading control. n ≥ 2. **B:** CLSM images of a mixed culture of HEK 293A LATS1/2KO cells with or without CAV1 KD. Cells were fixed and labelled for CAV1 (green), YAP (red) and counterstained with DAPI (blue). Arrows: CAV1 KD cells. Scale bars = 25 µm. **C:** Quantification of nuclear to cytoplasmic ratio of YAP signal in cells as in images in B. Each dot represents one cell. n ≥ 120. T-test, mean ± SEM. **D:** RT-qPCR analysis of HEK 293A LATS1/2 KO cells with CAV1 KD, relative to control cells. ns = no significant difference between the groups. n = 3. Mann-Whitney test, mean ± SD.

4.3.4 CAV1 KD Induces Anchorage-independent Growth

The ability of cells to grow in an anchor-free environment is one of the hallmarks of cancer [217] and has been shown to be increased in several cell lines upon YAP/TAZ hyperactivation [218, 219]. Culturing CAV1 KD cells in agarose led to increased numbers of colonies compared to control and CAV1 re-expressing cells (**Figure 30A,B**). Consequently, CAV1 deficiency not only increases YAP/TAZ activity, but also induces the cancerous phenotype of cells with hyperactive YAP/TAZ. However, further confirmation by, for instance, KD of YAP/TAZ and TEADs is needed to validate these finding and will allow to fully evaluate, if the increased ability of anchorage-independent growth in U2OS CAV1-deficient cells is YAP/TAZ-TEAD dependent.

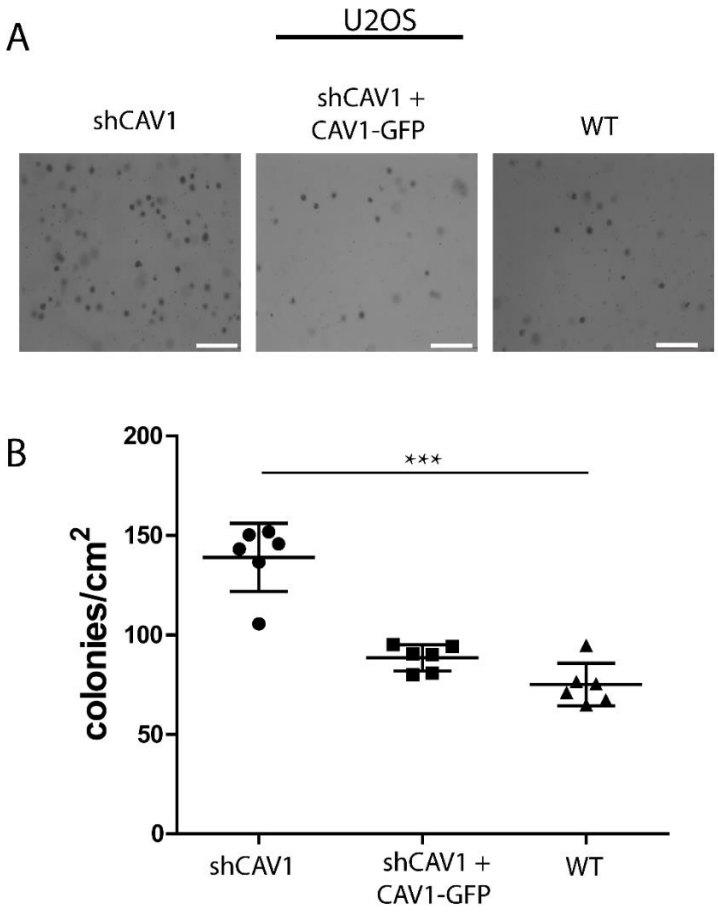

Figure 30: CAV1-deficiency facilitates anchor-free growth.

A: Soft agar colony formation assay of U2OS WT, CAV1 KD and CAV1-GFP expressing CAV1 KD cells. Images of crystal violet-stained cell colonies in agar. Scale bars = 500 µm.
B: Quantification of colonies per cm^2. Each dot represents one biological replicate. n = 2. Kruskal-Wallis test, mean ± SD.

4.4 Caveolae Facilitate YAP/TAZ-mediated Flow Response

Both the Hippo pathway and caveolae are known to regulate and transduce cellular responses to shear stress [193, 194, 220, 221]. Caveolae are recognised as mechanosensors and protectors and have been shown to flatten out under severe shear stress, which protects from membrane rupture [110]. Similarly, YAP/TAZ activity is induced upon mechanical stimuli, including shear stress [194, 220, 222]. Consequently, I aimed to determine whether caveolae and the Hippo pathway are mechanistically linked in the response to mechanical stimuli.

4.4.1 Shear Stress induces YAP/TAZ Activity

Confluent HEK 293A WT and YAP/TAZ KO cells were cultured at two different flow rates (2.1 and $4.7x10^{-5}$ Dyn/cm^2) for 18 hours and compared to steady state (0 Dyn/cm^2) cell cultures. WT cells experiencing shear stress showed decreased YAP phosphorylation, indicating an activation of YAP upon increased flow rates (**Figure 31A**). Moreover, on total proteins levels, an increase of CYR61 expression was evident (**Figure 31B**), verifying that shear stress-induced YAP/TAZ activity in the system used here. As expected, no CYR61 was detected in YAP/TAZ KO cells even under high flow rates, confirming CYR61 as an appropriate marker for YAP activation in this system (**Figure 31B**). Since $2.1x10^{-5}$ Dyn/cm^2 is within the physiological range [189, 223], and sufficient to induce YAP/TAZ activation, all following experiments were performed at this flow rate. A further indication that shear stress induces YAP activity was provided by immunofluorescence images of WT cells experiencing flow, which showed a significant increase of nuclear YAP compared to cells cultured at steady

state (**Figure 31C,D**). Finally, RT-qPCR analyses revealed that shear stress indeed inducted YAP/TAZ activity as both *CTGF* and *CYR61* mRNA levels were significantly elevated (**Figure 31E**).

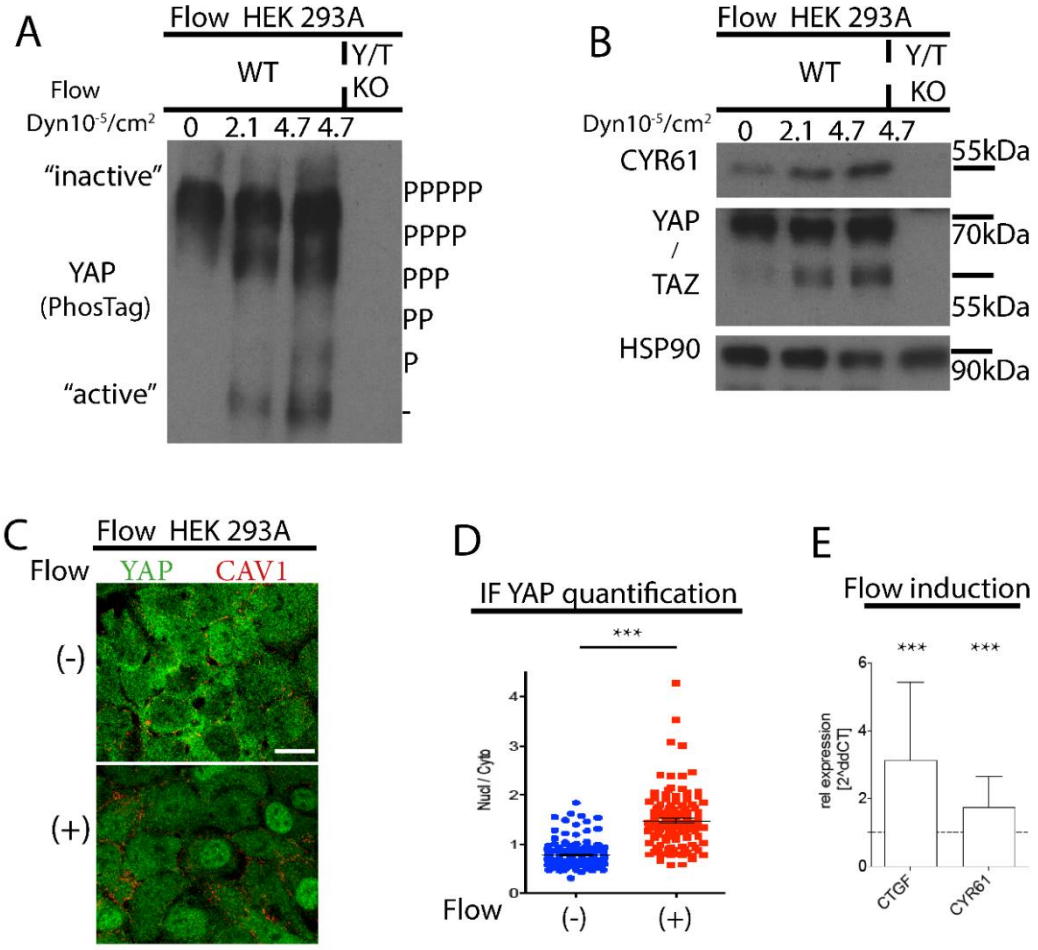

Figure 31: Shear stress-induced YAP/TAY activity.

A: Western blot based on a PhosTag SDS-gel blotted for YAP of lysates from HEK 293A WT cells cultures at steady state (0 Dyn/cm^2), or under flow (2.1 or 4.7x10^{-5} Dyn/cm^2) and YAP/TAZ#1 (Y/T) KO cells experiencing 4.7x10^{-5} Dyn/cm^2. n = 1. **B:** Western blot analysis of lysates as in A. **C:** CLSM images of HEK 293A WT cells cultures at steady state (-) of 2.1x10^{-5} Dyn/cm^2 (+). Cells were fixed straight immediately after stopping the exposure to flow and labelled for YAP (green) and CAV1 (red). Scale bar = 20 µm. **D:** Quantification of nuclear to cytoplasmic ratio of YAP signal in cells as in C. Each dot represents one cell. n ≥ 100. T-test, mean ± SEM. **E:** RT-qPCR analysis of expression of two YAP/TAZ target genes by HEK 293A WT cells cultured at 2.1x10^{-5} Dyn/cm^2, relative to cells experiencing no shear stress. n ≥ 5. Mann-Whitney test, mean ± SD.

4.4.2 Shear Stress Response of YAP/TAZ is Diminished in CAV1-deficient Cells

In order to determine whether the shear stress-induced activation of YAP/TAZ is mediated via caveolae, CAV1-deficient cells were cultured in the flow system. KD of CAV1 led to an increase of CYR61 expression at steady state (no shear stress (-)) (**Figure 32A**). However, under flow conditions the fold induction of CYR61 protein expression was significantly reduced in CAV1 KD cells (by 40%) compared to control cells (**Figure 32B**). Moreover, also shear stress-induced *CTGF* and *CYR61* was less pronounced in CAV1 KD compared to control cells (**Figure 32C**). In order to verify those results, HEK 293A CAV1 KO cell lines were generated (**Figure 32D**). The KO of CAV1 resulted in a reduction of CAVIN1 (**Figure 32D**) and shows, as demonstrated above, that the stability of CAVIN1 depends on CAV1. In detail, the CAV1 KO cell lines showed a strong reduction of CAVIN1 signal compared to WT cells, both on total protein as well as single cell level, as seen by immunofluorescence assays (**Figure 32D,E**). Furthermore, as in KD cells, the CAV1 KO led to YAP hypo-phosphorylation, shown here in two independent CAV1 KO cell lines (**Figure 32F**), which goes along with the nuclear accumulation of YAP as a result of lack of caveolae (**Figure 32G**). Interestingly, when the CAV1 KO cells experienced shear stress the nuclear to cytoplasmic YAP ratio was less induced compared to WT cells (**Figure 32H**). Meaning, shear stress does not increase nuclear translocation of YAP to the same extent in CAV1-deficient cells as in the WT. These results are coherent with RT-qPCR data revealing a less pronounced induction of expression of the YAP/TAZ-TEAD target genes *CTGF* and *CYR61* upon flow sensing in CAV1 KO cells (**Figure 32I**). In conclusion, the induction of YAP activity, as a response to shear stress, was inhibited in CAV1-deficient cells, pointing towards a caveolae-mediated shear stress response of YAP.

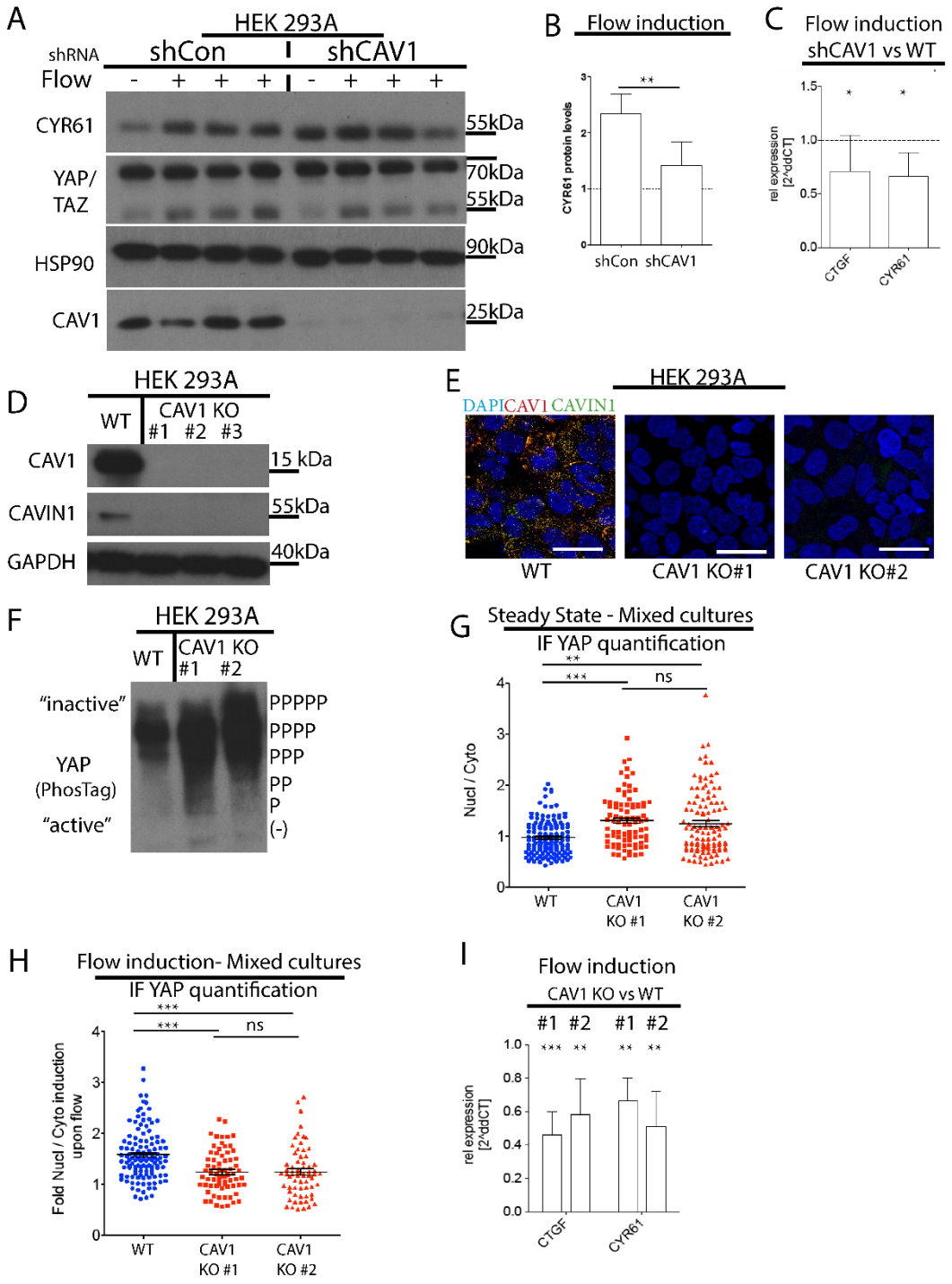

Figure 32: Flow-induced YAP/TAZ activity blunted under CAV1 deficiency.

A: Western blot analysis of HEK 293A shCon and shCAV1 cells cultured at steady state (-) and 2.1x10^{-5} Dyn/cm^2 (+). n ≥ 1. **B:** Quantification of CYR61 protein levels in shCon and shCAV1 cells as in A. n ≥ 3. **C:** RT-qPCR analysis of the relative fold induction of YAP/TAZ target genes expression in shCAV1 upon flow compared to control cells. n ≥ 5. Mann-Whitney test, mean ± SD. **D:** Western blot analysis of three independent HEK 293A CAV1 KO cell lines and WT cells.

n ≥ 1. **E:** CLSM images of HEK 293A WT and two of the CAV1 KO cell lines. Cells were fixed and labelled for CAV1 (red), CAVIN1 (green) and counterstained with DAPI (blue). Scale bar = 30 µm. **F:** Western blot based on a PhosTag SDS-gel probing for YAP protein of lysates as in D. **G:** Quantification of the ratio of nuclear to cytoplasmic YAP in cells cultured at steady state. Each dot represents one cell. n ≥ 120. T-test, mean ± SEM. **H:** Quantification of nuclear to cytoplasmic ratio of YAP signal displayed as normalised flow-induced values. Each dot represents one cell. n ≥ 100. T-test, mean ± SEM. **I:** RT-qPCR analysis of cells experiencing shear stress presented as relative fold induction of target gene expression in two separate CAV1 KO clones upon flow compared to control cells. n = 3. Mann-Whitney test, mean ± SD.

4.4.3 Re-expression of CAV1 Restores YAP/TAZ Response to Shear Stress

In order to further validate the above results, CAV1 was re-introduced into CAV1 KO cells (**Figure 33A**). Under steady state conditions the dependency of CAVIN1 stability on CAV1 expression was further confirmed [102, 105, 125]. In both generated CAV1 re-expressing cell lines the expression of CAVIN1 increased compared to the CAV1 KO parental cell lines (**Figure 33A-C**), highlighting that exogenous CAV1 is functional, as it stabilises CAVIN1 protein. Importantly, the re-introduction of CAV1 also modified YAP/TAZ expression. In both CAV1 re-expressing cell lines the ratio of nuclear to cytoplasmic YAP/TAZ was reduced compared to CAV1 KO cells (**Figure 33D-G**). In terms of the shear stress response, re-expression of CAV1 facilitated the flow-induced YAP/TAZ activation, resulting in increased nuclear YAP/TAZ (**Figure 33H,I**). In conclusion, these data show that shear stress-induced YAP/TAZ activation is, at least partly, mediated via caveolae.

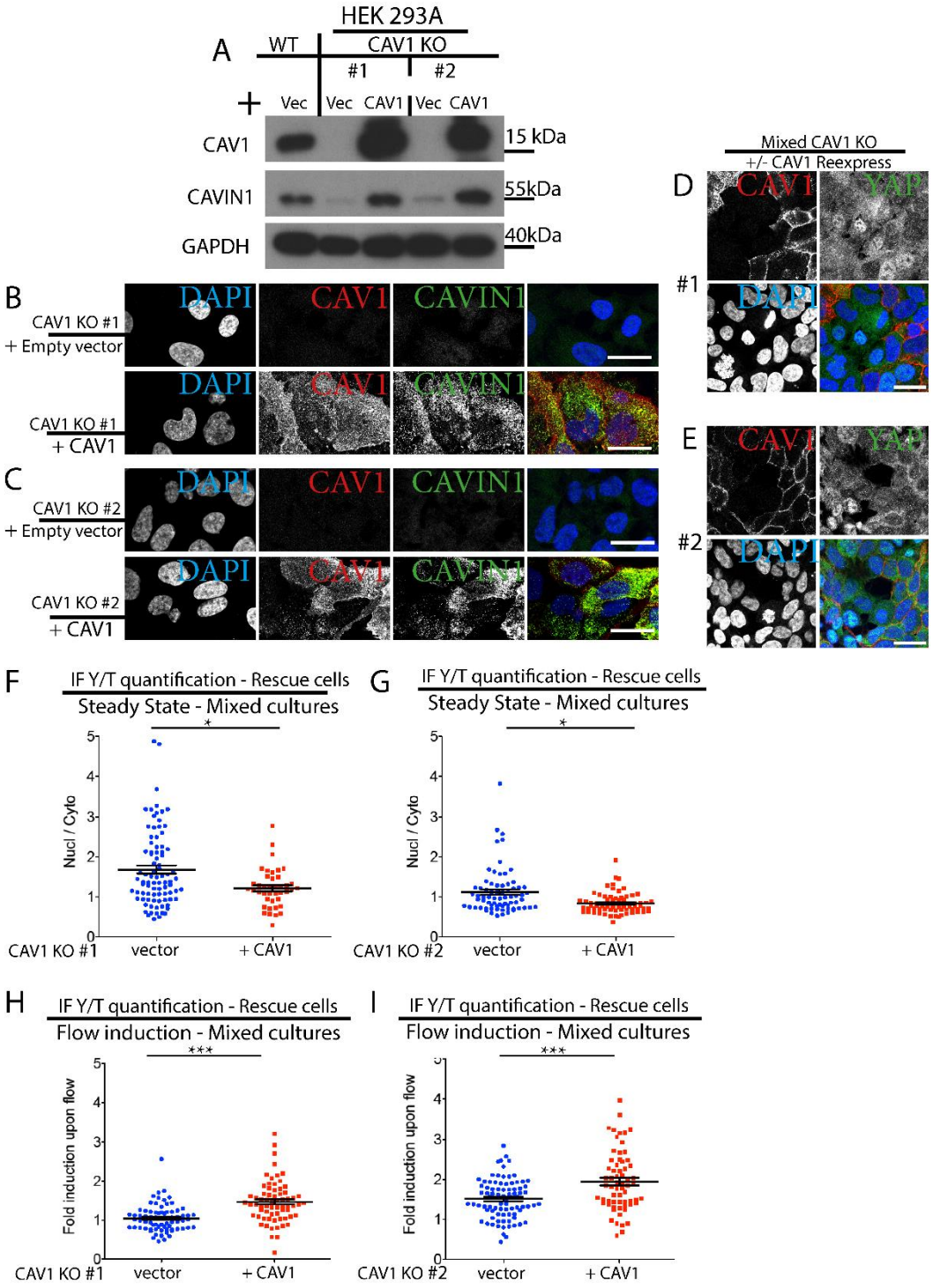

Figure 33: Re-expression of CAV1 restores YAP/TAZ response to shear stress.

A: Western blot analysis of HEK 293A WT and two independent CAV1 KO cell lines expressing vector control or CAV1 GAPDH served as a loading control. n ≥ 1. **B** and **C:** CLSM images of CAV1 KO cell lines (#1 and #2) expressing vector control (+empty vector) or CAV1. Cells were fixed and labelled for CAV1 (red), CAVIN1 (green) and counterstained with DAPI (blue). Scale bar = 30 µm. **D** and **E:** CLSM images of mixed cultures of CAV1 KO and CAV1 re-expressing cells,

fixed and labelled for CAV1 (red), YAP (green) and counterstained with DAPI (blue). Scale bar = 25 µm. **F** and **G:** Quantification of YAP/TAZ (Y/T) nuclear to cytoplasmic ratio in mixed steady state cultures of HEK 293A CAV1 KO (#1 and #2) vector control and CAV1 re-expressing cells. **H** and **I:** Quantification of fold induction of nuclear to cytoplasmic YAP/TAZ as in F and G of cells experiencing shear stress. Averages were normalised to steady state conditions. F-I: Each dot represents one cell. n ≥ 80. T-test, mean ± SEM.

4.5 Initial Characterisation of Blood Outgrowth Endothelial Cells (BOEC)

In the future, the results above should be complemented with additional physiological relevant systems. Therefore, I initiated the development of a primary cell derived endothelial cell line, which preserves its endothelial character over several passages. Endothelial progenitor cells were isolated from human blood and differentiated into blood outgrowth endothelial cells (BOECs), following the protocol established by Ormiston, et al. [198]. At passage 0 (after differentiation) the cells were labelled for endothelial markers VE-Cadherin and PECAM1 and compared to HEK 293A WT cells (**Figure 34A**). The BOECs but, as expected, not HEK 293A cells expressed both endothelial markers. To further establish these cells as a powerful endothelial *in vitro* system, I analysed the expression of endothelial markers at passage 9 (**Figure 34B**). Both VE-Cadherin and PECAM1 were strongly expressed throughout the culture. Moreover, cells showed expression of both YAP and TAZ.

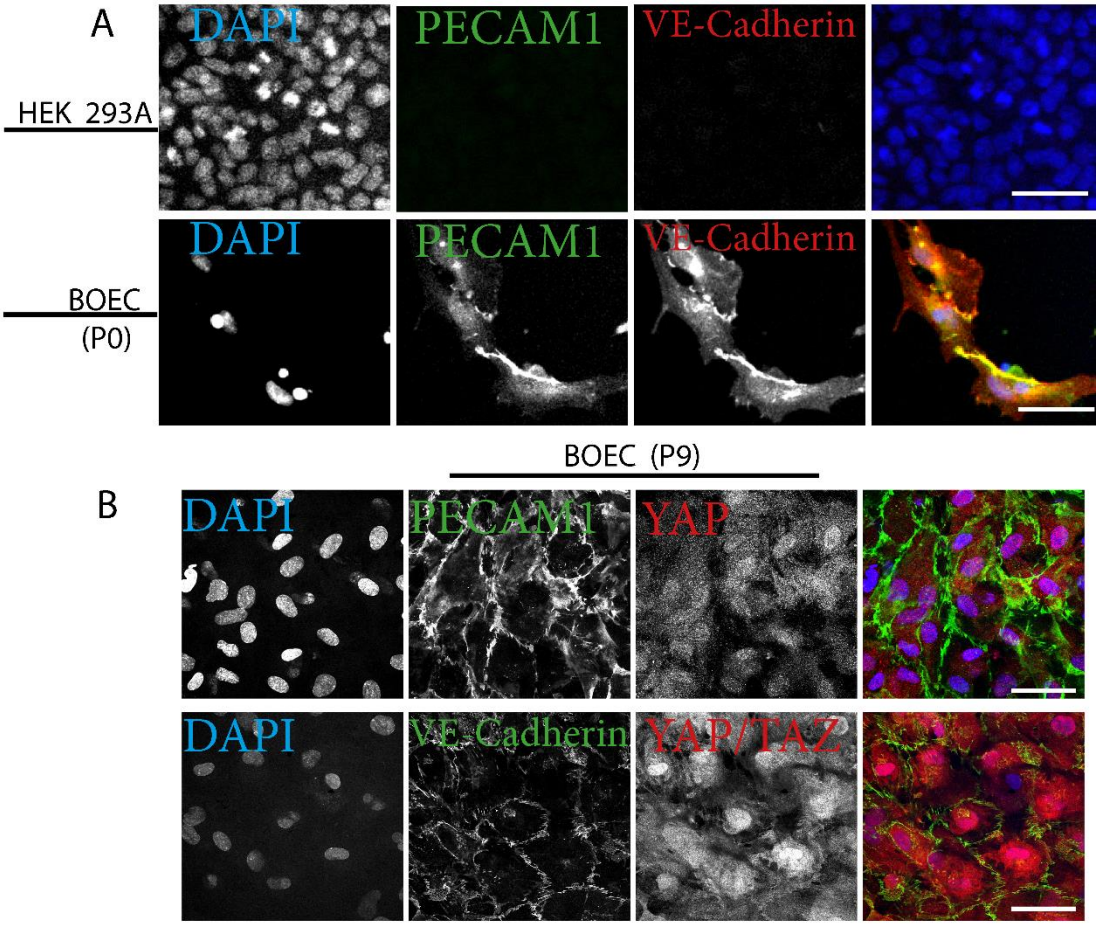

Figure 34: BOECs stably express endothelial markers.

A: CLSM images of HEK 293A and BOECs (passage 0). Cells were fixed and labelled for PECAM1 (green), VE-Cadherin (red) and counterstained with DAPI (blue). **B:** CLSM images of BOECs (passage 9), fixed and labelled for PECAM1 or VE-Cadherin (green), YAP or YAP/TAZ (red) and counterstained with DAPI (blue). Scale bars = 50µm. n = 1.

Also, on total protein levels, assayed by Western blotting, both endothelial markers were detected in BOECs, while the epithelial cell line was negative for PECAM1 and VE-Cadherin (**Figure 35**). Preliminary analysis of total protein levels of Hippo pathway (target) and caveolar proteins revealed an active Hippo pathway. However, it appears that TAZ covers a more significant role than YAP in BOECs, as it is higher expressed

compared to YAP. As a (most likely specific) YAP signal was detected by IF and a signal for unphosphorylated (active) YAP was obtained by Western blotting, the absence of total YAP signal may be explained by the use of unsuitable, YAP-specific antibodies or insufficient exposure while Western blotting. Furthermore, BOEC express the central caveolar components CAV1 and CAVIN1 stronger compared to the epithelial HEK 293A cells (**Figure 35**).

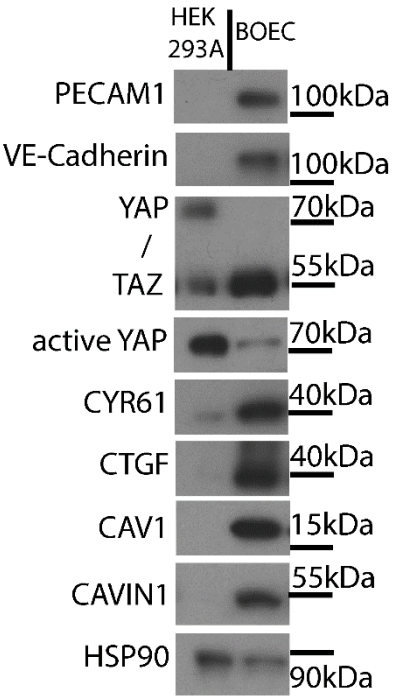

Figure 35: BOECs have a functional Hippo pathway and express essential caveolar components.

Western blot analysis of HEK 293A and BOECs (passage 9). Active YAP is an antibody specific to unphosphorylated YAP. HSP90 was used loading control. Please note that the absence of (CTGF, CAV1, CAVIN1) signal in HEK 293A is most likely due to a lower protein expression, which required a more extended exposure than the one chosen here. n = 1.

Finally, to further analysed the potential heterogeneity of cultures, the expression of the endothelial markers as well as CAV1 expression was established on single cell basis at passage 11. By flow cytometry analysis separate populations of BOEC and HEK 293A cells were labelled with VE-Cadherin, PECAM1 and CAV1, respectively. The populations were gated (**Figure 36A,B**) for cells, single cells and live cells.

Labelling with Zombie aqua (live/dead marker) revealed a viability of about 95% in HEK 293A and 80% in BOEC (**Figure 36A,B**).

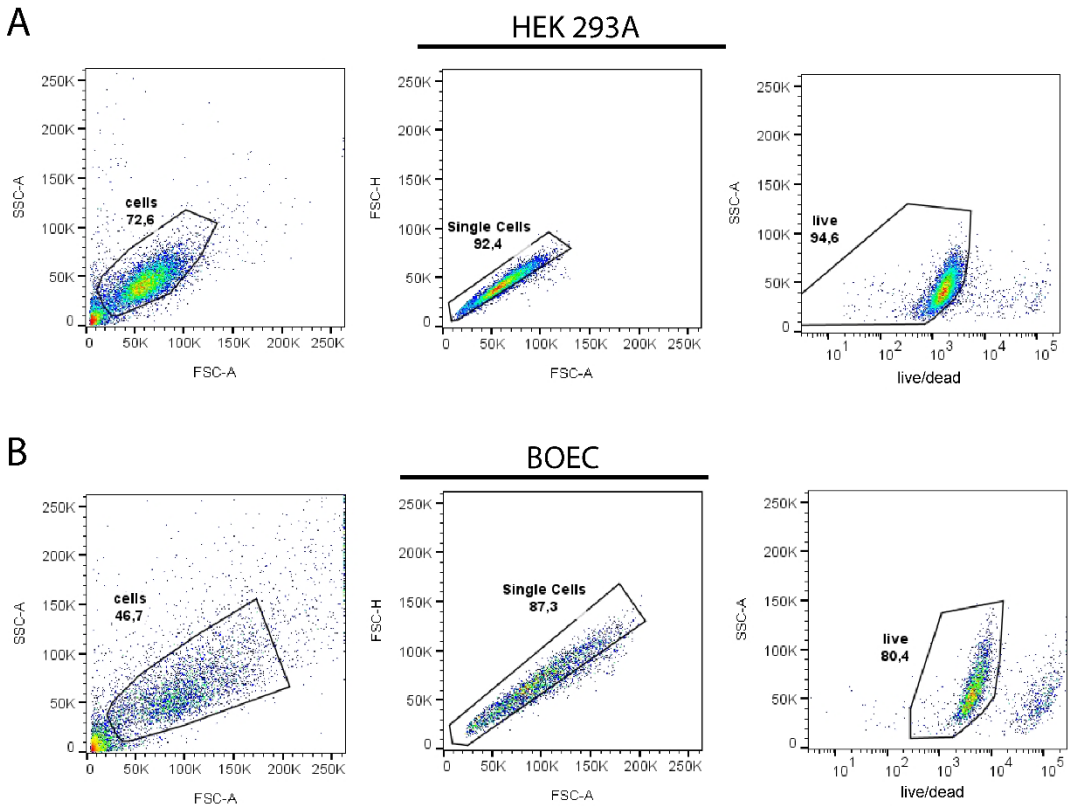

Figure 36: Gating strategy.

Flow cytometry analysis of HEK 293A cells and BOECs at passage 11. Gating strategy for HEK 293A (**A**) and BOECs (**B**). From left to right: Cells, single cells, live cells (identified by Zombie aqua labelling). Numbers in each graph indicate the percentage of total events of the previous gate. n = 1.

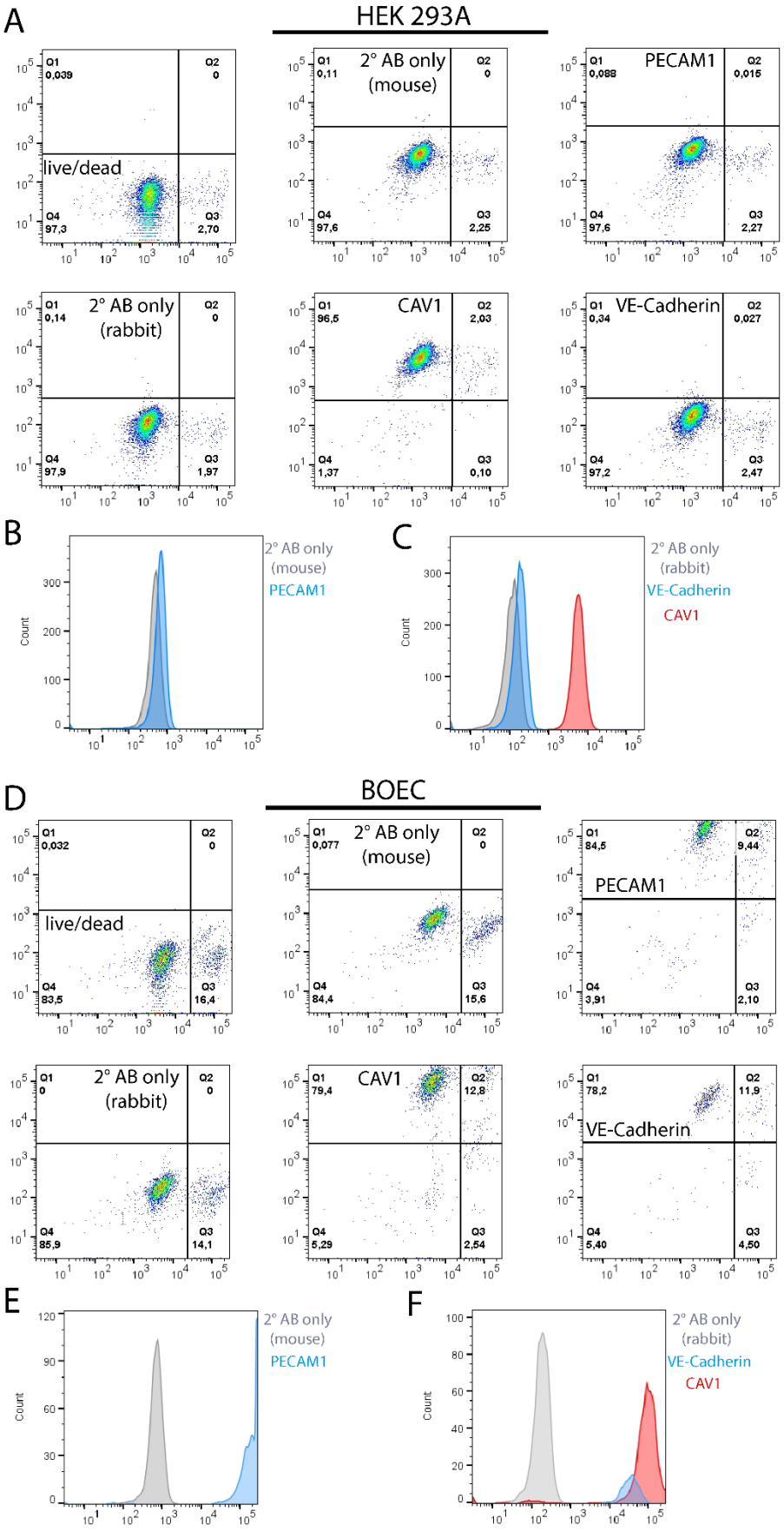
A
HEK 293A
live/dead
2° AB only (mouse)
PECAM1
2° AB only (rabbit)
CAV1
VE-Cadherin
B
2° AB only (mouse)
PECAM1
C
2° AB only (rabbit)
VE-Cadherin
CAV1
Count
D
BOEC
live/dead
2° AB only (mouse)
PECAM1
2° AB only (rabbit)
CAV1
VE-Cadherin
E
2° AB only (mouse)
PECAM1
F
2° AB only (rabbit)
VE-Cadherin
CAV1
Count

Figure 37: BOECs retain endothelial markers over many passages.

A: Flow cytometry analysis of HEK 293A WT cells. Percentages of live cells, cells labelled with secondary antibody only (2°), PECAM1, CAV1 and VE-Cadherin labelled cells. Labelling indicates the quadrant of positive cells per condition. Live cells are relative to single cells. All other conditions are relative to live cells. **B:** Histogram of detected cells incubated with anti-mouse secondary antibody only (grey) and anti-PECAM1 (antibody raised in mouse, blue). **C:** Histogram of detected cells incubated with anti-rabbit secondary antibody only (grey) and anti-VE-Cadherin (antibody raised in rabbit, blue) and anti-CAV1 (red). **D:** Flow cytometry analysis as in A but of BOECs. **E** and **F:** Histogram as in B and C but of BOECs. n = 1.

Both cell lines express CAV1, while BOECs express more CAV1 than HEK 293A indicated by the right shift (**Figure 37C,F**), which is consistent with the bulk analysis in the Western blot above (**Figure 35**). The secondary antibodies both showed low unspecific binding, as shown by the controls incubated with secondary antibody only (**Figure 37A-F**). At the same time, the specificity of the VE-Cadherin and the PECAM1 antibodies was evident from the low signal in epithelial cells. The comparison between the secondary-only treated HEK 293A cells (anti mouse, anti-rabbit) and the cells incubated with the combination of primary antibody against each of the endothelial markers (VE-Cadherin, PECAM1) and secondary antibody showed a high overlap (**Figure 37B,C**). Consequently, the HEK 293A cells were negative for both VE-Cadherin (0.34% positive of live cells) and PECAM1 (0.088% positive of live cells) expression (**Figure 37A-C**). BOECs on the other hand, highly expressed both endothelial markers VE-Cadherin (78.2% of live cells) and PECAM1 (84.5% of live cells, despite the suboptimal gating for PECAM1) (**Figure 37D-F**). There was a clear shift between the cells labelled for the endothelial markers compared to cells only incubated with the secondary antibodies (**Figure 37E,F**). The comparison between HEK 293A and BOECs underlines their endothelial character of the blood outgrowth endothelial cells and verifies that they stably express endothelial markers even at

passage 11. These data are exploratory, however, they emphasise that BOECs are a promising model to verify the physiological role and provide further mechanistic insights into the Hippo pathway and caveolae interaction in the context of shear stress.

5. Discussion

The Hippo pathway is widely recognised as a major driving force in multicellular, homeostatic and developmental processes [71, 212-214, 224-226]. Due to its central role, a tight regulation of the Hippo pathway is critical. A variety of regulatory mechanisms and feedback loops have been discovered. However, new findings constantly add novel interaction partners and feedback processes, emphasising that the understanding of Hippo pathway regulation is not yet complete [21, 58, 60, 84]. An accumulating number of studies show the role of the Hippo pathway in mechanotransduction and interactions with plasma membrane elements [79, 227-229]. A plasma membrane organelle, which is an important mechansosensor and protector are caveolae [109, 140, 173]. One stimulus that both the Hippo pathway and caveolae respond to is shear stress [171, 193, 194, 220]. Flow sensing plays major roles in multiple cell types especially during development [189, 223], in the cardiovascular system [223] or in the kidney [189]. Caveolae are enriched in cells experiencing shear stress, e.g. endothelial cells, and caveolae evolved to be important integrators of mechanical stimuli in those cells [168, 171, 230-232]. So far, the mechanistic insights into how the Hippo pathway is regulated by shear stress and how this cellular response is conferred has been limited [194, 220]. Due to the fact that both the regulation of caveolae and the Hippo pathway are still not fully understood, the question arose whether caveolae might influence the Hippo pathway, which further regulates the cellular response to mechanical stress. This work aimed to broadening the understanding of Hippo pathway regulation. Therefore, the potential reciprocal interaction between the multifunctional caveolae and the Hippo pathway was examined.

The key transcription co-activators of the Hippo pathway, YAP and TAZ, are known to activate transcription of genes central for proliferation and cell survival [22, 70, 197, 233]. Examining YAP/TAZ KO cells, in terms of expression of essential caveolar components, showed a strong reliance of key caveolae elements on the presence of YAP and TAZ activity. At the time these studies were undertaken, the relation between caveolae and Hippo pathway components was not known. Only recently, a study focusing on the interaction between YAP and CAV1 also identified that the expression of most YAP/TAZ target genes positively correlates with CAV1 expression [234]. However, we were the first to confirm that the expression of essential caveolar components depends on YAP/TAZ activity in different cell lines and species, and that CAV1 and CAVIN1 are direct target genes of YAP-TEAD1 [195]. Notably, YAP/TAZ hyperactivity only slightly increases CAV1 and CAVIN1 expression, while YAP/TAZ KO results in drastic loss of caveolae. Therefore, YAP/TAZ are essential for caveolae expression, though their activity appears not to be sufficient for CAV1 and CAVIN1 expression. Other factors that are regulating YAP/TAZ-TEAD activity are VGLL4, MRTF-SRF, AP-1 and SWI/SNF [27, 235-240] and might also play roles in regulating gene expression of caveolar components. Consequently, further studies are needed to identify the details of the expression of essential caveolar components and what roles the Hippo pathway and YAP/TAZ hyperactivation play in the regulation of caveolae expression.

The complexity of Hippo pathway regulation was revealed by identifying the negative feedback loop CAV1 and CAVIN1 exhibit on YAP/TAZ activity. YAP/TAZ induce the expression of CAV1 and CAVIN1, while caveolar components are inhibitors of YAP/TAZ activity. Loss of caveolae leads to the inactivation of the Hippo pathway kinase cascade and YAP/TAZ activation. As both caveolae and the Hippo pathway play central roles in metabolic signalling [103, 197, 241-244], regeneration [67, 245],

and cancers [214, 246], this negative feedback mechanism has the potential to be subject of new therapeutic approaches. One aspect that merits highlighting is that loss-of-function mutations within the muscle specific CAV3 as well as of CAVIN1 cause muscular dystrophy [109, 142, 247-249]. The Hippo pathway is a potent regulator of muscle cells [250-254] and intriguingly there are overlapping gene sets between those upregulated in muscular dystrophy caused by CAVIN1 or CAV3 mutations and those driven by muscular YAP/TAZ-TEAD transcription [142, 249-254]. It might therefore be worth pursuing to examine the state of the Hippo pathway within caveolae-deficient muscular dystrophy patients. Targeting the Hippo pathway within these patients may allow for therapeutic intervention [225, 226, 255, 256].

Another aspect where the YAP/TAZ and caveolae interplay is likely be identified as an important mechanism is cancer. Deregulation of Hippo pathway components and YAP/TAZ hyperactivity play key roles in carcinogenesis and cancer progression [201, 257, 258]. Upregulation and activation of YAP/TAZ is a general phenomenon in most, if not all solid tumours, including colon, lung and liver carcinoma [71, 259]. Similarly, caveolae have been shown to play roles in cancer [143-145, 260]. Here, CAV1 KD was sufficient to increase the ability of U2OS cells to grow in an anchor-independent environment, a characteristic of cancer cells [217]. Nonetheless, the role of caveolae in cancer is regarded as cell type and cancer specific as in some cancers CAV1 is upregulation while in other cancers it is downregulated [261]. Therefore, studies targeting the interplay between the Hippo pathway and caveolae have to determine the role of this interaction in carcinogenesis, cancer progression and metastasis in a cancer type specific manner. What is undebatable however, is the role caveolae play in neovascularisation and angiogenesis, which are further hallmarks of cancer [172, 217, 260, 261]. Also the role of the Hippo pathway in angiogenesis has been widely identified [222]. CAV1 deficiency promotes angiogenesis via induction of the nitric

oxide pathway or VEGF expression, while active YAP/TAZ promote proliferation, survival and migration of endothelial cells to promote angiogenesis [222, 262-264]. The vessel-lining endothelial cells are central for angiogenesis [77, 173, 188, 265]. These cells are constantly exposed to mechanical forces, in particular shear stress [165, 190]. So far, the mechanistic insights into how the Hippo pathway is regulated by shear stress and how this cellular response is conferred, has been limited [194, 220]. Caveolae have been reported to mediate shear stress stimuli into the cell [173, 193]. However, how caveolae perform mechanotransduction and the response to shear stress in particular, is not well understood [98, 171, 173, 174, 193, 202, 266]. Hence, the final objective of this thesis was to identify, if the newly establishing link between the Hippo pathway and caveolae plays a role in the shear stress response. The flow system used here induced expression of *CTGF* and *CYR61* in WT cells, which is in agreement with previous studies [267, 268]. Significantly, the results obtained reveal that shear stress-mediated induction of these YAP/TAZ-TEAD target genes is caveolae-dependent. So far, there is no complete and detailed mechanistic understanding of this process. However, the caveolae-dependent regulation occurs via LATS-mediated inhibitory phosphorylation of YAP/TAZ.

Caveolae are known to protect cells from mechanical stress [109, 173, 174, 193, 202, 266, 269]. Major insights into the composition of caveolae have been facilitated by the identification of additional caveolar proteins, like CAVINs [103-105, 120, 125, 270], PACSINs [126, 130] and EHDs [102, 126-128, 270, 271]. In combination with the recent technical advancement in EM and biophysical technologies, these discoveries have allowed impressive and detailed understanding into the molecular composition of caveolae [102-104, 120, 125, 270, 272-275]. Nonetheless, how caveolae gene expression is regulated as well as how they mediate flow sensing to the interior of the cell demand further investigations [101, 109, 173, 174, 193, 202, 266, 269]. Still, the

data presented here highlight that YAP/TAZ are activated in caveolae-deficient cells, and that these cells are therefore insensitive to shear stress mediated YAP/TAZ activation, which indicates caveolae and the Hippo pathway as a cardinal nexus for cellular flow sensing.

In order to verify the caveolae-dependent YAP/TAZ activation in a more physiological system than epithelial cells, primary cell derived endothelial cell lines were generated. The protocol established by Ormiston, et al. [198] allowed the isolation of endothelial progenitor cells from human blood which were then differentiated into endothelial cells. Those blood outgrowth endothelial cells (BOECs) stably express endothelial markers throughout many passages which is promising, considering other established endothelial *in vitro* models. The HUVEC (Human umbilical vein endothelial cells) line for example is costly and does not stably express endothelial markers over many passages, which limits their applicability for genetic and functional studies [276-278]. The BOEC line generated here appears stably expressing endothelial markers PECAM1 and VE-Cadherin, though evaluation of later passages is required to confirm its stability. BOECs therefore appear to offer a reliable model to investigate the Hippo pathway and caveolae interaction in an endothelial system.

BOECs will further allow to elucidate possible changes of VE-Cadherin expression in the context of Hippo pathway and caveolae interaction. VE-Cadherin locates at the junctions of vascular endothelial cells, where it mediates adhesion and regulates vascular permeability and leukocyte extravasation [279]. It will be interesting to evaluate if endothelial barrier functions are affected and the expression of VE-Cadherin is changed upon YAP/TAZ deficiency-induced caveolae reduction. It has been shown that CAV1 interacts with VE-Cadherin/catenin complexes at cell junctions and that VE-Cadherin expression is reduced in CAV1-deficient cells [231, 280]. Still,

endothelial barrier integrity was not affected in those cells under unstimulated conditions. However, thrombin stimulation increased the paracellular permeability in a CAV1-dependent manner [231]. Thrombin further induces YAP/TAZ activity in an epithelial cell model [281]. Consequently, it is worth investigating if thrombin disrupts the endothelial barrier integrity and if this process is mediated via the YAP/TAZ and CAV1 axis.

Moreover, hypertension is another aspect where the newly discovered link between the Hippo pathway and caveolae might be important and potentially opens new therapeutic approaches. Caveolae deficiency induces hypertension [140, 170, 282, 283]. It is speculative, however caveolae deficiency-induced YAP/TAZ hyperactivity might be a self-regulatory mechanism. YAP/TAZ-induced expression of caveolar components might be a compensatory route to protect vessels from increased force they are exposed to in hypertension. Verifying how YAP/TAZ and caveolae are regulated in the context of hypertension might open up new points of action to treat hypertension.

Finally, it is important to mention that somewhat contradicting to the findings discussed here, a recent study identified CAV1 as a YAP activator [234]. CAV1 deficiency led to the cytoplasmic retention of YAP and decreased YAP/TAZ target gene expression in mouse embryonic fibroblasts (MEF) and MDA-MB-231 cells in a LATS1/2-independent manner [234]. These results highlight the complexity and context dependency of the Hippo pathway. So far, details of how YAP/TAZ and caveolae interact are not fully understood. The interplay is likely to be cell type and context dependent and might involve yet unidentified regulators which govern the manifestation of this interaction.

6. Future Directions

The interplay between the Hippo pathway and caveolae has the potential to be of therapeutic importance. To fully take advantage of this potential, further lines of research are needed to gain additional and detailed insights into the molecular mechanisms and conservation across cell types and disease states.

The established BOEC line is a promising model to investigate the relationship between the Hippo pathway, YAP/TAZ and caveolae in human primary cell derived endothelial cells and therefore in a physiological and therapeutically relevant context. The caveolae-rich endothelium lines blood vessels and is therefore constantly exposed to shear stress. Thus, the first step should be to validate the results obtained here in the generated endothelial cell lines, BOEC. Furthermore, KD and/or KO BOEC lines of central Hippo pathway and caveolar components will provide powerful tools to study details of this interplay. Preliminary results revealed that KD of CAV1 is possible and it affects CAVIN1 expression as predicted. These results require further validation, though they are promising in the prospect of the feasibility of generating KD and potentially KO cell lines to study the interaction of the Hippo pathway and caveolae both at steady state and under shear stress conditions.

Initial attempts to study the shear stress response of BOECs were not successful, however they still revealed that it is possible to culture those endothelial cells in the Quasi Vivo flow system. I am confident that under appropriate conditions it will be possible to evaluate the interplay between the Hippo pathway and caveolae and their shear stress response in this system. As the flow rates in the Quasi Vivo setup are variable, it provides the opportunity to study the response to different share stress

strengths. Possibly, by culturing cells at high flow rates or infarction by disrupting the medium flow and/or starving cells from nutrients, high blood pressure may be simulated to provide valuable insights into the Hippo pathway and caveolae under these pathological conditions.

Moreover, the protocol of Ormiston, et al. [198] opens the opportunity to isolate endothelial progenitor cells from patients with CAV1 or CAVIN1 deficiency. However, these CAV1 and CAVIN1-deficient patients are rare [140, 142, 284], and so patient material might be challenging to obtain. Yet, obtaining patient material from either aged or other patient groups is feasible and could provide insight into the aged-dependency of the differentiation potential, YAP/TAZ activity and caveolar component expression patterns. Likewise, it will be of interest to determine if there are differences in YAP/TAZ and caveolae activity and expression in progenitors from patients with hypertension, for example. Still, epigenetic changes during the differentiation process might impair the relevance of studying these patient-derived endothelial cells *in vitro*, which need to be considered. However, investigating cells from different background, in terms of their differentiation capacity and their activity levels of YAP/TAZ during this process, will provide further insights into the impact and relevance of the Hippo pathway and caveolae interaction in development.

In the future, the combination of the blood endothelial progenitor cells and the Quasi Vivo flow system may allow to investigate the changes in expression levels of Hippo pathway and caveolar components during cell differentiation in the context of shear stress exposure. Comparing these data with cells originating from patients with caveolae related mutations offers the possibility to elucidate potential dependences of endothelial differentiation and the response of Hippo pathway during differentiation in a caveolae-deficient background. Finally, although technically challenging, it might be worth aiming to induce KD of Hippo pathway or caveolar components by lentivirus-

mediated shRNA transduction of progenitor cells of healthy donors. If successful, those cells will provide important data on expression patterns of Hippo pathway and caveolar components during differentiation at steady state and under shear stress.

Apart from the Quasi Vivo system, the relationship between the Hippo pathway and caveolae could be investigated in 3D cultures. 2D cultures have their limitations [285, 286] and both the Hippo pathway and caveolae are sensitive to mechanical stimuli [77, 78, 82, 97, 111, 195, 234]. The response to different ECM compositions, investigated in 3D cultures, e.g. by hydrogels of different stiffnesses, would provide additional understanding of the interplay between the Hippo pathway and caveolae. Following the findings reported in this thesis it is plausible that ECM stiffening induced activation of YAP/TAZ might increases caveolar gene expression. Verifying this response is of interest in the field of cancer research, for example, as stiffness within a tumour changes during cancer progression [76].

In order to investigate if the YAP/TAZ deficiency-induced reduction of caveolae indeed impairs the integrity of the endothelial barrier, transendothelial electrical resistance (TEER) measurements may be performed. Using for example the Electric Cell-substrate Impedance Sensing (ECIS) system and compare potential differences in TEER of BOEC WT and KD or KO cell lines will provide insights into the permeability of YAP/TAZ-deficient cells. Exploring alterations in the endothelial layer will provide insight into knock-on effects of Hippo pathway-regulated caveolae deficiency. Moreover, a biochemical analysis of CAVIN and caveolae complexes in these caveolae-rich endothelial cells under flow and in KD or KO cells might also reveal important mechanistic insights.

Interestingly, overexpression of CAV1 induces endothelial tube formation [232], which stands in contrast to other studies, which reported an inhibition of CAV1-induced

vessel formation [287]. Consequently, the function of CAV1 in angiogenesis is yet to be fully elucidated and the BOEC model has the potential to enhance our understanding of angiogenic processes and what role caveolae and the Hippo pathway and their interaction play in this context.

In conclusion, the list of further investigations is not exhaustive. Detailed insights into the regulatory interaction of the Hippo pathway, caveolae and their role in shear stress response is yet to be fully obtained. Nevertheless, the findings discussed in this thesis pave the way to further exploration of caveolae as a link, that explains some of the diverse effects of the Hippo pathway to cellular responses.

7. References

1. Karin, M. and H. Clevers, *Reparative inflammation takes charge of tissue regeneration.* Nature, 2016. **529**(7586): p. 307-15.
2. Hansen, C.G., T. Moroishi, and K.L. Guan, *YAP and TAZ: a nexus for Hippo signaling and beyond.* Trends Cell Biol, 2015. **25**(9): p. 499-513.
3. Justice, R.W., et al., *The Drosophila tumor suppressor gene warts encodes a homolog of human myotonic dystrophy kinase and is required for the control of cell shape and proliferation.* Genes Dev, 1995. **9**(5): p. 534-546.
4. Xu, T., et al., *Identifying tumor suppressors in genetic mosaics: the Drosophila lats gene encodes a putative protein kinase.* Development, 1995. **121**(4): p. 1053-1063.
5. Lai, Z.C., et al., *Control of cell proliferation and apoptosis by mob as tumor suppressor, mats.* Cell, 2005. **120**(5): p. 675-85.
6. Wu, S., et al., *hippo Encodes a Ste-20 Family Protein Kinase that Restricts Cell Proliferation and Promotes Apoptosis in Conjunction with salvador and warts.* Cell, 2003. **114**(4): p. 445-456.
7. Pan, D., *The hippo signaling pathway in development and cancer.* Dev Cell, 2010. **19**(4): p. 491-505.
8. Tapon, N., et al., *salvador Promotes both cell cycle exit and apoptosis in Drosophila and is mutated in human cancer cell lines.* Cell, 2002. **110**(4): p. 467-78.
9. Harvey, K.F., C.M. Pfleger, and I.K. Hariharan, *The Drosophila Mst Ortholog, hippo, Restricts Growth and Cell Proliferation and Promotes Apoptosis.* Cell, 2003. **114**(4): p. 457-467.
10. Pantalacci, S., N. Tapon, and P. Leopold, *The Salvador partner Hippo promotes apoptosis and cell-cycle exit in Drosophila.* Nat Cell Biol, 2003. **5**(10): p. 921-7.
11. Udan, R.S., et al., *Hippo promotes proliferation arrest and apoptosis in the Salvador/Warts pathway.* Nat Cell Biol, 2003. **5**(10): p. 914-20.
12. Jia, J., et al., *The Drosophila Ste20 family kinase dMST functions as a tumor suppressor by restricting cell proliferation and promoting apoptosis.* Genes Dev, 2003. **17**(20): p. 2514-9.
13. Huang, J., et al., *The Hippo signaling pathway coordinately regulates cell proliferation and apoptosis by inactivating Yorkie, the Drosophila Homolog of YAP.* Cell, 2005. **122**(3): p. 421-34.
14. Zhang, L., et al., *The TEAD/TEF family of transcription factor Scalloped mediates Hippo signaling in organ size control.* Dev Cell, 2008. **14**(3): p. 377-87.
15. Zhao, B., et al., *TEAD mediates YAP-dependent gene induction and growth control.* Genes Dev, 2008. **22**(14): p. 1962-71.
16. Vassilev, A., et al., *TEAD/TEF transcription factors utilize the activation domain of YAP65, a Src/Yes-associated protein localized in the cytoplasm.* Genes Dev, 2001. **15**(10): p. 1229-41.
17. Kitagawa, M., *A Sveinsson's chorioretinal atrophy-associated missense mutation in mouse Tead1 affects its interaction with the co-factors YAP and TAZ.* Biochem Biophys Res Commun, 2007. **361**(4): p. 1022-6.
18. Zhang, H., et al., *TEAD transcription factors mediate the function of TAZ in cell growth and epithelial-mesenchymal transition.* J Biol Chem, 2009. **284**(20): p. 13355-62.
19. Dong, J., et al., *Elucidation of a universal size-control mechanism in Drosophila and mammals.* Cell, 2007. **130**(6): p. 1120-33.
20. Gokhale, R. and C.M. Pfleger, *The Power of Drosophila Genetics: The Discovery of the Hippo Pathway*, in *The Hippo Pathway: Methods and Protocols*, A. Hergovich, Editor. 2019, Springer New York: New York, NY. p. 3-26.
21. Meng, Z., T. Moroishi, and K.L. Guan, *Mechanisms of Hippo pathway regulation.* Genes Dev, 2016. **30**(1): p. 1-17.

22. Lei, Q.Y., et al., *TAZ promotes cell proliferation and epithelial-mesenchymal transition and is inhibited by the hippo pathway.* Mol Cell Biol, 2008. **28**(7): p. 2426-36.
23. Chen, Y.A., et al., *WW Domain-Containing Proteins YAP and TAZ in the Hippo Pathway as Key Regulators in Stemness Maintenance, Tissue Homeostasis, and Tumorigenesis.* Front Oncol, 2019. **9**: p. 60.
24. Kim, M.K., J.W. Jang, and S.C. Bae, *DNA binding partners of YAP/TAZ.* BMB Rep, 2018. **51**(3): p. 126-133.
25. Li, Z., et al., *Structural insights into the YAP and TEAD complex.* Genes Dev, 2010. **24**(3): p. 235-40.
26. Lin, K.C., H.W. Park, and K.L. Guan, *Regulation of the Hippo Pathway Transcription Factor TEAD.* Trends Biochem Sci, 2017. **42**(11): p. 862-872.
27. Zanconato, F., et al., *Genome-wide association between YAP/TAZ/TEAD and AP-1 at enhancers drives oncogenic growth.* Nat Cell Biol, 2015. **17**(9): p. 1218-27.
28. Anbanandam, A., et al., *Insights into transcription enhancer factor 1 (TEF-1) activity from the solution structure of the TEA domain.* PNAS, 2006. **103**(46): p. 17225-17230.
29. Yoshida, T., *MCAT elements and the TEF-1 family of transcription factors in muscle development and disease.* Arterioscler Thromb Vasc Biol, 2008. **28**(1): p. 8-17.
30. Ota, M. and H. Sasaki, *Mammalian Tead proteins regulate cell proliferation and contact inhibition as transcriptional mediators of Hippo signaling.* Development, 2008. **135**(24): p. 4059-69.
31. Zhao, B., et al., *Inactivation of YAP oncoprotein by the Hippo pathway is involved in cell contact inhibition and tissue growth control.* Genes Dev, 2007. **21**(21): p. 2747-61.
32. Hergovich, A., *Regulation and functions of mammalian LATS/NDR kinases: looking beyond canonical Hippo signalling.* Cell & Bioscience, 2013. **3**(1): p. 32.
33. Sudol, M., *YAP1 oncogene and its eight isoforms.* Oncogene, 2013. **32**(33): p. 3922.
34. Liu, C.Y., et al., *The hippo tumor pathway promotes TAZ degradation by phosphorylating a phosphodegron and recruiting the SCF{beta}-TrCP E3 ligase.* J Biol Chem, 2010. **285**(48): p. 37159-69.
35. Zhao, B., et al., *A coordinated phosphorylation by Lats and CK1 regulates YAP stability through SCF(beta-TRCP).* Genes Dev, 2010. **24**(1): p. 72-85.
36. Wang, S., et al., *YAP antagonizes innate antiviral immunity and is targeted for lysosomal degradation through IKKvarepsilon-mediated phosphorylation.* Nat Immunol, 2017. **18**(7): p. 733-743.
37. Callus, B.A., A.M. Verhagen, and D.L. Vaux, *Association of mammalian sterile twenty kinases, Mst1 and Mst2, with hSalvador via C-terminal coiled-coil domains, leads to its stabilization and phosphorylation.* FEBS J, 2006. **273**(18): p. 4264-76.
38. Praskova, M., F. Xia, and J. Avruch, *MOBKL1A/MOBKL1B phosphorylation by MST1 and MST2 inhibits cell proliferation.* Curr Biol, 2008. **18**(5): p. 311-21.
39. Hergovich, A., D. Schmitz, and B.A. Hemmings, *The human tumour suppressor LATS1 is activated by human MOB1 at the membrane.* Biochem Biophys Res Commun, 2006. **345**(1): p. 50-8.
40. Yin, F., et al., *Spatial organization of Hippo signaling at the plasma membrane mediated by the tumor suppressor Merlin/NF2.* Cell, 2013. **154**(6): p. 1342-55.
41. Rouleau, G.A., et al., *Alteration in a new gene encoding a putative membrane-organizing protein causes neuro-fibromatosis type 2.* Nature, 1993. **363**(6429): p. 515-521.
42. Meng, Z., et al., *MAP4K family kinases act in parallel to MST1/2 to activate LATS1/2 in the Hippo pathway.* Nat Commun, 2015. **6**: p. 8357.
43. Hergovich, A., *The Roles of NDR Protein Kinases in Hippo Signalling.* Genes (Basel), 2016. **7**(5).
44. Zheng, Y., et al., *Identification of Happyhour/MAP4K as Alternative Hpo/Mst-like Kinases in the Hippo Kinase Cascade.* Dev Cell, 2015. **34**(6): p. 642-55.
45. Li, Q., et al., *The conserved misshapen-warts-Yorkie pathway acts in enteroblasts to regulate intestinal stem cells in Drosophila.* Dev Cell, 2014. **31**(3): p. 291-304.

46. Lim, S., et al., *Identification of the kinase STK25 as an upstream activator of LATS signaling.* Nat Commun, 2019. **10**(1): p. 1547.
47. Millward, T., P. Cron, and B.A. Hemmings, *Molecular cloning and characterization of a conserved nuclear serine(threonine) protein kinase.* PNAS, 1995. **92**(11): p. 5022-6.
48. Hergovich, A., et al., *NDR kinases regulate essential cell processes from yeast to humans.* Nat Rev Mol Cell Biol, 2006. **7**(4): p. 253-64.
49. Selimoglu, R., et al., *RalA GTPase and MAP4K4 Function through NDR1 Activation in Stress Response and Apoptotic Signaling.* Cell Biology & Cell Metabolism, 2014. **1**(1): p. 1-11.
50. Zhang, L., et al., *NDR functions as a physiological YAP1 kinase in the intestinal epithelium.* Curr Biol, 2015. **25**(3): p. 296-305.
51. Byun, M.R., et al., *SRC activates TAZ for intestinal tumorigenesis and regeneration.* Cancer Lett, 2017. **410**: p. 32-40.
52. Li, P., et al., *alphaE-catenin inhibits a Src-YAP1 oncogenic module that couples tyrosine kinases and the effector of Hippo signaling pathway.* Genes Dev, 2016. **30**(7): p. 798-811.
53. Lamar, J.M., et al., *SRC tyrosine kinase activates the YAP/TAZ axis and thereby drives tumor growth and metastasis.* J Biol Chem, 2019. **294**(7): p. 2302-2317.
54. Kim, N.G. and B.M. Gumbiner, *Adhesion to fibronectin regulates Hippo signaling via the FAK-Src-PI3K pathway.* J Cell Biol, 2015. **210**(3): p. 503-15.
55. Huh, H.D., et al., *Regulation of TEAD Transcription Factors in Cancer Biology.* Cells, 2019. **8**(6).
56. Basu, S., et al., *Akt phosphorylates the Yes-associated protein, YAP, to induce interaction with 14-3-3 and attenuation of p73-mediated apoptosis.* molecular cell, 2003. **11**(1): p. 11-23.
57. Strano, S., et al., *Physical interaction with Yes-associated protein enhances p73 transcriptional activity.* J Biol Chem, 2001. **276**(18): p. 15164-73.
58. Kim, W. and E.H. Jho, *The history and regulatory mechanism of the Hippo pathway.* BMB Rep, 2018. **51**(3): p. 106-118.
59. Morin-Kensicki, E.M., et al., *Defects in yolk sac vasculogenesis, chorioallantoic fusion, and embryonic axis elongation in mice with targeted disruption of Yap65.* Mol Cell Biol, 2006. **26**(1): p. 77-87.
60. Plouffe, S.W., et al., *The Hippo pathway effector proteins YAP and TAZ have both distinct and overlapping functions in the cell.* J Biol Chem, 2018. **293**(28): p. 11230-11240.
61. Hu, J., et al., *Yes-associated protein (yap) is required for early embryonic development in zebrafish (danio rerio).* Int J Biol Sci, 2013. **9**(3): p. 267-78.
62. Astone, M., et al., *Zebrafish mutants and TEAD reporters reveal essential functions for Yap and Taz in posterior cardinal vein development.* Sci Rep, 2018. **8**(1): p. 10189.
63. Makita, R., et al., *Multiple renal cysts, urinary concentration defects, and pulmonary emphysematous changes in mice lacking TAZ.* Am J Physiol Renal Physiol, 2008. **294**(3): p. F542-53.
64. Nishioka, N., et al., *The Hippo signaling pathway components Lats and Yap pattern Tead4 activity to distinguish mouse trophectoderm from inner cell mass.* Dev Cell, 2009. **16**(3): p. 398-410.
65. Kimelman, D., et al., *Regulation of posterior body and epidermal morphogenesis in zebrafish by localized Yap1 and Wwtr1.* Elife, 2017. **6**.
66. Miesfeld, J.B., et al., *Yap and Taz regulate retinal pigment epithelial cell fate.* Development, 2015. **142**(17): p. 3021-32.
67. Yimlamai, D., et al., *Hippo pathway activity influences liver cell fate.* Cell, 2014. **157**(6): p. 1324-38.
68. Patel, S.H., F.D. Camargo, and D. Yimlamai, *Hippo Signaling in the Liver Regulates Organ Size, Cell Fate, and Carcinogenesis.* Gastroenterology, 2017. **152**(3): p. 533-545.

69. Wang, J., et al., *The Hippo pathway in the heart: pivotal roles in development, disease, and regeneration.* Nat Rev Cardiol, 2018. **15**(11): p. 672-684.
70. Grijalva, J.L., et al., *Dynamic alterations in Hippo signaling pathway and YAP activation during liver regeneration.* Am J Physiol Gastrointest Liver Physiol, 2014. **307**(2): p. G196-204.
71. Zanconato, F., M. Cordenonsi, and S. Piccolo, *YAP/TAZ at the Roots of Cancer.* Cancer Cell, 2016. **29**(6): p. 783-803.
72. Petrilli, A.M. and C. Fernandez-Valle, *Role of Merlin/NF2 inactivation in tumor biology.* Oncogene, 2016. **35**(5): p. 537-48.
73. Sekido, Y., *Molecular pathogenesis of malignant mesothelioma.* Carcinogenesis, 2013. **34**(7): p. 1413-9.
74. Twist, E.C., et al., *The neurofibromatosis type 2 gene is inactivated in schwannomas.* Hum Mol Genet, 1994. **3**(1): p. 147-51.
75. Han, Y., *Analysis of the role of the Hippo pathway in cancer.* J Transl Med, 2019. **17**(1): p. 116.
76. Broders-Bondon, F., et al., *Mechanotransduction in tumor progression: The dark side of the force.* J Cell Biol, 2018. **217**(5): p. 1571-1587.
77. Dupont, S., et al., *Role of YAP/TAZ in mechanotransduction.* Nature, 2011. **474**(7350): p. 179-83.
78. Panciera, T., et al., *Mechanobiology of YAP and TAZ in physiology and disease.* Nat Rev Mol Cell Biol, 2017.
79. Nardone, G., et al., *YAP regulates cell mechanics by controlling focal adhesion assembly.* Nat Commun, 2017. **8**: p. 15321.
80. Sansores-Garcia, L., et al., *Modulating F-actin organization induces organ growth by affecting the Hippo pathway.* EMBO J, 2011. **30**(12): p. 2325-35.
81. Dobrokhotov, O., et al., *Mechanoregulation and pathology of YAP/TAZ via Hippo and non-Hippo mechanisms.* Clin Transl Med, 2018. **7**(1): p. 23.
82. Liu, F., et al., *Mechanosignaling through YAP and TAZ drives fibroblast activation and fibrosis.* Am J Physiol Lung Cell Mol Physiol, 2015. **308**(4): p. L344-57.
83. Yu, F.X. and K.L. Guan, *The Hippo pathway: regulators and regulations.* Genes Dev, 2013. **27**(4): p. 355-71.
84. Moon, S., S. Yeon Park, and H. Woo Park, *Regulation of the Hippo pathway in cancer biology.* Cell Mol Life Sci, 2018. **75**(13): p. 2303-2319.
85. Gaspar, P. and N. Tapon, *Sensing the local environment: actin architecture and Hippo signalling.* Curr Opin Cell Biol, 2014. **31**: p. 74-83.
86. Wada, K., et al., *Hippo pathway regulation by cell morphology and stress fibers.* Development, 2011. **138**(18): p. 3907-14.
87. Yu, F.X., et al., *Regulation of the Hippo-YAP pathway by G-protein-coupled receptor signaling.* Cell, 2012. **150**(4): p. 780-91.
88. Miller, E., et al., *Identification of serum-derived sphingosine-1-phosphate as a small molecule regulator of YAP.* Chem Biol, 2012. **19**(8): p. 955-62.
89. Jang, J.W., M.K. Kim, and S.C. Bae, *Reciprocal regulation of YAP/TAZ by the Hippo pathway and the Small GTPase pathway.* Small GTPases, 2018: p. 1-9.
90. Shi, X., et al., *Rho differentially regulates the Hippo pathway by modulating the interaction between Amot and Nf2 in the blastocyst.* Development, 2017. **144**(21): p. 3957-3967.
91. Zhao, B., et al., *Cell detachment activates the Hippo pathway via cytoskeleton reorganization to induce anoikis.* Genes Dev, 2012. **26**(1): p. 54-68.
92. Stan, R.V., *Structure of caveolae.* Biochim Biophys Acta, 2005. **1746**(3): p. 334-48.
93. Palade, G.E. and R.R. Bruns, *Structural modulations of plasmalemmal vesicles.* The journal of call biology, 1968. **37**(3): p. 633-649.
94. Yamada, E., *The fine structure of the gall bladder epithelium of the mouse.* J Biophys Biochem Cytol, 1955. **1**(5): p. 445-58.
95. Rothberg, K.G., et al., *Caveolin, a protein component of caveolae membrane coats.* Cell, 1992. **68**(4): p. 673-682.
96. Parton, R.G., *Caveolae: Structure, Function, and Relationship to Disease.* Annu Rev Cell Dev Biol, 2018. **34**: p. 111-136.

97. Cheng, J.P. and B.J. Nichols, *Caveolae: One Function or Many?* Trends Cell Biol, 2016. **26**(3): p. 177-89.
98. Hansen, C.G. and B.J. Nichols, *Exploring the caves: cavins, caveolins and caveolae.* Trends Cell Biol, 2010. **20**(4): p. 177-86.
99. Hayer, A., et al., *Biogenesis of caveolae: stepwise assembly of large caveolin and cavin complexes.* Traffic, 2010. **11**(3): p. 361-82.
100. Bastiani, M., et al., *MURC/Cavin-4 and cavin family members form tissue-specific caveolar complexes.* J Cell Biol, 2009. **185**(7): p. 1259-73.
101. Shvets, E., A. Ludwig, and B.J. Nichols, *News from the caves: update on the structure and function of caveolae.* Curr Opin Cell Biol, 2014. **29**: p. 99-106.
102. Hansen, C.G., et al., *Deletion of cavin genes reveals tissue-specific mechanisms for morphogenesis of endothelial caveolae.* Nat Commun, 2013. **4**: p. 1831.
103. Liu, L., et al., *Deletion of Cavin/PTRF causes global loss of caveolae, dyslipidemia, and glucose intolerance.* Cell Metab, 2008. **8**(4): p. 310-7.
104. Hill, M.M., et al., *PTRF-Cavin, a conserved cytoplasmic protein required for caveola formation and function.* Cell, 2008. **132**(1): p. 113-24.
105. Liu, L. and P.F. Pilch, *A critical role of cavin (polymerase I and transcript release factor) in caveolae formation and organization.* J Biol Chem, 2008. **283**(7): p. 4314-22.
106. Sotgia, F., et al., *Caveolin-1 and cancer metabolism in the tumor microenvironment: markers, models, and mechanisms.* Annu Rev Pathol, 2012. **7**: p. 423-67.
107. Zhuang, Z., et al., *Is caveolin involved in normal proximal tubule function? Presence in model PT systems but absence in situ.* American Journal of Physiology-Renal Physiology, 2011. **300**(1): p. F199-F206.
108. Fernandez-Rojo, M.A., et al., *Caveolin-1 orchestrates the balance between glucose and lipid-dependent energy metabolism: implications for liver regeneration.* Hepatology, 2012. **55**(5): p. 1574-84.
109. Lo, H.P., et al., *The caveolin-cavin system plays a conserved and critical role in mechanoprotection of skeletal muscle.* J Cell Biol, 2015. **210**(5): p. 833-49.
110. Parton, R.G. and M.A. del Pozo, *Caveolae as plasma membrane sensors, protectors and organizers.* Nat Rev Mol Cell Biol, 2013. **14**(2): p. 98-112.
111. Echarri, A. and M.A. Del Pozo, *Caveolae - mechanosensitive membrane invaginations linked to actin filaments.* J Cell Sci, 2015. **128**(15): p. 2747-58.
112. Ariotti, N., et al., *Molecular Characterization of Caveolin-induced Membrane Curvature.* J Biol Chem, 2015. **290**(41): p. 24875-90.
113. Parolini, I., et al., *Expression of caveolin-1 is required for the transport of caveolin-2 to the plasma membrane. Retention of caveolin-2 at the level of the golgi complex.* J Biol Chem, 1999. **274**(36): p. 25718-25725.
114. Scherer, P.E., et al., *Cell-type and tissue-specific expression of caveolin-2. Caveolins 1 and 2 co-localize and form a stable hetero-oligomeric complex in vivo.* J Biol Chem, 1997. **272**(46): p. 29337-29346.
115. de Almeida, C.J.G., *Caveolin-1 and Caveolin-2 Can Be Antagonistic Partners in Inflammation and Beyond.* Front Immunol, 2017. **8**: p. 1530.
116. Cao, H., A.R. Sanguinetti, and C.C. Mastick, *Oxidative stress activates both Src-kinases and their negative regulator Csk and induces phosphorylation of two targeting proteins for Csk: caveolin-1 and paxillin.* Exp Cell Res, 2004. **294**(1): p. 159-71.
117. Tonn Eisinger, K.R., et al., *Palmitoylation of caveolin-1 is regulated by the same DHHC acyltransferases that modify steroid hormone receptors.* J Biol Chem, 2018. **293**(41): p. 15901-15911.
118. Walser, P.J., et al., *Constitutive formation of caveolae in a bacterium.* Cell, 2012. **150**(4): p. 752-63.
119. Lobos-Gonzalez, L., et al., *Caveolin-1 in Melanoma Progression*, in *Advances in Malignant Melanoma - Clinical and Research Perspectives*. 2011.
120. Vinten, J., et al., *Identification of a major protein on the cytosolic face of caveolae.* Biochim Biophys Acta, 2005. **1717**(1): p. 34-40.

121. Aboulaich, N., et al., *Vectorial proteomics reveal targeting, phosphorylation and specific fragmentation of polymerase I and transcript release factor (PTRF) at the surface of caveolae in human adipocytes.* Biochem J., 2004. **383**(Pt 2): p. 237-48.
122. Gambin, Y., et al., *Single-molecule analysis reveals self assembly and nanoscale segregation of two distinct cavin subcomplexes on caveolae.* Elife, 2013. **3**: p. e01434.
123. Kovtun, O., et al., *Cavin family proteins and the assembly of caveolae.* J Cell Sci, 2015. **128**(7): p. 1269-78.
124. Kovtun, O., et al., *Structural insights into the organization of the cavin membrane coat complex.* Dev Cell, 2014. **31**(4): p. 405-19.
125. Hansen, C.G., et al., *SDPR induces membrane curvature and functions in the formation of caveolae.* Nat Cell Biol, 2009. **11**(7): p. 807-14.
126. Hansen, C.G., G. Howard, and B.J. Nichols, *Pacsin 2 is recruited to caveolae and functions in caveolar biogenesis.* J Cell Sci, 2011. **124**(Pt 16): p. 2777-85.
127. Stoeber, M., et al., *Oligomers of the ATPase EHD2 confine caveolae to the plasma membrane through association with actin.* EMBO J, 2012. **31**(10): p. 2350-64.
128. Moren, B., et al., *EHD2 regulates caveolar dynamics via ATP-driven targeting and oligomerization.* Mol Biol Cell, 2012. **23**(7): p. 1316-29.
129. Yeow, I., et al., *EHD Proteins Cooperate to Generate Caveolar Clusters and to Maintain Caveolae during Repeated Mechanical Stress.* Curr Biol, 2017. **27**(19): p. 2951-2962 e5.
130. Senju, Y., et al., *Essential role of PACSIN2/syndapin-II in caveolae membrane sculpting.* J Cell Sci, 2011. **124**(Pt 12): p. 2032-40.
131. Ritter, B., et al., *PACSIN 2, a novel member of the PACSIN family of cytoplasmic adapter proteins.* FEBS Lett, 1999. **454**(3): p. 356-62.
132. Seemann, E., et al., *Deciphering caveolar functions by syndapin III KO-mediated impairment of caveolar invagination.* Elife, 2017. **6**.
133. Martinez-Outschoorn, U.E., Sotgia, F., Lisanti, M. P., *Caveolae and signalling in cancer.* Nat Rev Cancer, 2015. **15**(4): p. 225-37.
134. Parton, R.G. and K. Simons, *The multiple faces of caveolae.* Nat Rev Mol Cell Biol, 2007. **8**(3): p. 185-94.
135. Ortegren, U., et al., *Lipids and glycosphingolipids in caveolae and surrounding plasma membrane of primary rat adipocytes.* Eur J Biochem, 2004. **271**(10): p. 2028-36.
136. Krishna, A. and D. Sengupta, *Interplay between Membrane Curvature and Cholesterol: Role of Palmitoylated Caveolin-1.* Biophys J, 2019. **116**(1): p. 69-78.
137. Dietzen, D.J., W.R. Hastings, and D.M. Lublin, *Caveolin is palmitoylated on multiple cysteine residues. Palmitoylation is not necessary for localization of caveolin to caveolae.* J Biol Chem, 1995. **270**(12): p. 6838-6842.
138. Zhu, Y., et al., *Lipoprotein promotes caveolin-1 and Ras translocation to caveolae: role of cholesterol in endothelial signaling.* Arterioscler Thromb Vasc Biol, 2000. **20**(11): p. 2465-2470.
139. Gustincich, S., et al., *The HumanSerum Deprivation ResponseGene (SDPR) Maps to 2q32–q33 and Codes for a Phosphatidylserine-Binding Protein.* genomics, 1999. **57**(1): p. 120-129.
140. Han, B., et al., *Characterization of a caveolin-1 mutation associated with both pulmonary arterial hypertension and congenital generalized lipodystrophy.* Traffic, 2016. **17**(12): p. 1297-1312.
141. Razani, B., et al., *Caveolin-1 null mice are viable but show evidence of hyperproliferative and vascular abnormalities.* J Biol Chem, 2001. **276**(41): p. 38121-38.
142. Hayashi, Y.K., et al., *Human PTRF mutations cause secondary deficiency of caveolins resulting in muscular dystrophy with generalized lipodystrophy.* J Clin Invest, 2009. **119**(9): p. 2623-33.
143. Goetz, J.G., et al., *Caveolin-1 in tumor progression: the good, the bad and the ugly.* Cancer Metastasis Rev, 2008. **27**(4): p. 715-35.

144. Arpaia, E., et al., *The interaction between caveolin-1 and Rho-GTPases promotes metastasis by controlling the expression of alpha5-integrin and the activation of Src, Ras and Erk.* Oncogene, 2012. **31**(7): p. 884-96.
145. Basu Roy, U.K., et al., *Caveolin-1 is a novel regulator of K-RAS-dependent migration in colon carcinogenesis.* Int J Cancer, 2013. **133**(1): p. 43-57.
146. Calizo, R.C. and S. Scarlata, *A role for G-proteins in directing G-protein-coupled receptor-caveolae localization.* Biochemistry, 2012. **51**(47): p. 9513-23.
147. Li, S., R. Seitz, and M.P. Lisanti, *Phosphorylation of caveolin by src tyrosine kinases. The alpha-isoform of caveolin is selectively phosphorylated by v-Src in vivo.* J Biol Chem, 1996. **271**(7): p. 3863-8.
148. Razani, B. and M.P. Lisanti, *Two distinct caveolin-1 domains mediate the functional interaction of caveolin-1 with protein kinase A.* Am J Physiol Cell Physiol, 2001. **281**(4): p. C1241-50.
149. Collins, B.M., et al., *Structure-based reassessment of the caveolin signaling model: do caveolae regulate signaling through caveolin-protein interactions?* Dev Cell, 2012. **23**(1): p. 11-20.
150. Jung, W., et al., *Cell-free formation and interactome analysis of caveolae.* J Cell Biol, 2018. **217**(6): p. 2141-2165.
151. Echarri, A., et al., *Caveolar domain organization and trafficking is regulated by Abl kinases and mDia1.* J Cell Sci, 2012. **125**(Pt 13): p. 3097-113.
152. Muriel, O., et al., *Phosphorylated filamin A regulates actin-linked caveolae dynamics.* J Cell Sci, 2011. **124**(Pt 16): p. 2763-76.
153. Torrino, S., et al., *EHD2 is a mechanotransducer connecting caveolae dynamics with gene transcription.* J Cell Biol, 2018. **217**(12): p. 4092-4105.
154. Head, B.P., et al., *Microtubules and actin microfilaments regulate lipid raft/caveolae localization of adenylyl cyclase signaling components.* J Biol Chem, 2006. **281**(36): p. 26391-9.
155. Stahlhut, M. and B. van Deurs, *Identification of filamin as a novel ligand for caveolin-1: evidence for the organization of caveolin-1-associated membrane domains by the actin cytoskeleton.* Mol Biol Cell, 2000. **11**(1): p. 325-37.
156. Tamura, K., et al., *Nano-mechanical properties of living cells expressing constitutively active RhoA effectors.* Biochem Biophys Res Commun, 2010. **403**(3-4): p. 363-7.
157. Wickström, S.A., et al., *Integrin-Linked Kinase Controls Microtubule Dynamics Required for Plasma Membrane Targeting of Caveolae.* Developmental Cell, 2010. **19**(4): p. 574-588.
158. Stossel, T.P., et al., *Filamins as integrators of cell mechanics and signalling.* Nat Rev Mol Cell Biol, 2001. **2**(2): p. 138-45.
159. Sverdlov, M., et al., *Filamin A regulates caveolae internalization and trafficking in endothelial cells.* Mol Biol Cell, 2009. **20**(21): p. 4531-40.
160. del Pozo, M.A., et al., *Phospho-Caveolin-1 Mediates Integrin-Regulated Membrane Domain Internalisation.* Nat Cell Biol, 2005. **7**(9): p. 901-8.
161. Burridge, K. and E.S. Wittchen, *The tension mounts: stress fibers as force-generating mechanotransducers.* J Cell Biol, 2013. **200**(1): p. 9-19.
162. Peng, F., et al., *RhoA activation in mesangial cells by mechanical strain depends on caveolae and caveolin-1 interaction.* J Am Soc Nephrol, 2007. **18**(1): p. 189-98.
163. Lisanti, M.P., et al., *Characterization of caveolin-rich membrane domains isolated from an endothelial-rich source: implications for human disease.* J Cell Biol, 1994. **126**(1): p. 111-26.
164. Razani, B., S.E. Woodman, and M.P. Lisanti, *Caveolae: From Cell Biology to Animal Physiology.* Pharmacol Rev, 2002. **54**(3): p. 431-67.
165. Collins, C. and E. Tzima, *Hemodynamic forces in endothelial dysfunction and vascular aging.* Exp Gerontol, 2011. **46**(2-3): p. 185-8.
166. García-Cardeña, G., et al., *Targeting of nitric oxide synthase to endothelial cell caveolae via palmitoylation: implications for nitric oxide signaling.* PNAS, 1996. **93**(13): p. 6448-6453.

167. Le Lay, S. and T.V. Kurzchalia, *Getting rid of caveolins: phenotypes of caveolin-deficient animals.* Biochim Biophys Acta, 2005. **1746**(3): p. 322-33.
168. Murata, T., et al., *Reexpression of caveolin-1 in endothelium rescues the vascular, cardiac, and pulmonary defects in global caveolin-1 knockout mice.* J Exp Med, 2007. **204**(10): p. 2373-82.
169. Wunderlich, C., et al., *Chronic NOS inhibition prevents adverse lung remodeling and pulmonary arterial hypertension in caveolin-1 knockout mice.* Pulm Pharmacol Ther, 2008. **21**(3): p. 507-15.
170. Zhao, Y.Y., et al., *Persistent eNOS activation secondary to caveolin-1 deficiency induces pulmonary hypertension in mice and humans through PKG nitration.* J Clin Invest, 2009. **119**(7): p. 2009-18.
171. Chai, Q., et al., *Role of caveolae in shear stress-mediated endothelium-dependent dilation in coronary arteries.* Cardiovasc Res, 2013. **100**(1): p. 151-9.
172. Chang, S.H., et al., *Vascular permeability and pathological angiogenesis in caveolin-1-null mice.* Am J Pathol, 2009. **175**(4): p. 1768-76.
173. Cheng, J.P., et al., *Caveolae protect endothelial cells from membrane rupture during increased cardiac output.* J Cell Biol, 2015. **211**(1): p. 53-61.
174. Sinha, B., et al., *Cells respond to mechanical stress by rapid disassembly of caveolae.* Cell, 2011. **144**(3): p. 402-13.
175. Pekar, O., et al., *EHD2 shuttles to the nucleus and represses transcription.* Biochem J, 2012. **444**(3): p. 383-94.
176. Thompson, C., et al., *Loss of caveolin-1 alters extracellular matrix protein expression and ductal architecture in murine mammary glands.* PLoS One, 2017. **12**(2): p. e0172067.
177. Ding, S.Y., et al., *Pleiotropic effects of cavin-1 deficiency on lipid metabolism.* J Biol Chem, 2014. **289**(12): p. 8473-83.
178. Mendoza-Topaz, C., et al., *Cells respond to deletion of CAV1 by increasing synthesis of extracellular matrix.* PLoS One, 2018. **13**(10): p. e0205306.
179. Wang, X.M., et al., *Caveolin-1: a critical regulator of lung fibrosis in idiopathic pulmonary fibrosis.* J Exp Med, 2006. **203**(13): p. 2895-906.
180. Govender, P., et al., *Cavin1; a regulator of lung function and macrophage phenotype.* PLoS One, 2013. **8**(4): p. e62045.
181. Taniguchi, T., et al., *PTRF/Cavin-1 Deficiency Causes Cardiac Dysfunction Accompanied by Cardiomyocyte Hypertrophy and Cardiac Fibrosis.* PLoS One, 2016. **11**(9): p. e0162513.
182. Minetti, C., et al., *Mutations in the caveolin-3 gene cause autosomal dominant limb-girdle muscular dystrophy.* Natue Genetics, 1998. **18**(4): p. 365-368.
183. Repetto, S., et al., *Increased number of caveolae and caveolin-3 overexpression in Duchenne muscular dystrophy.* Biochem Biophys Res Commun, 1999. **261**(3): p. 547-550.
184. Volonte, D., A.J. Peoples, and F. Galbiati, *Modulation of myoblast fusion by caveolin-3 in dystrophic skeletal muscle cells: implications for Duchenne muscular dystrophy and limb-girdle muscular dystrophy-1C.* Mol Biol Cell, 2003. **14**(10): p. 4075-88.
185. Paluch, E.K., et al., *Mechanotransduction: use the force(s).* BMC Biol, 2015. **13**: p. 47.
186. Jansen, K.A., P. Atherton, and C. Ballestrem, *Mechanotransduction at the cell-matrix interface.* Semin Cell Dev Biol, 2017. **71**: p. 75-83.
187. Najrana, T. and J. Sanchez-Esteban, *Mechanotransduction as an Adaptation to Gravity.* Front Pediatr, 2016. **4**: p. 140.
188. Chatterjee, S., *Endothelial Mechanotransduction, Redox Signaling and the Regulation of Vascular Inflammatory Pathways.* Front Physiol, 2018. **9**: p. 524.
189. Mammoto, T., A. Mammoto, and D.E. Ingber, *Mechanobiology and developmental control.* Annu Rev Cell Dev Biol, 2013. **29**: p. 27-61.
190. Fernandes, D.C., et al., *Hemodynamic Forces in the Endothelium: From Mechanotransduction to Implications on Development of Atherosclerosis*, in *Endothelium and Cardiovascular Diseases*. 2018. p. 85-95.

191. Nigro, P., J. Abe, and B.C. Berk, *Flow shear stress and atherosclerosis: a matter of site specificity.* Antioxid Redox Signal, 2011. **15**(5): p. 1405-1414
192. Li, Y.S., J.H. Haga, and S. Chien, *Molecular basis of the effects of shear stress on vascular endothelial cells.* J Biomech, 2005. **38**(10): p. 1949-71.
193. Yu, J., et al., *Direct evidence for the role of caveolin-1 and caveolae in mechanotransduction and remodeling of blood vessels.* J Clin Invest, 2006. **116**(5): p. 1284-91.
194. Nakajima, H., et al., *Flow-Dependent Endothelial YAP Regulation Contributes to Vessel Maintenance.* Dev Cell, 2017. **40**(6): p. 523-536 e6.
195. Rausch, V., et al., *The Hippo Pathway Regulates Caveolae Expression and Mediates Flow Response via Caveolae.* Curr Biol, 2019. **29**(2): p. 242-255 e6.
196. Moroishi, T., et al., *A YAP/TAZ-induced feedback mechanism regulates Hippo pathway homeostasis.* Genes Dev, 2015. **29**: p. 1271-1284.
197. Hansen, C.G., et al., *The Hippo pathway effectors YAP and TAZ promote cell growth by modulating amino acid signaling to mTORC1.* Cell Res, 2015. **25**(12): p. 1299-313.
198. Ormiston, M.L., et al., *Generation and Culture of Blood Outgrowth Endothelial Cells from Human Peripheral Blood.* J Vis Exp, 2015(106): p. e53384.
199. Wang, X., et al., *PrimerBank: a PCR primer database for quantitative gene expression analysis, 2012 update.* Nucleic Acids Res, 2012. **40**(Database issue): p. D1144-9.
200. Soules, K.A. and B.A. Link, *Morphogenesis of the anterior segment in the zebrafish eye.* BMC Dev Biol, 2005. **5**: p. 12.
201. Holden, J.K. and C.N. Cunningham, *Targeting the Hippo Pathway and Cancer through the TEAD Family of Transcription Factors.* Cancers (Basel), 2018. **10**(3).
202. Garcia, J., et al., *Sheath Cell Invasion and Trans-differentiation Repair Mechanical Damage Caused by Loss of Caveolae in the Zebrafish Notochord.* Curr Biol, 2017. **27**(13): p. 1982-1989 e3.
203. Rausch, V. and C.G. Hansen, *Immunofluorescence Study of Endogenous YAP in Mammalian Cells*, in *The Hippo Pathway: Methods and Protocols*, A. Hergovich, Editor. 2019, Springer New York: New York, NY. p. 97-106.
204. Vinten, J., et al., *A 60-kDa protein abundant in adipocyte caveolae.* Cell Tissue Res, 2001. **305**(1): p. 99-106.
205. Stein, C., et al., *YAP1 Exerts Its Transcriptional Control via TEAD-Mediated Activation of Enhancers.* PLoS Genet, 2015. **11**(8): p. e1005465.
206. Liu-Chittenden, Y., et al., *Genetic and pharmacological disruption of the TEAD-YAP complex suppresses the oncogenic activity of YAP.* Genes Dev, 2012. **26**(12): p. 1300-5.
207. Michels, S. and U. Schmidt-Erfurth, *Photodynamic therapy with verteporfin: a new treatment in ophthalmology.* Semin Ophthalmol, 2001. **16**(4): p. 201-6.
208. Wang, C., et al., *Verteporfin inhibits YAP function through up-regulating 14-3-3σ sequestering YAP in the cytoplasm.* Am J Cancer Res, 2016. **6**(1): p. 27-37.
209. Elisi, G.M., et al., *Repurposing of Drugs Targeting YAP-TEAD Functions.* Cancers (Basel), 2018. **10**(9).
210. Lui, J.W., et al., *The Efficiency of Verteporfin as a Therapeutic Option in Pre-Clinical Models of Melanoma.* J Cancer, 2019. **10**(1): p. 1-10.
211. Gomez, M., V. Gomez, and A. Hergovich, *The Hippo pathway in disease and therapy: cancer and beyond.* Clinical and Translational Medicine, 2014. **3**(22): p. 1-12.
212. Johnson, R. and G. Halder, *The two faces of Hippo: targeting the Hippo pathway for regenerative medicine and cancer treatment.* Nat Rev Drug Discov, 2014. **13**(1): p. 63-79.
213. Yu, F.X., B. Zhao, and K.L. Guan, *Hippo Pathway in Organ Size Control, Tissue Homeostasis, and Cancer.* Cell, 2015. **163**(4): p. 811-28.
214. Moroishi, T., C.G. Hansen, and K.L. Guan, *The emerging roles of YAP and TAZ in cancer.* Nat Rev Cancer, 2015. **15**(2): p. 73-9.

215. Hamaratoglu, F., et al., *The tumour-suppressor genes NF2/Merlin and Expanded act through Hippo signalling to regulate cell proliferation and apoptosis.* Nat Cell Biol, 2006. **8**(1): p. 27-36.
216. Xin, M., et al., *Hippo pathway effector Yap promotes cardiac regeneration.* Proc Natl Acad Sci U S A, 2013. **110**(34): p. 13839-44.
217. Hanahan, D. and R.A. Weinberg, *Hallmarks of cancer: the next generation.* Cell, 2011. **144**(5): p. 646-74.
218. Overholtzer, M., et al., *Transforming properties of YAP, a candidate oncogene on the chromosome 11q22 amplicon.* PNAS, 2006. **103**(33): p. 12405-12410.
219. Hiemer, S.E., A.D. Szymaniak, and X. Varelas, *The transcriptional regulators TAZ and YAP direct transforming growth factor beta-induced tumorigenic phenotypes in breast cancer cells.* J Biol Chem, 2014. **289**(19): p. 13461-74.
220. Lee, H.J., et al., *Fluid shear stress activates YAP1 to promote cancer cell motility.* Nat Commun, 2017. **8**: p. 14122.
221. Wang, L., et al., *Integrin-YAP/TAZ-JNK cascade mediates atheroprotective effect of unidirectional shear flow.* Nature, 2016. **540**(7634): p. 579-582.
222. Boopathy, G.T.K. and W. Hong, *Role of Hippo Pathway-YAP/TAZ Signaling in Angiogenesis.* Front Cell Dev Biol, 2019. **7**: p. 49.
223. Potente, M. and T. Makinen, *Vascular heterogeneity and specialization in development and disease.* Nat Rev Mol Cell Biol, 2017. **18**(8): p. 477-494.
224. Mohamed, A.D., et al., *The Hippo signal transduction pathway in soft tissue sarcomas.* Biochim Biophys Acta, 2015. **1856**(1): p. 121-9.
225. Gomez, M., V. Gomez, and A. Hergovich, *The Hippo pathway in disease and therapy: cancer and beyond.* Clin Transl Med, 2014. **3**: p. 22.
226. Park, J.H., J.E. Shin, and H.W. Park, *The Role of Hippo Pathway in Cancer Stem Cell Biology.* Mol Cells, 2018. **41**(2): p. 83-92.
227. Kim, J., et al., *Actin remodelling factors control ciliogenesis by regulating YAP/TAZ activity and vesicle trafficking.* Nat Commun, 2015. **6**: p. 6781.
228. Ando, T., et al., *Tissue inhibitor of metalloproteinase-1 promotes cell proliferation through YAP/TAZ activation in cancer.* Oncogene, 2018. **37**(2): p. 263-270.
229. Zuidema, A., et al., *Mechanisms of integrin alphaVbeta5 clustering in flat clathrin lattices.* J Cell Sci, 2018. **131**(21).
230. Nguyen, K.T., et al., *Shear stress reduces protease activated receptor-1 expression in human endothelial cells.* Ann Biomed Eng, 2001. **29**(2): p. 145-52.
231. Kronstein, R., et al., *Caveolin-1 opens endothelial cell junctions by targeting catenins.* Cardiovasc Res, 2012. **93**(1): p. 130-40.
232. Liu, J., et al., *Caveolin-1 expression enhances endothelial capillary tubule formation.* J Biol Chem, 2001. **277**(12): p. 10661-8.
233. Camargo, F.D., et al., *YAP1 increases organ size and expands undifferentiated progenitor cells.* Curr Biol, 2007. **17**(23): p. 2054-60.
234. Moreno-Vicente, R., et al., *Caveolin-1 Modulates Mechanotransduction Responses to Substrate Stiffness through Actin-Dependent Control of YAP.* Cell Rep, 2018. **25**(6): p. 1622-1635 e6.
235. Jiao, S., et al., *A peptide mimicking VGLL4 function acts as a YAP antagonist therapy against gastric cancer.* Cancer Cell, 2014. **25**(2): p. 166-80.
236. Zhang, W., et al., *VGLL4 functions as a new tumor suppressor in lung cancer by negatively regulating the YAP-TEAD transcriptional complex.* Cell Res, 2014. **24**(3): p. 331-43.
237. Kim, T., et al., *MRTF potentiates TEAD-YAP transcriptional activity causing metastasis.* EMBO J, 2017. **36**(4): p. 520-535.
238. Krawczyk, K.K., et al., *Myocardin Family Members Drive Formation of Caveolae.* PLoS One, 2015. **10**(8): p. e0133931.
239. Skibinski, A., et al., *The Hippo transducer TAZ interacts with the SWI/SNF complex to regulate breast epithelial lineage commitment.* Cell Rep, 2014. **6**(6): p. 1059-1072.
240. Witwicka, H., et al., *Calcineurin broadly regulates the initiation of skeletal muscle-specific gene expression by binding target promoters and facilitating the interaction of the SWI/SNF chromatin remodeling enzyme.* Mol Cell Biol, 2019.

241. Mo, J.S., et al., *Cellular energy stress induces AMPK-mediated regulation of YAP and the Hippo pathway.* Nat Cell Biol, 2015. **17**(4): p. 500-10.
242. Sorrentino, G., et al., *Metabolic control of YAP and TAZ by the mevalonate pathway.* Nat Cell Biol, 2014. **16**(4): p. 357-66.
243. Pilch, P.F. and L. Liu, *Fat caves: caveolae, lipid trafficking and lipid metabolism in adipocytes.* Trends Endocrinol Metab, 2011. **22**(8): p. 318-24.
244. Gailite, I., B.L. Aerne, and N. Tapon, *Differential control of Yorkie activity by LKB1/AMPK and the Hippo/Warts cascade in the central nervous system.* Proc Natl Acad Sci U S A, 2015. **112**(37): p. E5169-78.
245. Fernandez, M.A., et al., *Caveolin-1 is essential for liver regeneration.* Science, 2006. **313**(5793): p. 1628-32.
246. Nassoy, P. and C. Lamaze, *Stressing caveolae new role in cell mechanics.* Trends Cell Biol, 2012. **22**(7): p. 381-9.
247. Betz, R.C., et al., *Mutations in CAV3 cause mechanical hyperirritability of skeletal muscle in rippling muscle disease.* Nat Genet, 2001. **28**(3): p. 218-9.
248. Minetti, C., et al., *Mutations in the caveolin-3 gene cause autosomal dominant limb-girdle muscular dystrophy.* Nat Genet, 1998. **18**(4): p. 365-8.
249. Ding, S.Y., L. Liu, and P.F. Pilch, *Muscular dystrophy in PTFR/cavin-1 null mice.* JCI Insight, 2017. **2**(5): p. e91023.
250. Joshi, S., et al., *TEAD transcription factors are required for normal primary myoblast differentiation in vitro and muscle regeneration in vivo.* PLoS Genet, 2017. **13**(2): p. e1006600.
251. Sun, C., et al., *Common and Distinctive Functions of the Hippo Effectors Taz and Yap in Skeletal Muscle Stem Cell Function.* Stem Cells, 2017. **35**(8): p. 1958-1972.
252. Wackerhage, H., et al., *The Hippo signal transduction network in skeletal and cardiac muscle.* Sci Signal, 2014. **7**(337): p. re4.
253. Watt, K.I., et al., *The Hippo pathway effector YAP is a critical regulator of skeletal muscle fibre size.* Nat Commun, 2015. **6**: p. 6048.
254. Judson, R.N., et al., *The Hippo pathway member Yap plays a key role in influencing fate decisions in muscle satellite cells.* J Cell Sci, 2012. **125**(Pt 24): p. 6009-19.
255. Plouffe, S.W., A.W. Hong, and K.L. Guan, *Disease implications of the Hippo/YAP pathway.* Trends Mol Med, 2015. **21**(4): p. 212-22.
256. Mercuri, E. and F. Muntoni, *Muscular dystrophies.* Lancet, 2013. **381**(9869): p. 845-60.
257. Calvo, F., et al., *Mechanotransduction and YAP-dependent matrix remodelling is required for the generation and maintenance of cancer-associated fibroblasts.* Nat Cell Biol, 2013. **15**(6): p. 637-46.
258. Garcia-Rendueles, M.E., et al., *NF2 Loss Promotes Oncogenic RAS-Induced Thyroid Cancers via YAP-Dependent Transactivation of RAS Proteins and Sensitizes Them to MEK Inhibition.* Cancer Discov, 2015. **5**(11): p. 1178-93.
259. Steinhardt, A.A., et al., *Expression of Yes-associated protein in common solid tumors.* Hum Pathol, 2008. **39**(11): p. 1582-9.
260. Celus, W., et al., *Loss of Caveolin-1 in Metastasis-Associated Macrophages Drives Lung Metastatic Growth through Increased Angiogenesis.* Cell Rep, 2017. **21**(10): p. 2842-2854.
261. Lamaze, C. and S. Torrino, *Caveolae and cancer: A new mechanical perspective.* Biomed J, 2015. **38**(5): p. 367-79.
262. Gratton, J.-P., et al., *Selective inhibition of tumor microvascular permeability by cavtratin blocks tumor progression in mice.* Cancer Cell, 2003. **4**(1): p. 31-39.
263. Lin, M.I., et al., *Caveolin-1-deficient mice have increased tumor microvascular permeability, angiogenesis, and growth.* Cancer Res, 2007. **67**(6): p. 2849-56.
264. Yasuda, D., et al., *Lysophosphatidic acid-induced YAP/TAZ activation promotes developmental angiogenesis by repressing Notch ligand Dll4.* J Clin Invest, 2019. **130**.
265. Wang, K.C., et al., *Flow-dependent YAP/TAZ activities regulate endothelial phenotypes and atherosclerosis.* Proc Natl Acad Sci U S A, 2016. **113**(41): p. 11525-11530.

266. Gervasio, O.L., et al., *Caveolae respond to cell stretch and contribute to stretch-induced signaling.* J Cell Sci, 2011. **124**(Pt 21): p. 3581-90.
267. Garcia-Cardena, G., et al., *Biomechanical activation of vascular endothelium as a determinant of its functional phenotype.* Proc Natl Acad Sci U S A, 2001. **98**(8): p. 4478-85.
268. Riser, B.L. and P. Cortes, *Connective tissue growth factor and its regulation: a new element in diabetic glomerulosclerosis.* Ren Fail, 2001. **23**(3-4): p. 459-70.
269. Corrotte, M., et al., *Caveolae internalization repairs wounded cells and muscle fibers.* Elife, 2013. **2**: p. e00926.
270. Aboulaich, N., et al., *Vectorial proteomics reveal targeting, phosphorylation and specific fragmentation of polymerase I and transcript release factor (PTRF) at the surface of caveolae in human adipocytes.* Biochem J, 2004. **383**(Pt 2): p. 237-48.
271. Hoernke, M., et al., *EHD2 restrains dynamics of caveolae by an ATP-dependent, membrane-bound, open conformation.* Proc Natl Acad Sci U S A, 2017. **114**(22): p. E4360-E4369.
272. Stoeber, M., et al., *Model for the architecture of caveolae based on a flexible, net-like assembly of Cavin1 and Caveolin discs.* Proc Natl Acad Sci U S A, 2016. **113**(50): p. E8069-E8078.
273. Ludwig, A., et al., *Molecular composition and ultrastructure of the caveolar coat complex.* PLoS Biol, 2013. **11**(8): p. e1001640.
274. Ludwig, A., B.J. Nichols, and S. Sandin, *Architecture of the caveolar coat complex.* J Cell Sci, 2016. **129**(16): p. 3077-83.
275. Hansen, C.G. and B.J. Nichols, *Molecular mechanisms of clathrin-independent endocytosis.* J Cell Sci, 2009. **122**(Pt 11): p. 1713-21.
276. Hampel, B., et al., *Increased expression of extracellular proteins as a hallmark of human endothelial cell in vitro senescence.* Exp Gerontol, 2006. **41**(5): p. 474-81.
277. Unterluggauer, H., et al., *Identification of cultivation-independent markers of human endothelial cell senescence in vitro.* Biogerontology, 2007. **8**(4): p. 383-97.
278. Martin-Ramirez, J., et al., *Establishment of outgrowth endothelial cells from peripheral blood.* Nat Protoc, 2012. **7**(9): p. 1709-15.
279. Vestweber, D., *VE-cadherin: the major endothelial adhesion molecule controlling cellular junctions and blood vessel formation.* Arterioscler Thromb Vasc Biol, 2008. **28**(2): p. 223-32.
280. Song, L., S. Ge, and J.S. Pachter, *Caveolin-1 regulates expression of junction-associated proteins in brain microvascular endothelial cells.* Blood, 2007. **109**(4): p. 1515-23.
281. Mo, J.S., et al., *Regulation of the Hippo-YAP pathway by protease-activated receptors (PARs).* Genes Dev, 2012. **26**(19): p. 2138-43.
282. Lian, X., et al., *Pathophysiological Role of Caveolae in Hypertension.* Front Med (Lausanne), 2019. **6**: p. 153.
283. Zhao, Y.Y., et al., *Defects in caveolin-1 cause dilated cardiomyopathy and pulmonary hypertension in knockout mice.* Proc Natl Acad Sci U S A, 2002. **99**(17): p. 11375-11380.
284. Kim, C.A., et al., *Association of a homozygous nonsense caveolin-1 mutation with Berardinelli-Seip congenital lipodystrophy.* J Clin Endocrinol Metab, 2008. **93**(4): p. 1129-34.
285. Duval, K., et al., *Modeling Physiological Events in 2D vs. 3D Cell Culture.* Physiology, 2017. **32**(4): p. 266-277.
286. Kapalczynska, M., et al., *2D and 3D cell cultures - a comparison of different types of cancer cell cultures.* Arch Med Sci, 2018. **14**(4): p. 910-919.
287. Brouet, A., et al., *Antitumor effects of in vivo caveolin gene delivery are associated with the inhibition of the proangiogenic and vasodilatory effects of nitric oxide.* FASEB J, 2005. **19**(6): p. 602-4.

Fica Tudo Bem

(* Y *)